Table 4. Thickness statistics of hydrogeologic units in model nearfield.

[Total number of active nearfield cells = 88,335; total active nearfield area = 82,817 square miles]

Unit	System	Top layer	Bottom layer	Number of cells present	Area (square miles)	Average thickness (feet)	Maximum thickness (feet)
QRNR	QRNR	1	3	84,406	78,787	176	1,107
JURA	PENN	4	4	3,892	3,491	60	195
PEN1	PENN	5	5	9,280	8,656	200	601
PEN2	PENN	6	6	9,917	9,247	163	527
MICH	MSHL	7	7	13,647	12,634	250	720
MSHL	MSHL	8	8	16,864	15,559	193	493
DVMS	SLDV	9	9	40,540	36,791	926	1,940
SLDV	SLDV	10	12	71,807	64,833	1,981	7,148
MAQU	C-O	13	13	73,319	66,189	426	2,162
SNNP	C-O	14	14	79,535	71,929	375	1,400
STPT	C-O	15	15	67,102	60,665	363	1,364
PCFR	C-O	16	16	84,164	78,269	467	1,615
IRGA	C-O	17	17	81,688	75,267	141	543
EACL	C-O	18	18	81,746	75,139	287	1,566
MTSM	C-O	19	20	88,275	82,815	630	2,611

The conversion of the three-dimensional stratigraphic database into the model grid produces hydrogeologic units and model layers with not only distinct thickness characteristics but also widely divergent lateral extent (fig. 20 and table 4). For example, the JURA confining unit in model layer 4 is present over only about 4 percent of the model nearfield, whereaswhereas the QRNR and MTSM systems are present over almost the entire nearfield. This complicated stratigraphic pattern is illustrated by selected hydrogeologic sections through the model domain (see fig. 21 for the section traces). Differences in layer thickness along north/south sections that cross the Wisconsin and Kankakee Arches (see fig. 22*A*, corresponding to column 48) and the Michigan Basin (see fig. 22*B*, corresponding to column 204) are quite apparent. The first section shows areas where Precambrian bedrock is shallow and overlain by a thin layer of unconsolidated material and sedimentary rock, whereas in the second section sedimentary rocks attain a combined thickness well over 10,000 ft in the center of the Michigan Basin. The west/east sections reveal more of the structure of the Wisconsin and Kankakee Arches and the Michigan Basin. The PENN and MSHL aquifer systems are not present along the northernmost section (fig. 23*A*, corresponding to row 80), which skirts the southern boundary of the UP_MI and extends into the NLP_MI at the northern edge of the Michigan Basin. The two west/east sections that cross the middle of the Michigan Basin (fig. 23*B*, corresponding to row 170 and fig. 23*C*, corresponding to row 260) express its full bowl-like form, with all or almost all of the 20 model layers present and none or few pinched. The southernmost section, crossing from northeastern Illinois into the northern edge of Indiana (fig. 23*D*, corresponding to row 350), indicates the presence of the Kankakee Arch to the west and the limited thickness of sedimentary rock at the southern margin of the Michigan Basin to the east.

Grouping model layers into aquifer systems along west/east sections (fig. 24*A*–*D*) is a useful way to simplify the visualization of the subsurface geometry. The volume of the Michigan Basin is clearly dominated by the lowermost aquifer systems, the SLDV and C-O, with the QRNR system constituting a thin veneer relative to the overall thickness. In the center of the basin, the PENN and MSHL systems are dominant. The pattern is different west of Lake Michigan, where the QRNR and C-O systems constitute most of the subsurface above the Precambrian bedrock; however, near the lake they are separated by the SLDV system thickening to the east.

Some model layers represent confining units that define the top of aquifer systems:

- JURA (layer 4) at the top of the PENN aquifer system
- MICH (layer 7) at the top of the MSHL aquifer system
- DVMS (layer 9) at the top of the SLDV aquifer system
- MAQU (layer 13) at the top of the C-O aquifer system

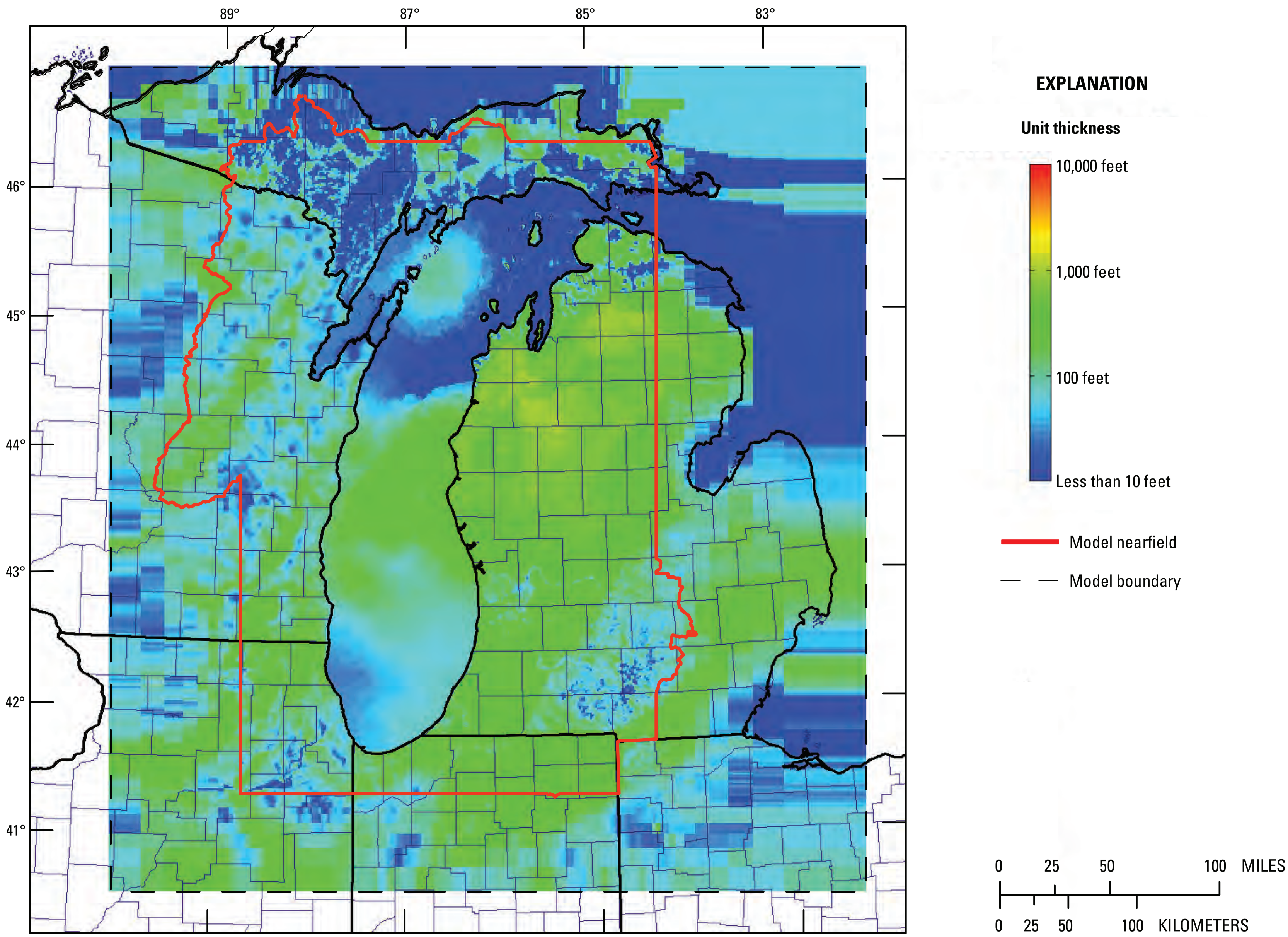

Base from U.S. Geological Survey digital data
1:100,000 1983. Universal Transverse Mercator projection
Zone 16, Standard Parallel 0° (Equator), Central Meridian 87° W,
North American Datum 1983

Figure 20*A*. Thickness of hydrogeologic units: Quaternary deposits (QRNR = layers 1–3).

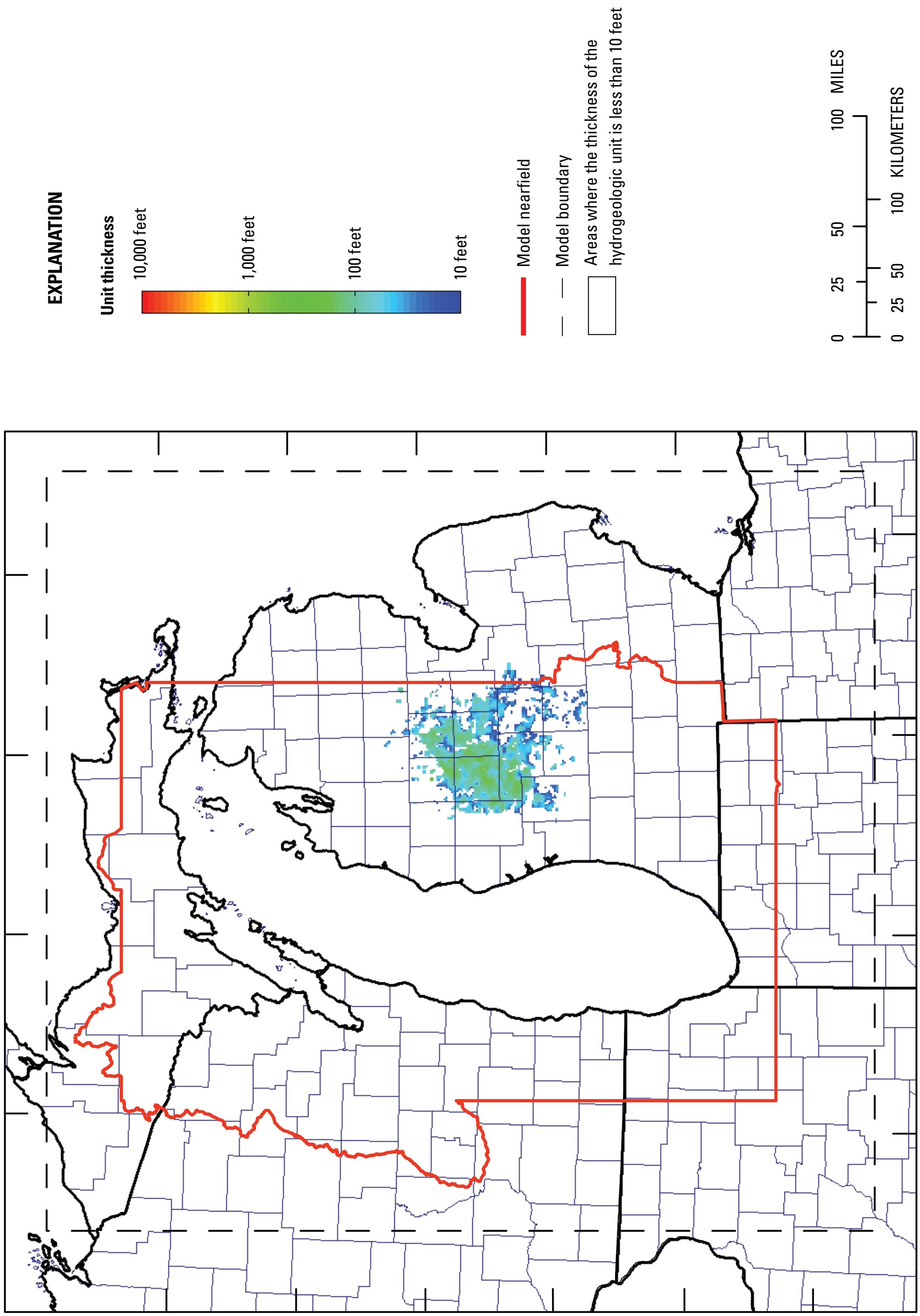

Base from U.S. Geological Survey digital data
1:100,000 1983. Universal Transverse Mercator projection
Zone 16, Standard Parallel 0° (Equator), Central Meridian 87° W,
North American Datum 1983

Figure 20*B*. Thickness of hydrogeologic units: Jurassic red beds (JURA = layer 4).

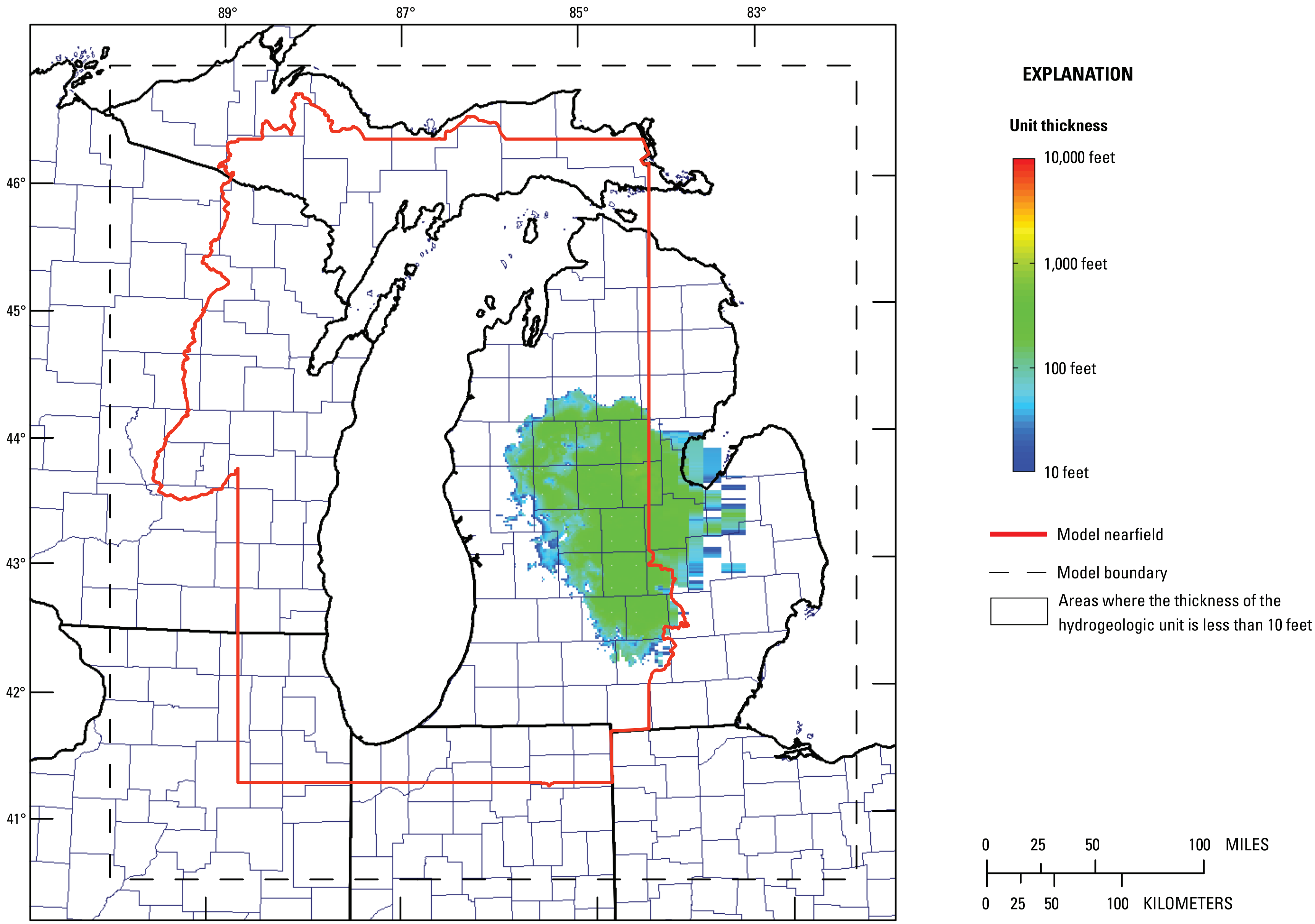

Base from U.S. Geological Survey digital data
1:100,000 1983. Universal Transverse Mercator projection
Zone 16, Standard Parallel 0° (Equator), Central Meridian 87° W,
North American Datum 1983

Figure 20*C*. Thickness of hydrogeologic units: Upper Pennsylvanian sandstone (PEN1 = layer 5).

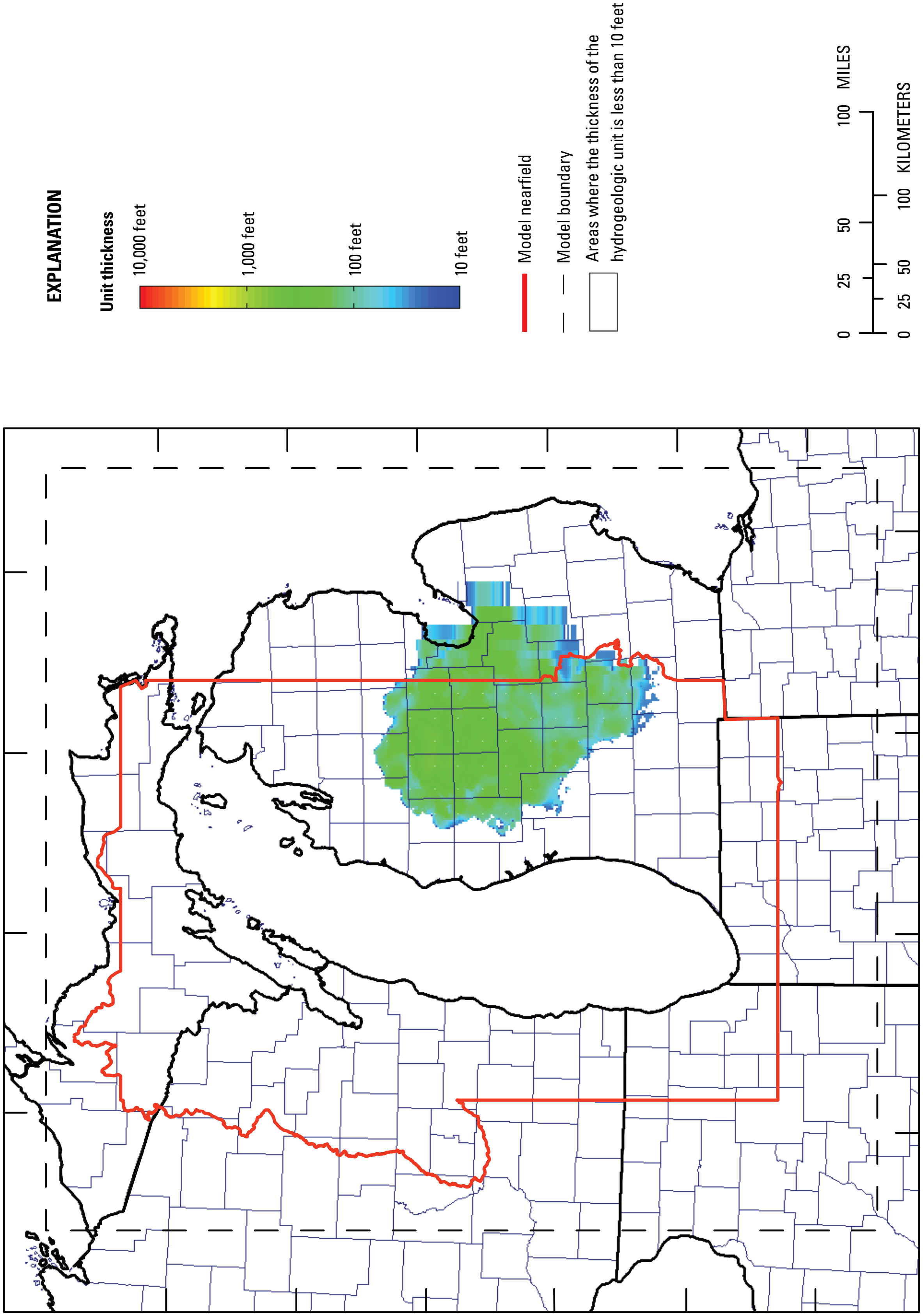

Base from U.S. Geological Survey digital data
1:100,000 1983. Universal Transverse Mercator projection
Zone 16, Standard Parallel 0° (Equator), Central Meridian 87° W,
North American Datum 1983

Figure 20*D*. Thickness of hydrogeologic units: Lower Pennsylvanian sandstone, limestones, and shales (PEN2 = layer 6).

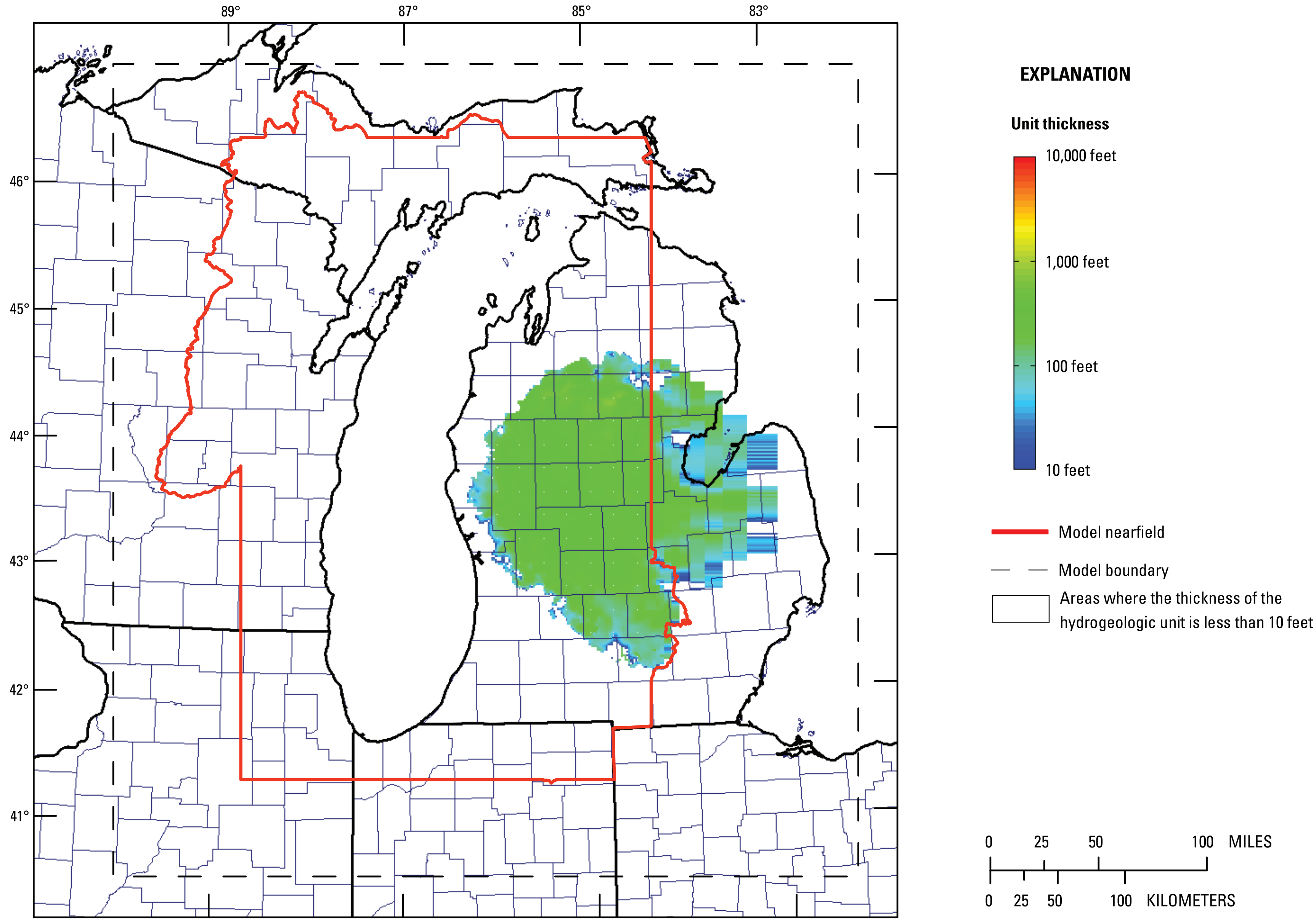

Base from U.S. Geological Survey digital data
1:100,000 1983. Universal Transverse Mercator projection
Zone 16, Standard Parallel 0° (Equator), Central Meridian 87° W,
North American Datum 1983

Figure 20*E*. Thickness of hydrogeologic units: Michigan Formation shale (MICH = layer 7).

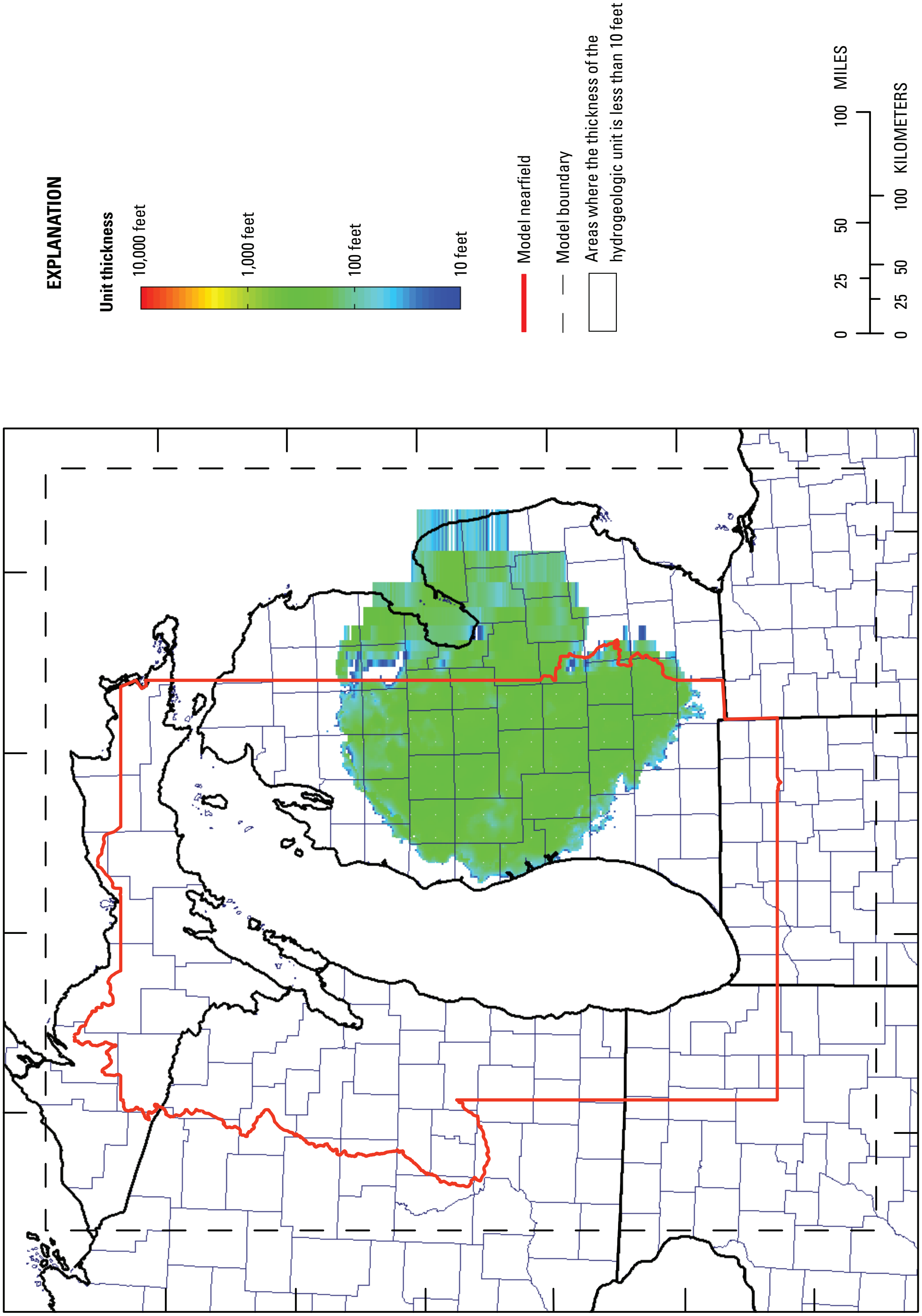

Base from U.S. Geological Survey digital data
1:100,000 1983. Universal Transverse Mercator projection
Zone 16, Standard Parallel 0° (Equator), Central Meridian 87° W,
North American Datum 1983

Figure 20*F*. Thickness of hydrogeologic units: Marshall Sandstone (MSHL = layer 8).

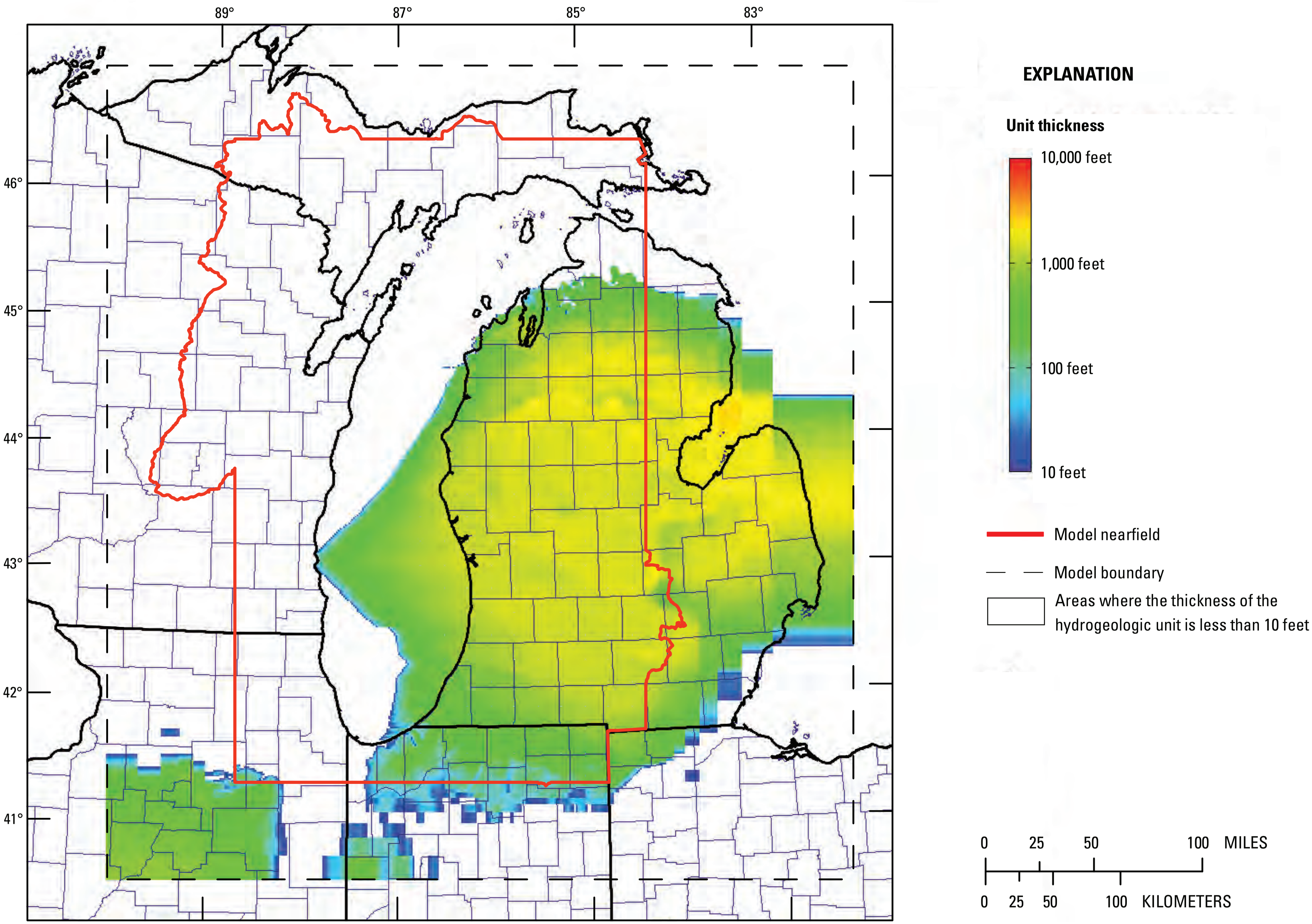

Base from U.S. Geological Survey digital data
1:100,000 1983. Universal Transverse Mercator projection
Zone 16, Standard Parallel 0° (Equator), Central Meridian 87° W,
North American Datum 1983

Figure 20*G*. Thickness of hydrogeologic units: Devonian-Mississippian shale (DVMS = layer 9).

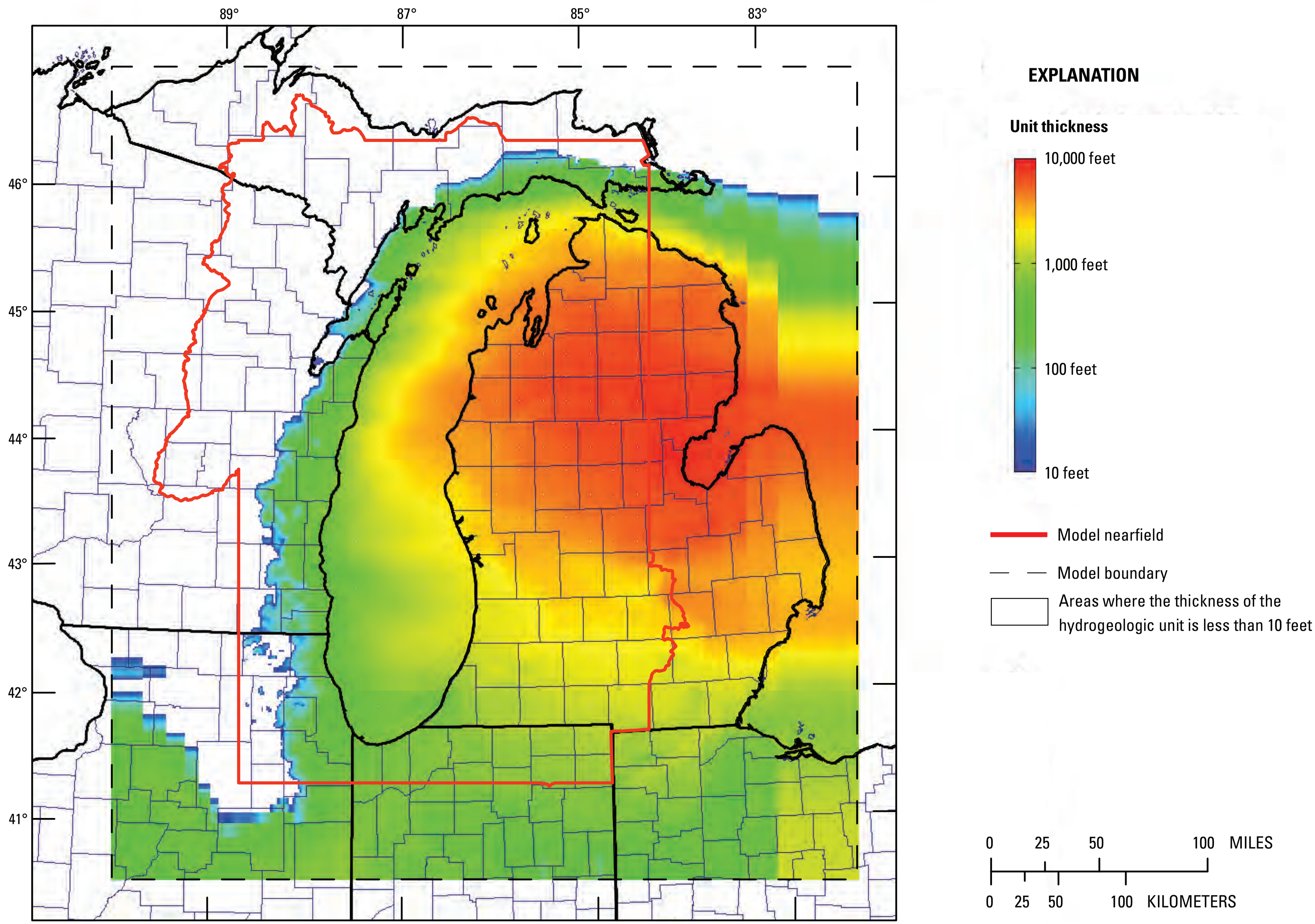

Base from U.S. Geological Survey digital data
1:100,000 1983. Universal Transverse Mercator projection
Zone 16, Standard Parallel 0° (Equator), Central Meridian 87° W,
North American Datum 1983

Figure 20*H*. Thickness of hydrogeologic units: Silurian-Devonian carbonate and evaporites (SLDV = layers 10–12).

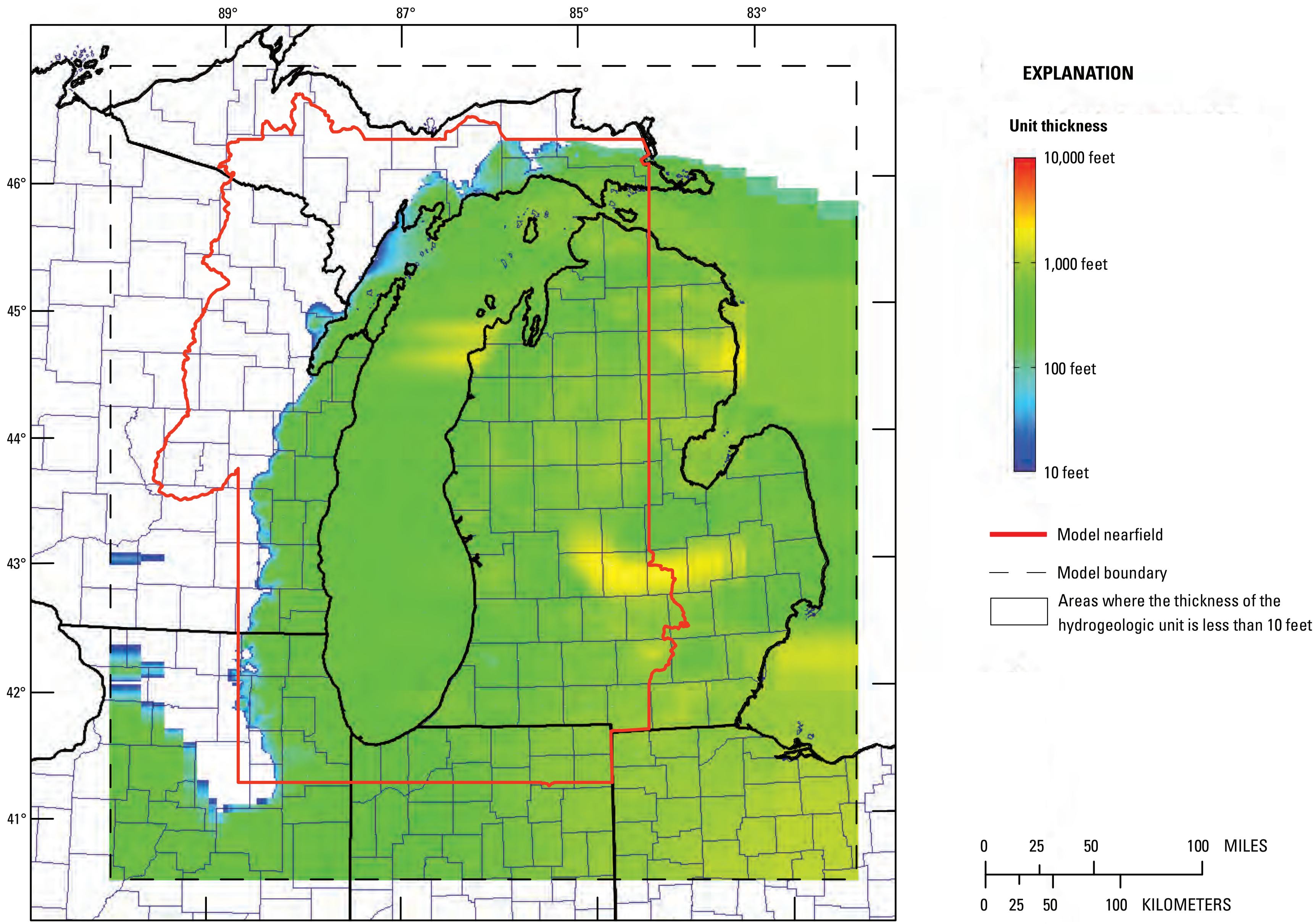

Base from U.S. Geological Survey digital data
1:100,000 1983. Universal Transverse Mercator projection
Zone 16, Standard Parallel 0° (Equator), Central Meridian 87° W,
North American Datum 1983

Figure 20*I*. Thickness of hydrogeologic units: Maquoketa shale (MAQU = layer 13).

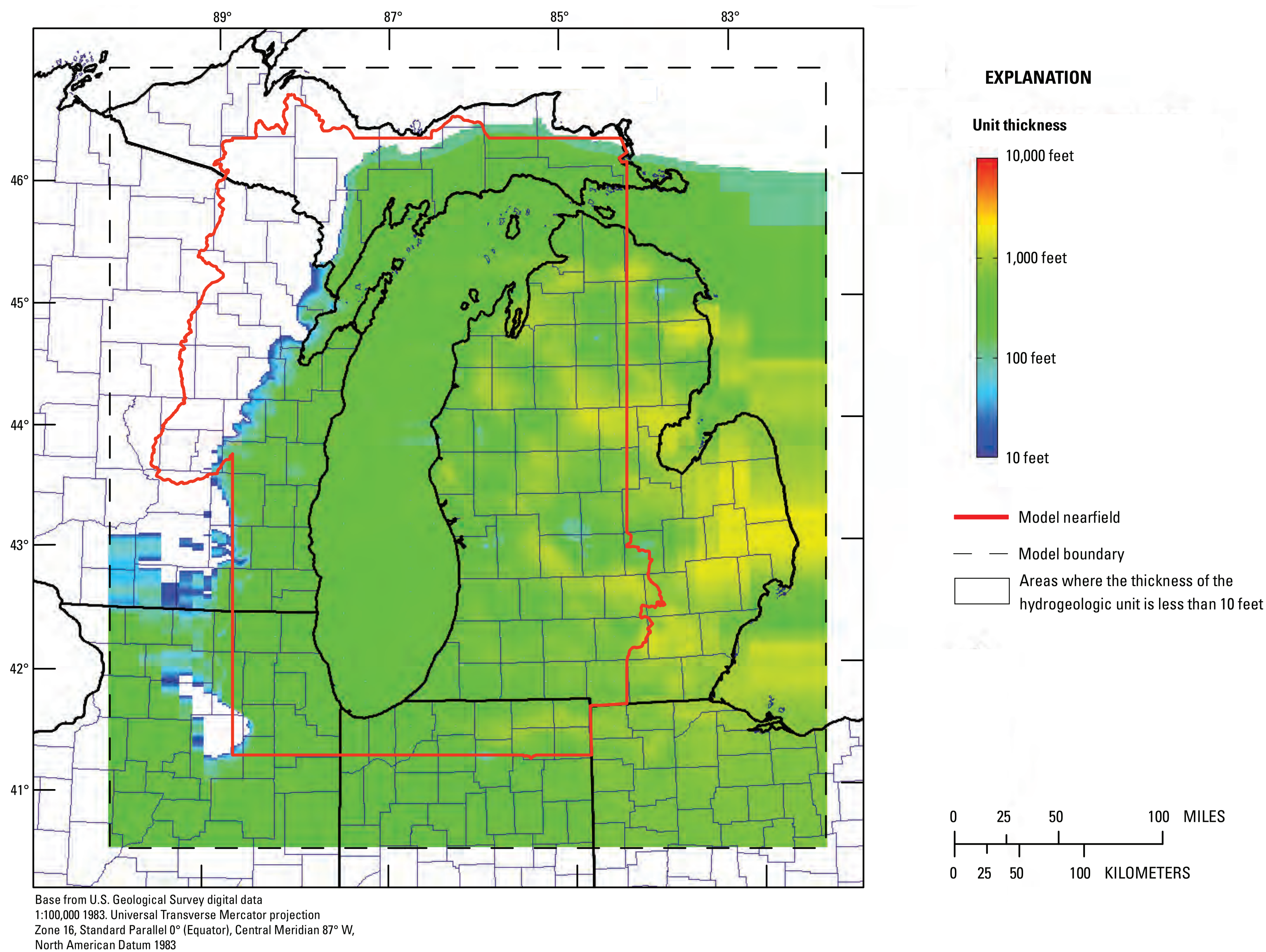

Figure 20*J*. Thickness of hydrogeologic units: Sinnipee dolomite (SNNP = layer 14).

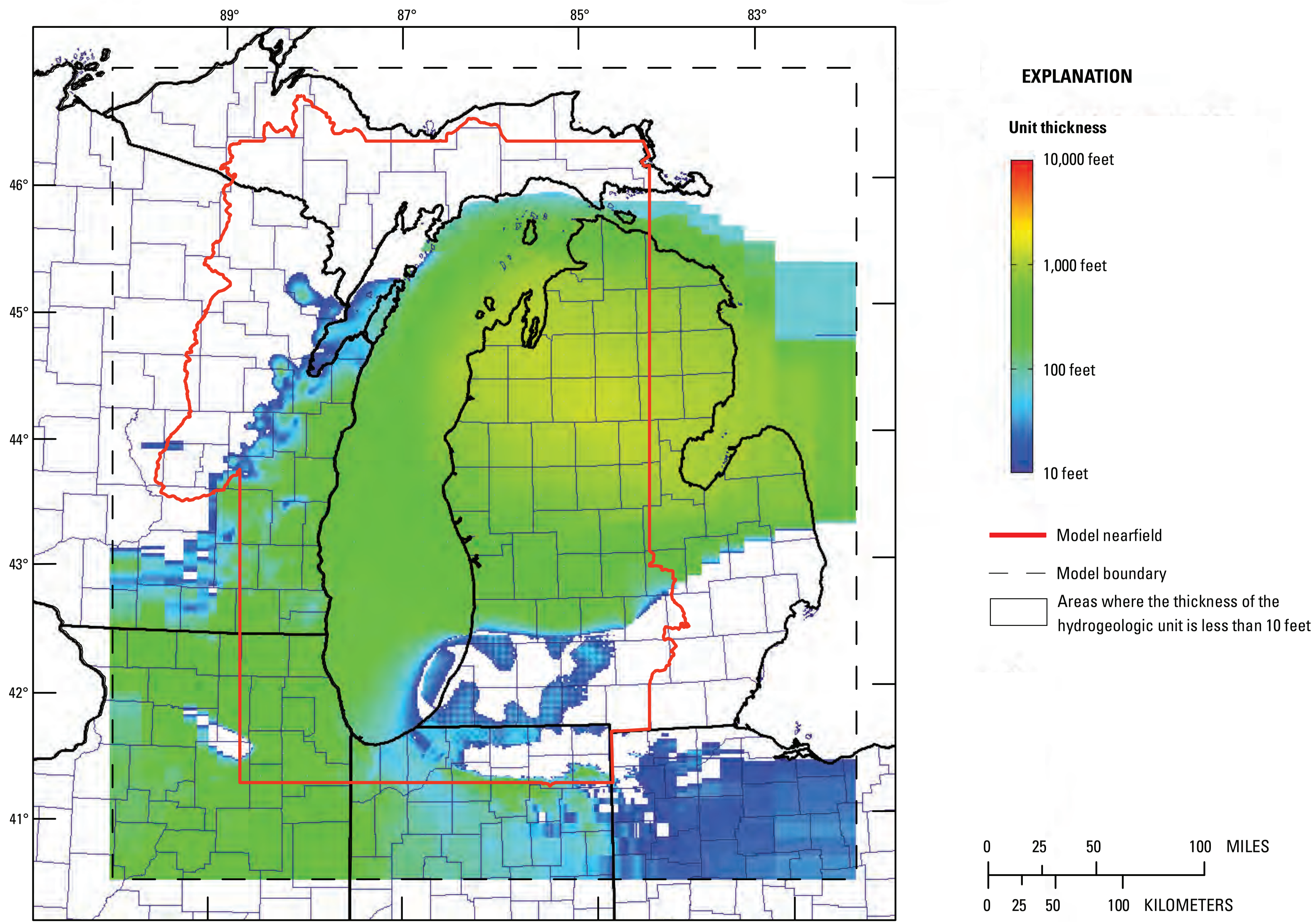

Base from U.S. Geological Survey digital data
1:100,000 1983. Universal Transverse Mercator projection
Zone 16, Standard Parallel 0° (Equator), Central Meridian 87° W,
North American Datum 1983

Figure 20*K*. Thickness of hydrogeologic units: St. Peter sandstone (STPT = layer 15).

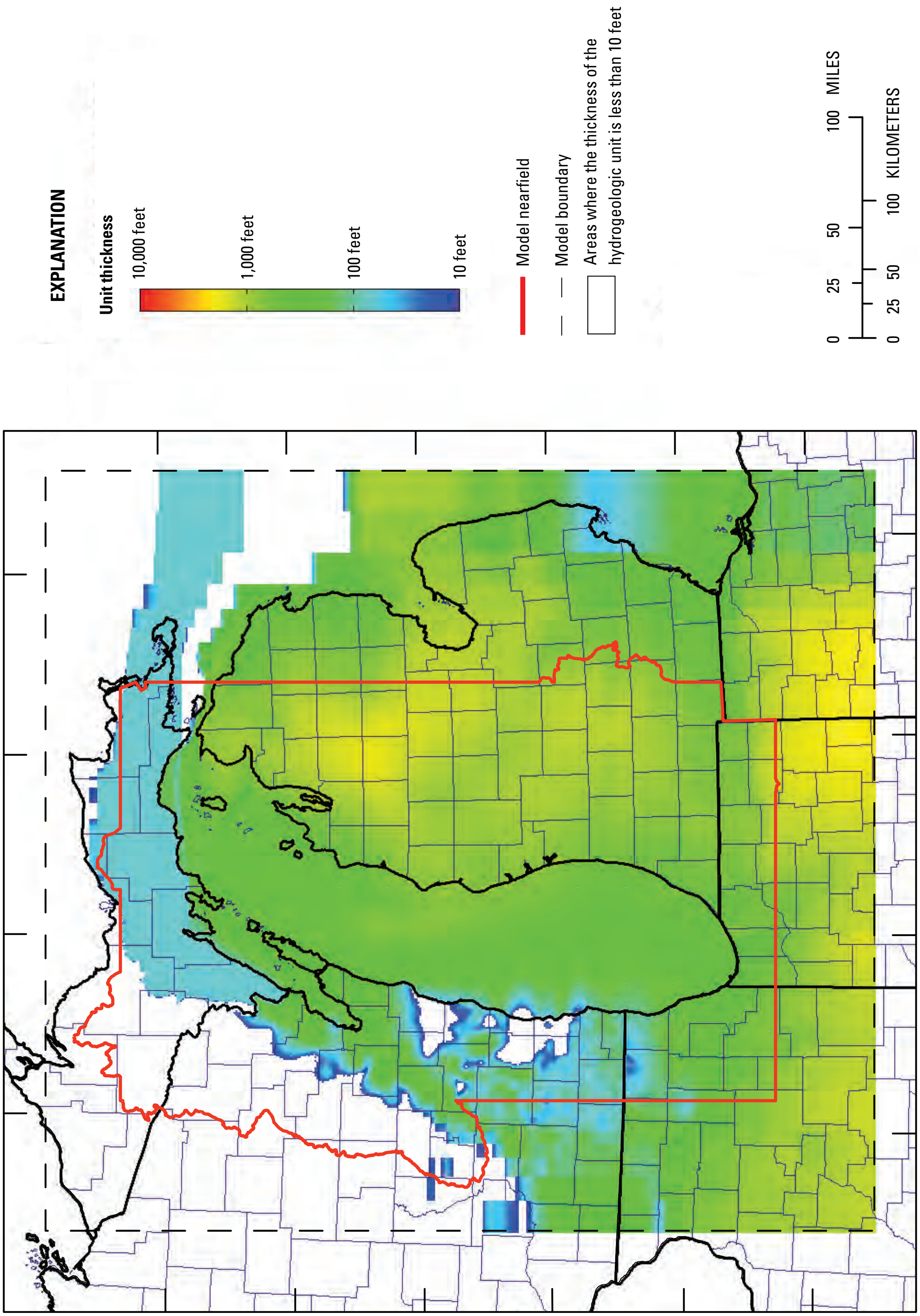

Base from U.S. Geological Survey digital data
1:100,000 1983. Universal Transverse Mercator projection
Zone 16, Standard Parallel 0° (Equator), Central Meridian 87° W,
North American Datum 1983

Figure 20*L*. Thickness of hydrogeologic units: Prairie du Chien dolomite and Franconia sandstone/shale (PCFR = layer 16).

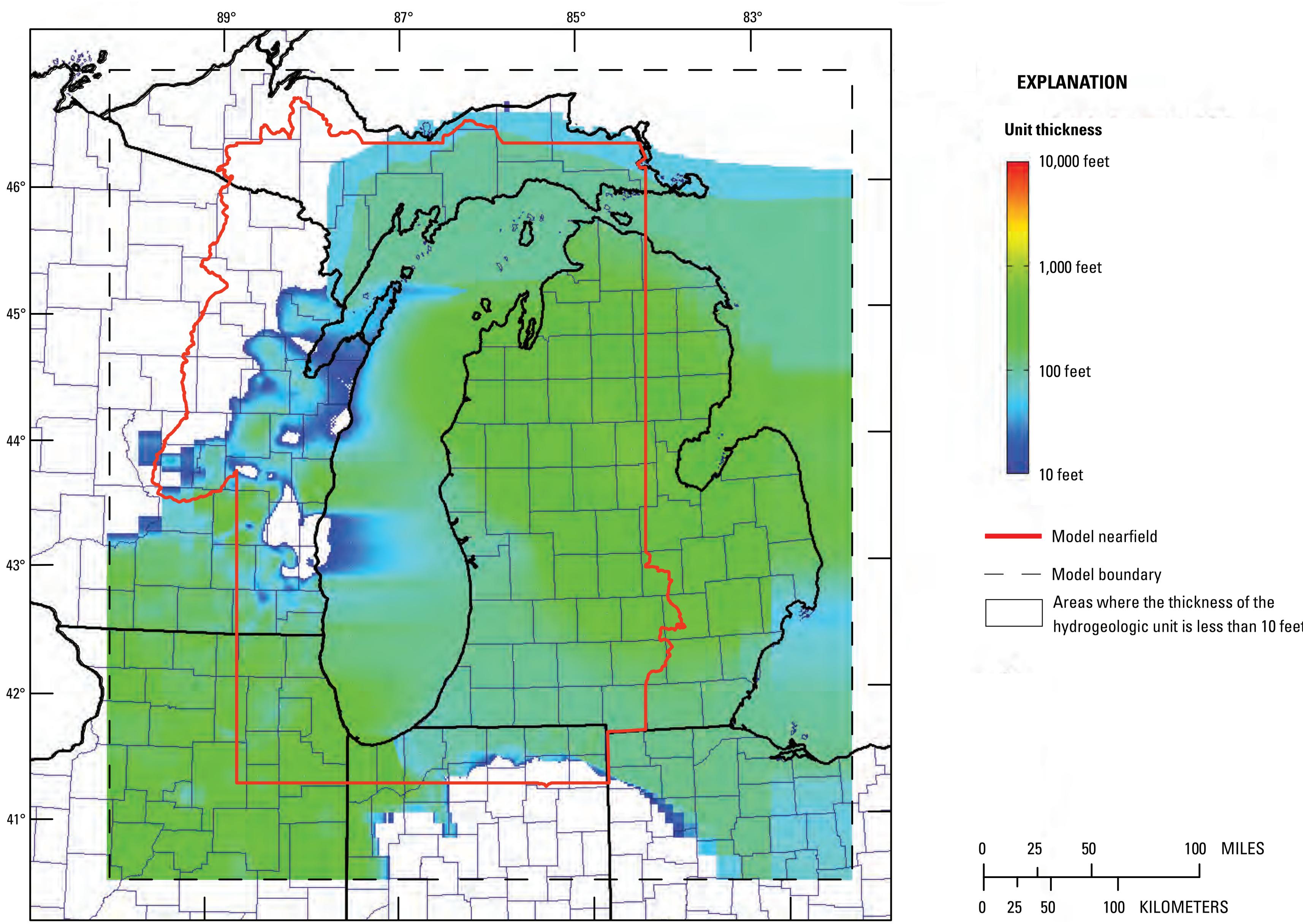

Base from U.S. Geological Survey digital data
1:100,000 1983. Universal Transverse Mercator projection
Zone 16, Standard Parallel 0° (Equator), Central Meridian 87° W,
North American Datum 1983

Figure 20*M*. Thickness of hydrogeologic units: Ironton-Galesville sandstone (IRGA = layer 17).

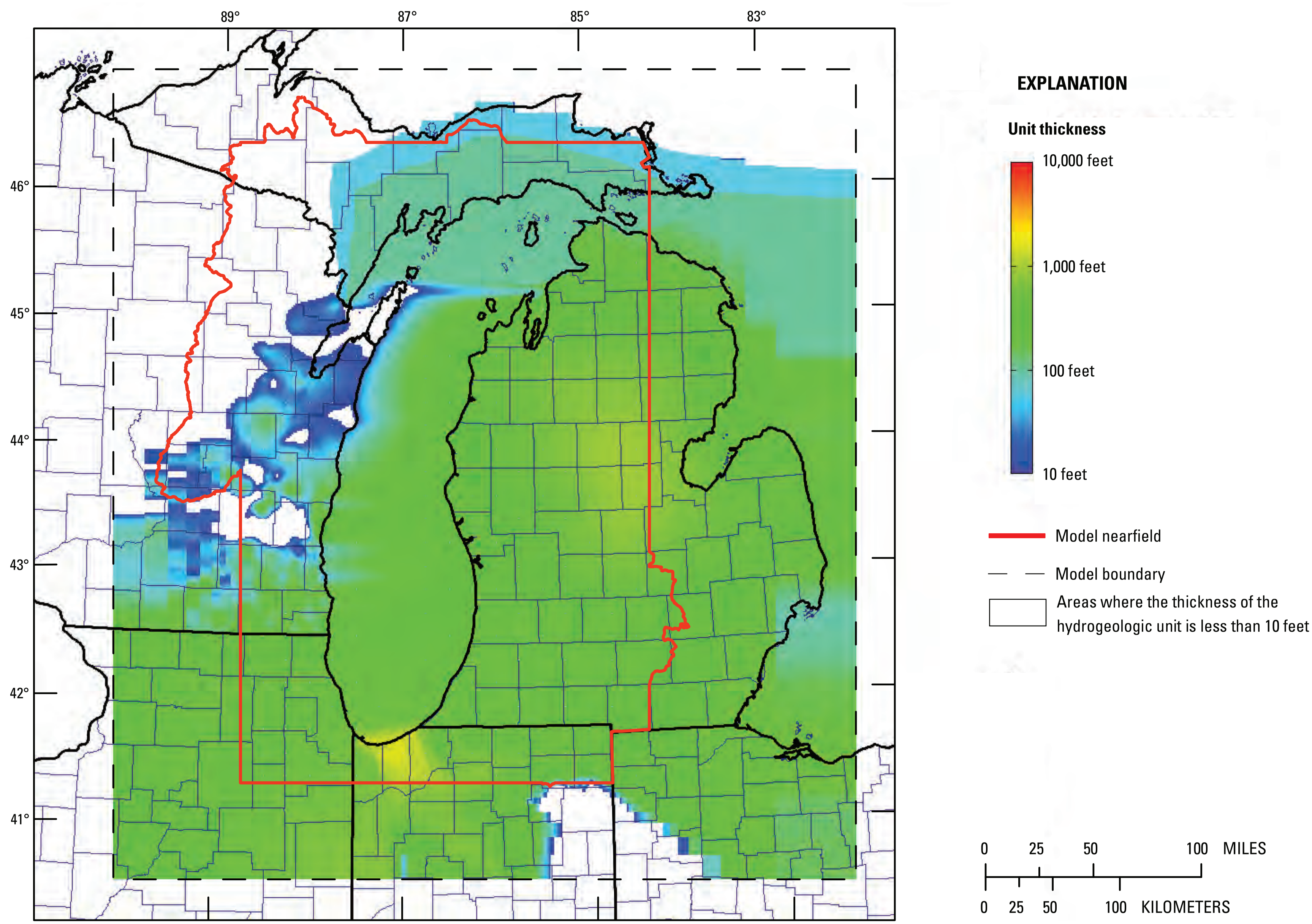

Base from U.S. Geological Survey digital data
1:100,000 1983. Universal Transverse Mercator projection
Zone 16, Standard Parallel 0° (Equator), Central Meridian 87° W,
North American Datum 1983

Figure 20*N*. Thickness of hydrogeologic units: Eau Claire sandstone/shale (EACL = layer 18).

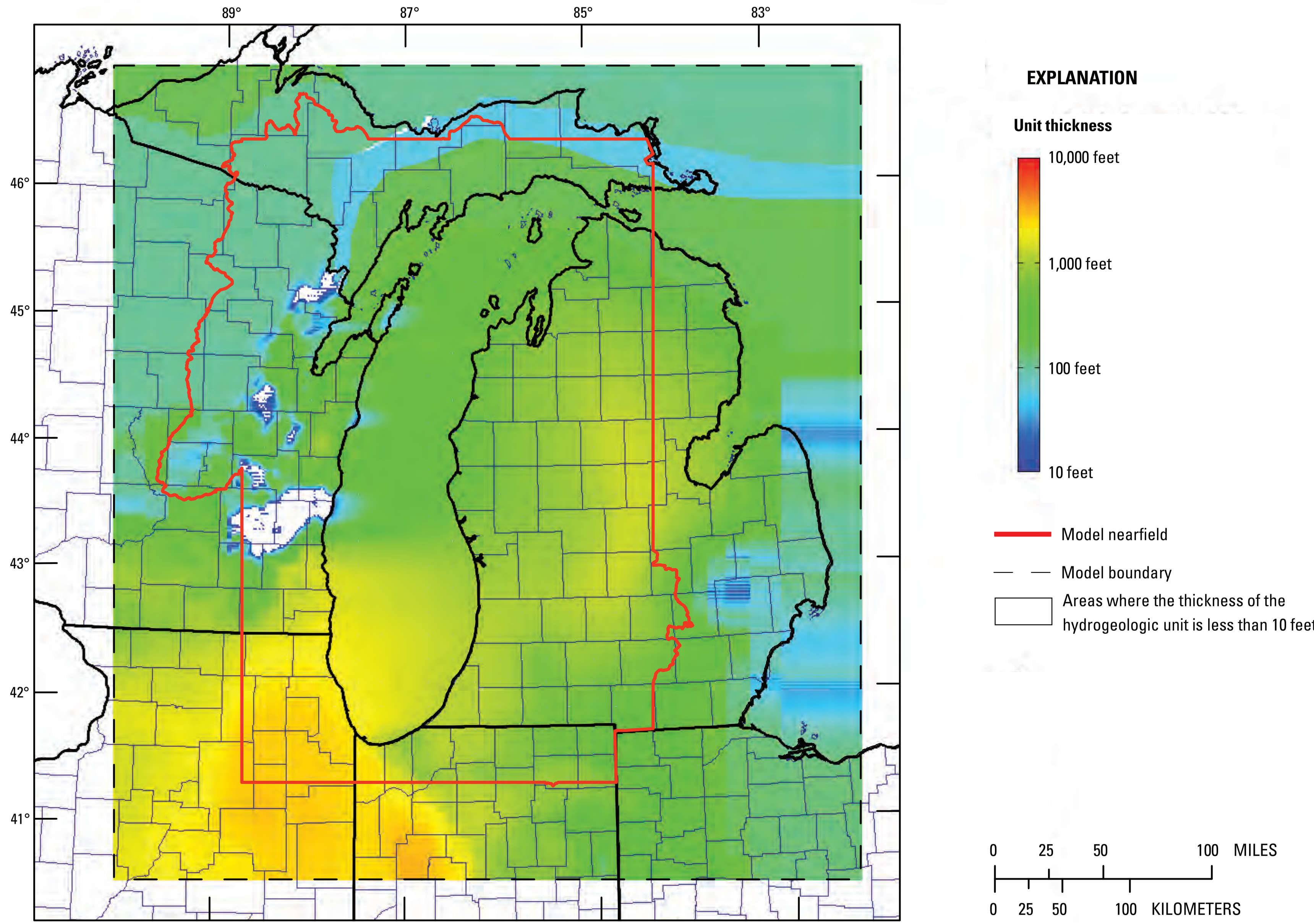

Base from U.S. Geological Survey digital data
1:100,000 1983. Universal Transverse Mercator projection
Zone 16, Standard Parallel 0° (Equator), Central Meridian 87° W,
North American Datum 1983

Figure 20*O*. Thickness of hydrogeologic units: Mount Simon sandstone (MTSM = layers 19, 20).

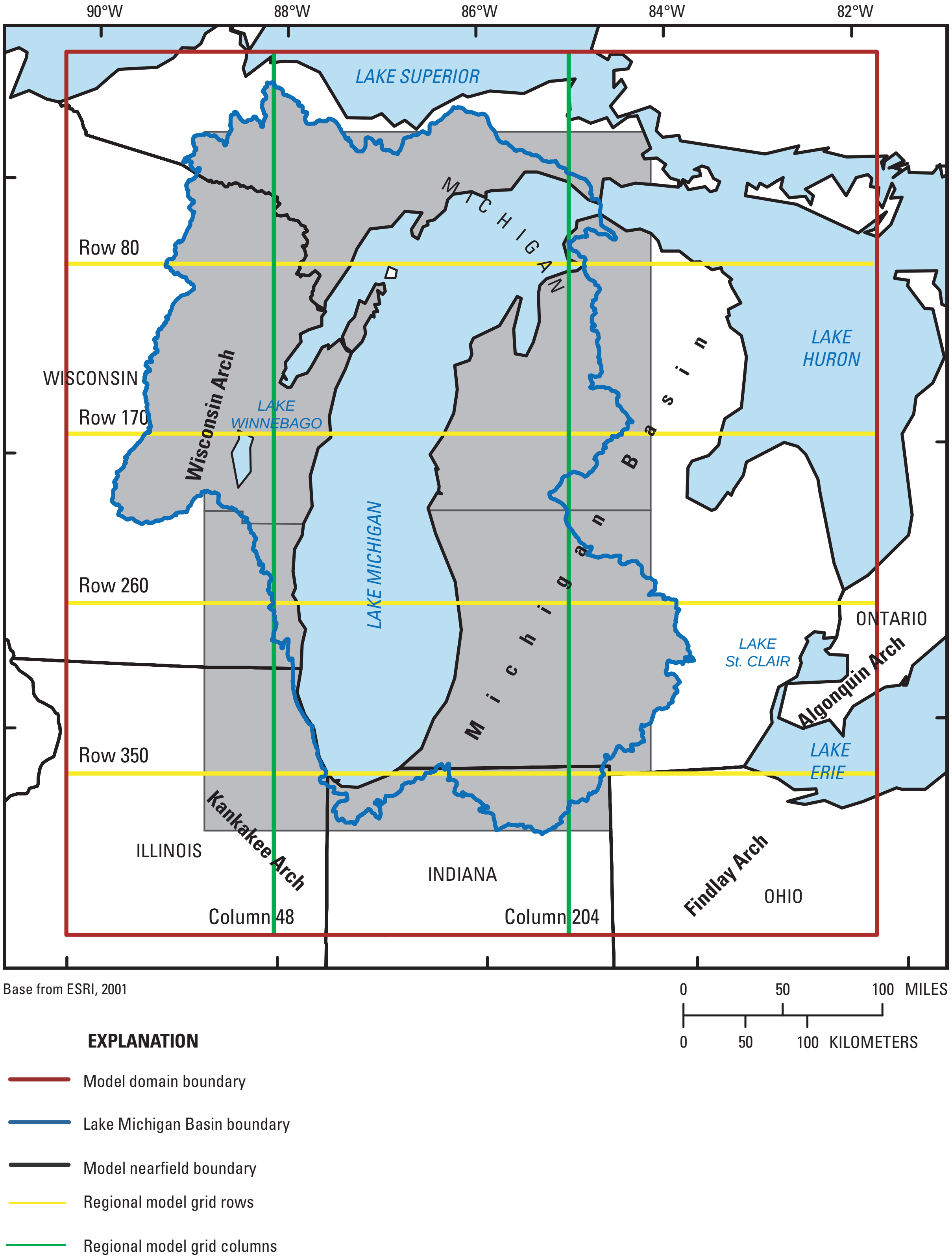

Figure 21. Traces for two north/south and four west/east hydrogeologic cross sections. (North south sections are along model columns. West east sections are along model rows.)

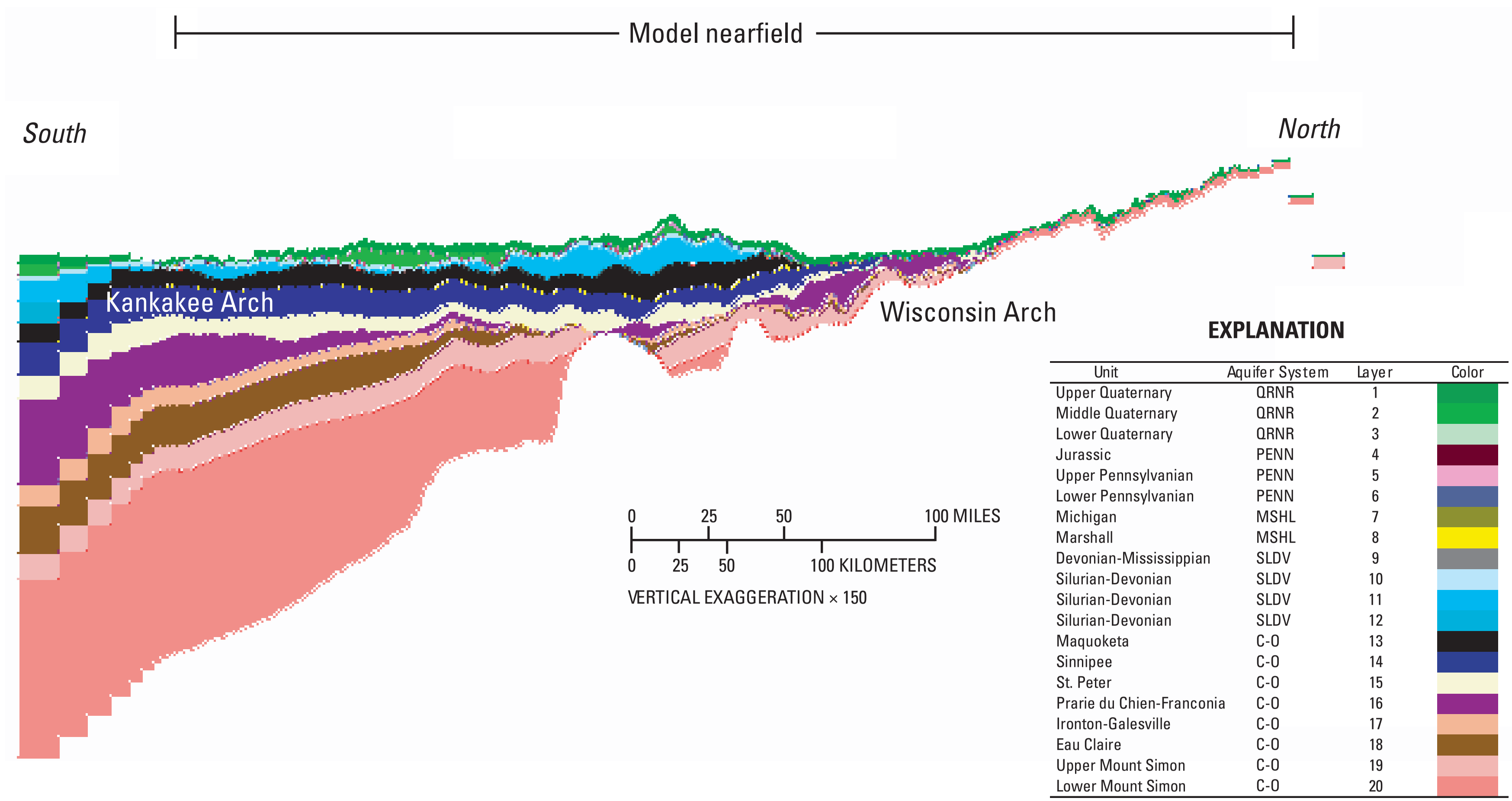

Figure 22*A*. Layering along model column 48.

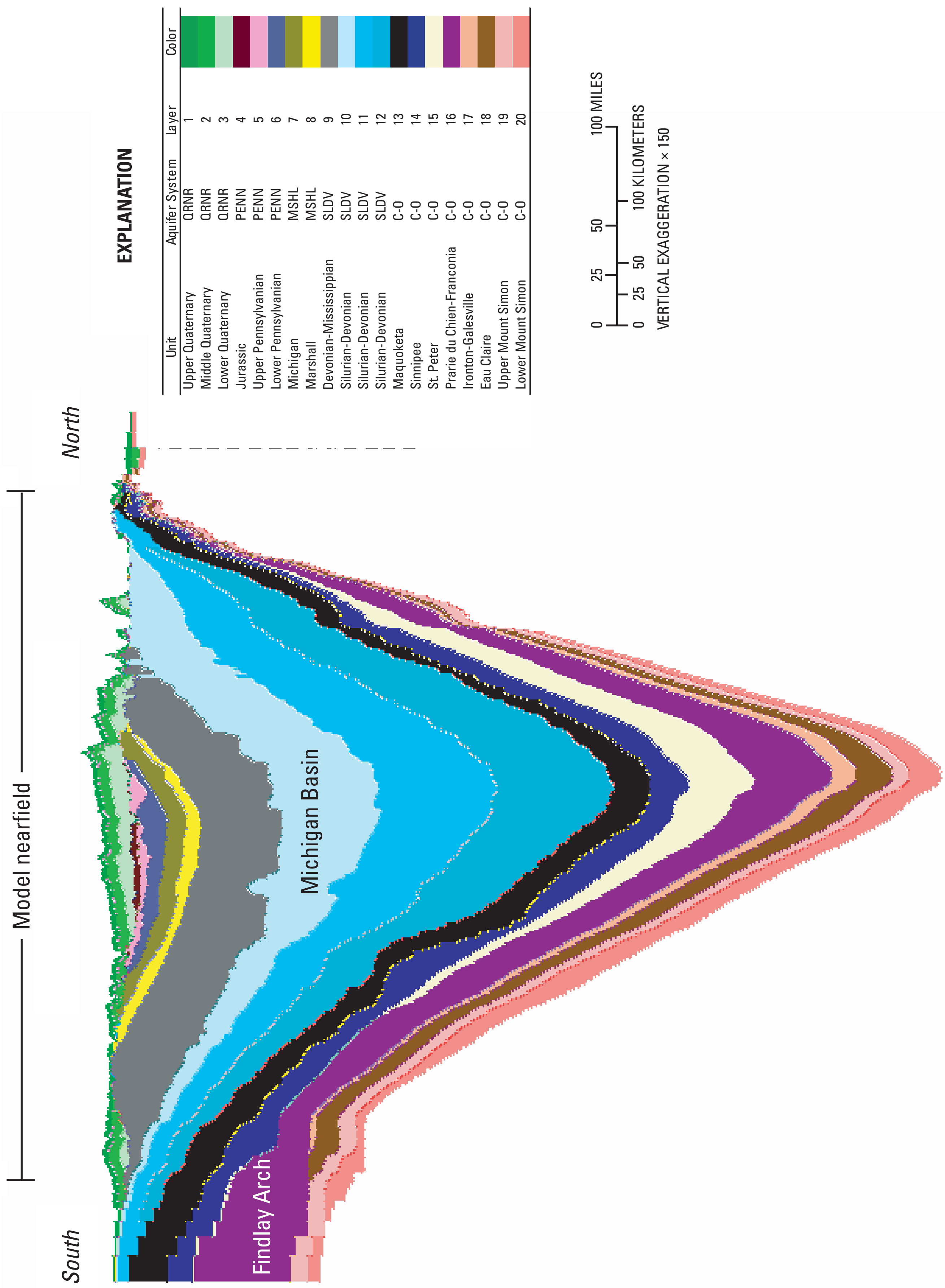

Figure 22B. Layering along model column 204.

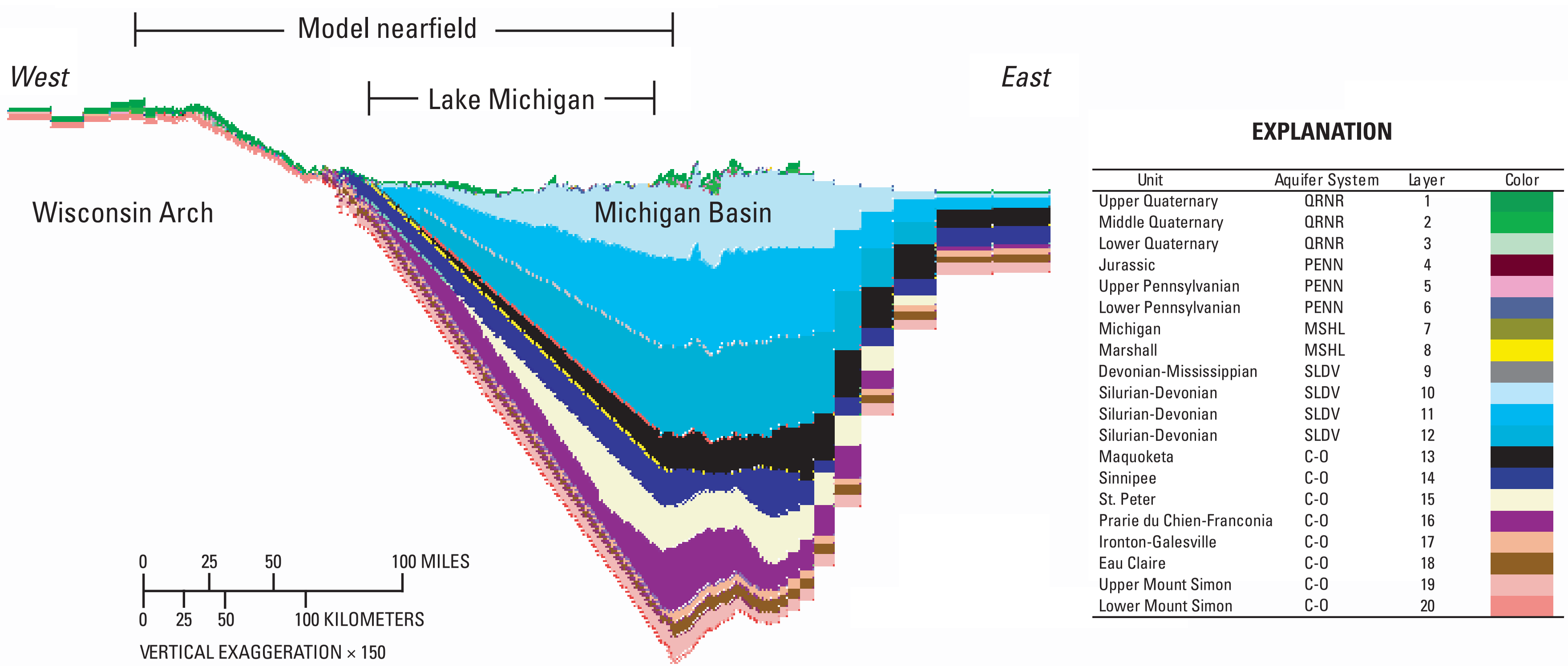

Unit	Aquifer System	Layer	Color
Upper Quaternary	QRNR	1	
Middle Quaternary	QRNR	2	
Lower Quaternary	QRNR	3	
Jurassic	PENN	4	
Upper Pennsylvanian	PENN	5	
Lower Pennsylvanian	PENN	6	
Michigan	MSHL	7	
Marshall	MSHL	8	
Devonian-Mississippian	SLDV	9	
Silurian-Devonian	SLDV	10	
Silurian-Devonian	SLDV	11	
Silurian-Devonian	SLDV	12	
Maquoketa	C-O	13	
Sinnipee	C-O	14	
St. Peter	C-O	15	
Prarie du Chien-Franconia	C-O	16	
Ironton-Galesville	C-O	17	
Eau Claire	C-O	18	
Upper Mount Simon	C-O	19	
Lower Mount Simon	C-O	20	

Figure 23*A*. Layering along model row 80.

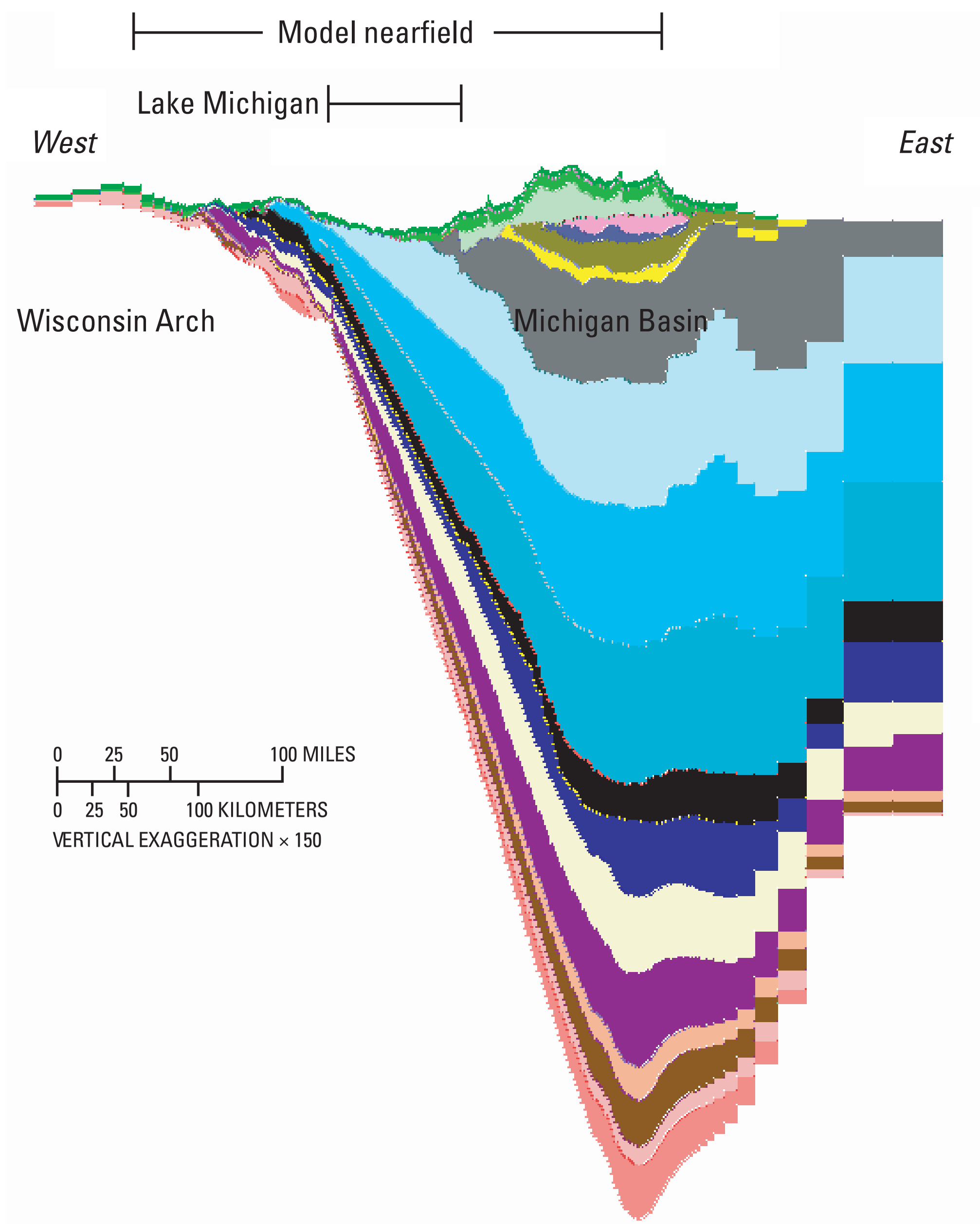

EXPLANATION

Unit	Aquifer System	Layer	Color
Upper Quaternary	QRNR	1	
Middle Quaternary	QRNR	2	
Lower Quaternary	QRNR	3	
Jurassic	PENN	4	
Upper Pennsylvanian	PENN	5	
Lower Pennsylvanian	PENN	6	
Michigan	MSHL	7	
Marshall	MSHL	8	
Devonian-Mississippian	SLDV	9	
Silurian-Devonian	SLDV	10	
Silurian-Devonian	SLDV	11	
Silurian-Devonian	SLDV	12	
Maquoketa	C-O	13	
Sinnipee	C-O	14	
St. Peter	C-O	15	
Prarie du Chien-Franconia	C-O	16	
Ironton-Galesville	C-O	17	
Eau Claire	C-O	18	
Upper Mount Simon	C-O	19	
Lower Mount Simon	C-O	20	

Figure 23*B*. Layering along model row 170.

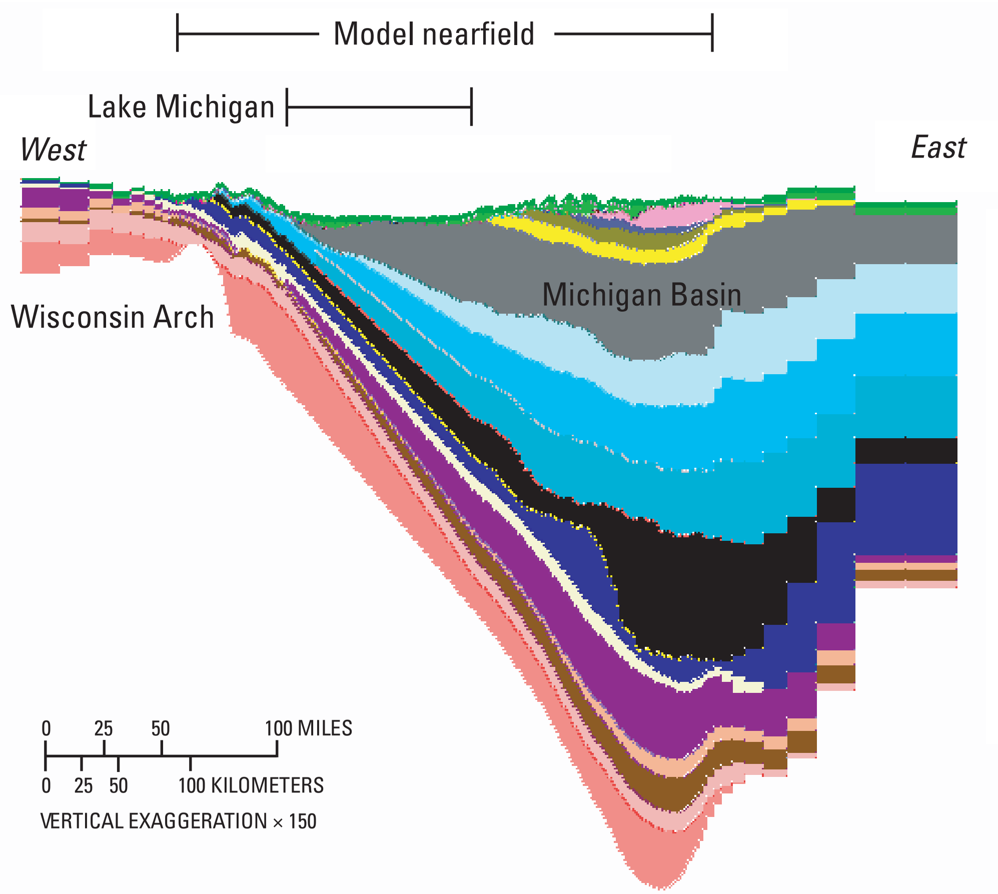

EXPLANATION

Unit	Aquifer System	Layer	Color
Upper Quaternary	QRNR	1	
Middle Quaternary	QRNR	2	
Lower Quaternary	QRNR	3	
Jurassic	PENN	4	
Upper Pennsylvanian	PENN	5	
Lower Pennsylvanian	PENN	6	
Michigan	MSHL	7	
Marshall	MSHL	8	
Devonian-Mississippian	SLDV	9	
Silurian-Devonian	SLDV	10	
Silurian-Devonian	SLDV	11	
Silurian-Devonian	SLDV	12	
Maquoketa	C-O	13	
Sinnipee	C-O	14	
St. Peter	C-O	15	
Prarie du Chien-Franconia	C-O	16	
Ironton-Galesville	C-O	17	
Eau Claire	C-O	18	
Upper Mount Simon	C-O	19	
Lower Mount Simon	C-O	20	

Figure 23*C*. Layering along model row 260.

EXPLANATION

Unit	Aquifer System	Layer	Color
Upper Quaternary	QRNR	1	
Middle Quaternary	QRNR	2	
Lower Quaternary	QRNR	3	
Jurassic	PENN	4	
Upper Pennsylvanian	PENN	5	
Lower Pennsylvanian	PENN	6	
Michigan	MSHL	7	
Marshall	MSHL	8	
Devonian-Mississippian	SLDV	9	
Silurian-Devonian	SLDV	10	
Silurian-Devonian	SLDV	11	
Silurian-Devonian	SLDV	12	
Maquoketa	C-O	13	
Sinnipee	C-O	14	
St. Peter	C-O	15	
Prarie du Chien-Franconia	C-O	16	
Ironton-Galesville	C-O	17	
Eau Claire	C-O	18	
Upper Mount Simon	C-O	19	
Lower Mount Simon	C-O	20	

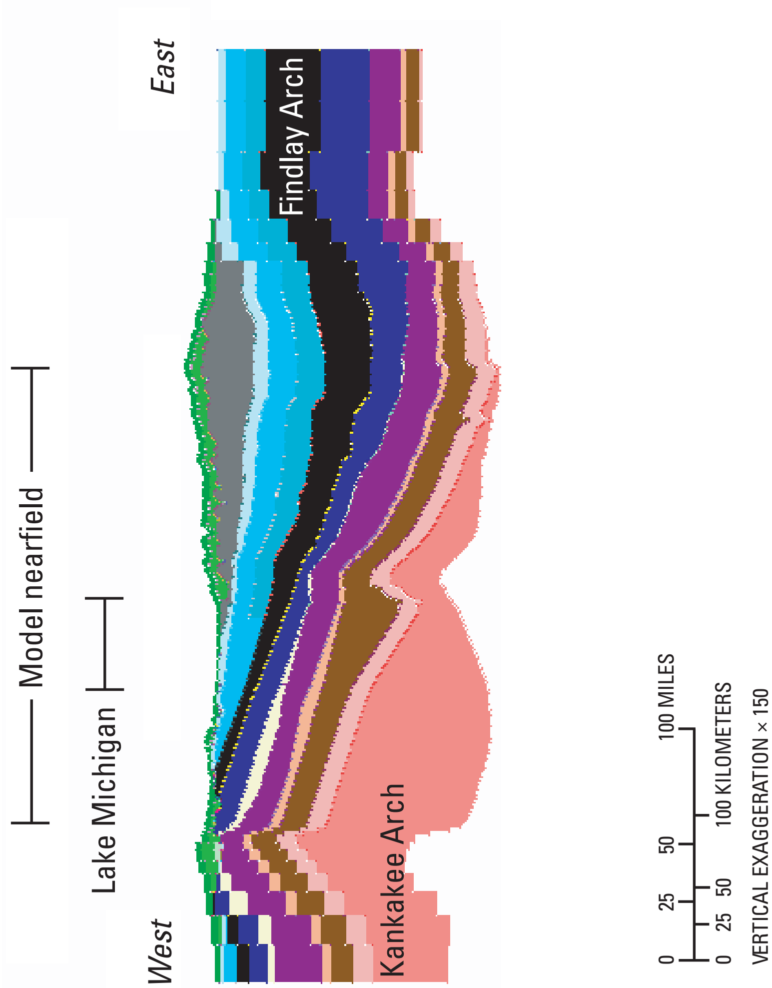

Figure 23*D*. Layering along model row 350.

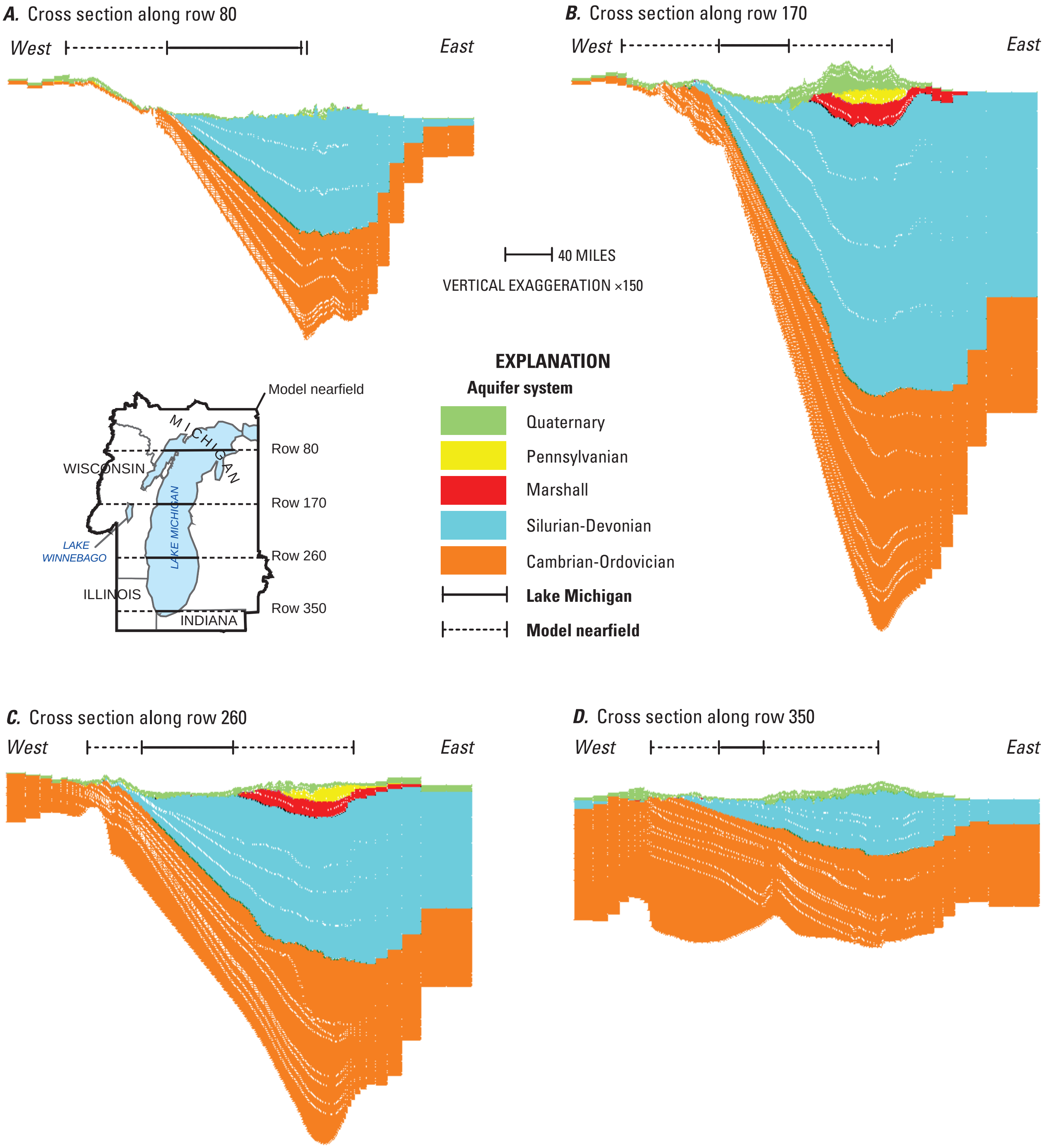

Figure 24. Aquifer systems along model rows.

Some model layers represent hydrogeologic units that, as a result of lateral facies changes, function as aquifers in some areas and confining units in other areas. The EACL is a confining unit in the central and southern parts of the model domain, but it functions more as an aquifer in the northern part. Several other units function as confining units only in the Michigan Basin:

- The shale part of the Saginaw Formation (layer 6), a discontinuous body within the PENN system.
- The Salina Group (layer 11) within the SLDV system.
- PCFR (layer 16) within the C-O system.
- Lower MTSM (layer 20) within the C-O system.

Overall, confining units represent a large proportion of the sedimentary bedrock east of Lake Michigan (fig. 25).

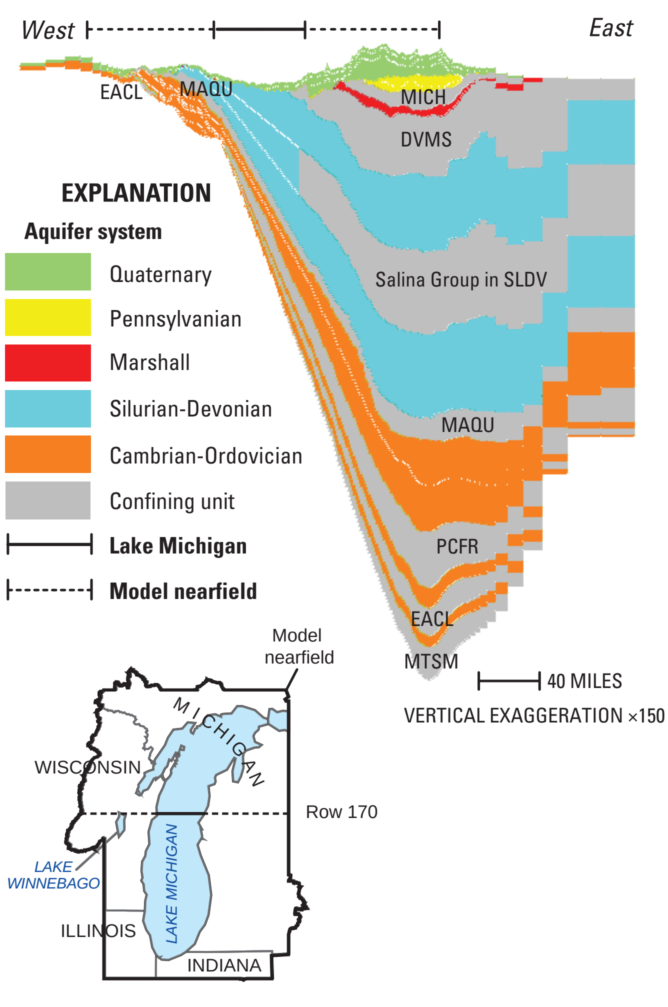

Figure 25. Major confining units along model row 170.

The relative thickness of an aquifer system is not always correlated with the amount of water that can be withdrawn from it or the rate of groundwater flow through it. Another major control on flow patterns and water use is the unconfined or confined condition of the aquifer system and, in the case where multiple aquifer systems are present, the degree of separation between relatively shallow unconfined and semiconfined layers and underlying (deeper) confined layers. The boundary between the shallow part of the flow system (consisting potentially of both unconsolidated and bedrock units) and the deep part of the flow system (consisting only of bedrock units) is defined vertically by the elevation of the uppermost unpinched bedrock confining unit (see discussion in section 3.2). The QRNR aquifer system is always shallow, but the other aquifer systems can be either shallow (unconfined or semiconfined) or deep (confined) depending on location. Where present in the nearfield model domain, 62 percent of the PENN aquifer system is shallow and 38 percent is deep; 19 percent of the MSHL system is shallow and 81 percent is deep; 44 percent of the SLDV system is shallow and 56 percent is deep; and 19 percent of the C-O system is shallow and 81 percent is deep. The PENN, MSHL, and SLDV systems tend to be much more heavily used for water supply where they are shallow; in contrast, the sedimentary sequence of the C-O system west of Lake Michigan is heavily pumped both where it is shallow and where it is deep.

4.3 Stress Periods

The time discretization of the model has two purposes:

1. To separate predevelopment conditions, which approximate the natural conditions before the advent of high-capacity pumping wells, from postdevelopment conditions, which have been influenced by variations in pumping and recharge.[8]
2. To simulate changes in recharge and pumping rates at a time scale sufficiently short to incorporate hydrologically important trends (for example, an increase in recharge across the Lake Michigan Basin or water-level recovery in response to shifting the source of an important center's public water supply from wells to surface water).

The first objective was met by constructing a combined steady-state/transient model, with the first stress period devoted to predevelopment conditions: its water-level output serves as the basis for calculating drawdown and recovery in subsequent transient stress periods. The second objective was met by assigning variable stress-period length as a function of the data available (for example, well records and climate and land-use records) and the rapidity of change. The first wells

[8] The terms "predevelopment" and "postdevelopment" distinguish the periods before and after high-capacity pumping started in 1864. However, because development and well discharge accelerated around the onset of World War II, the phrase "predevelopment (pre-1940)" is sometimes used, notably in the treatment of calibration targets, to include the time between 1864 and 1940.

in the Lake Michigan Basin area date to 1864 in the Chicago-Milwaukee area (Feinstein, Eaton, and others, 2005; Feinstein, Hart, and others, 2005). Water-use data over parts of the model domain are sparse until the latter half 20th century (for example, the Illinois water-use database is limited to total amounts from pumping centers before1964 and only afterwards incorporates discharge from individual wells, whereas the Michigan water-use database contains many gaps before the late 1970s). In the 1970s, climate changes linked to precipitation patterns across much of the eastern United States (Magnuson and others, 2003) gave rise to steplike increase in recharge rates, whereas the most important shift from groundwater to surface water occurred in the early 1980s, when the Chicago area began to supply itself from Lake Michigan. Relatively long stress periods (20 years or more) are used to represent the interval from 1864 to 1940, whereas shorter, 5-year periods represent the 1970s and 1980s, plus the last stress period from 2001 to 2005.

In all, there are 13 stress periods in the model, with the 12 transient stress periods extending over 141 years (table 5). Because the first stress period is steady state, the choice of initial head conditions in the model is arbitrary as long as it causes no part of the model (when in unconfined mode) to dewater and be rendered inactive. Setting the initial head for all layers at a row/column location to the average land-surface elevation over the row/column area fulfilled this requirement.

Table 5. Stress period setup for model.

Stress period	Duration	Time period
1	Steady state	Predevelopment: before Oct. 1864
2	36 years	Oct. 1864–Sept. 1900
3	20 years	Oct. 1900–Sept. 1920
4	20 years	Oct. 1920–Sept. 1940
5	10 years	Oct. 1940–Sept. 1950
6	10 years	Oct. 1950–Sept. 1960
7	10 years	Oct. 1960–Sept. 1970
8	5 years	Oct. 1970–Sept. 1975
9	5 years	Oct. 1975–Sept. 1980
10	5 years	Oct. 1980–Sept. 1985
11	5 years	Oct. 1985–Sept. 1990
12	10 years	Oct. 1990–Sept. 2000
13	5 years	Oct. 2000–Sept. 2005
Total	**141 years**	**Predevelopment–Sept. 2005**

The first model stress period consists of one steady-state time step. The subsequent transient stress periods are each divided into five time steps regardless of the stress-period length. All stresses (recharge, pumping, surface-water inputs) are automatically kept constant for the length of the stress period, but the evolution of the response to the continued and changed stresses between periods is influenced by the sequenced solutions for the period. Time-step lengths within each period are increased by a factor of 2 to better simulate changes heads and flows in response to changes in boundary conditions from one stress period to the next. Only the results from the final time step in each stress period are reported.

4.4 Farfield Boundary Conditions

The farfield of the model is composed mostly of cells belong to one of four boundary condition categories: no flow, constant head, general head, and specified non-zero flux.

4.4.1 No Flow

Boundaries at the north, east, south, and west sides of the model are no flow. Although this boundary condition does not reflect actual groundwater conditions at these locations, the effect of the boundary on simulated conditions in the model nearfield is small because (1) the model sides are distant from the model nearfield, (2) other farfield boundary conditions limit its influence, and (3) in some areas, important groundwater divides are present between the model nearfield and the no-flow boundary. The effect of the no-flow side boundaries is assessed in model-sensitivity simulations (see section 7).

No-flow boundaries also define the bottom of the model (at the interface with the Precambrian crystalline rock) and represent inactive areas within the model farfield where the Precambrian bedrock is shallow and the QRNR and bedrock systems are not present (fig. 26). The total area of the farfield inactive zones is 10,741 mi^2, comprising 5.9 percent of the full model domain. One large zone is in the northwest corner of the model in the Lake Superior Basin; another is in the northeast corner of the model in Ontario, Canada. Neither of these zones participates in the model solution.[9]

[9] The extent of inactive zones was determined by application of an unpublished U.S. Geologic Survey algorithm written by Arlen Harbaugh (called *MF2KCLST.EXE*, for MODFLOW-2000 Version 1.17.01, dated September 22, 2006) that identifies "islands" of cells in a MODFLOW model that are not in flow connection with the remainder of the domain because too many inactive or dry cells are distributed over one or more areas of the model. In the LMB model, connected clusters of cells in the northwest, northeast, and the far western parts of the model are cut off when Precambrian crystalline bedrock highs render inactive many row/column locations in a neighborhood, causing the entire cluster to become hydraulically isolated.

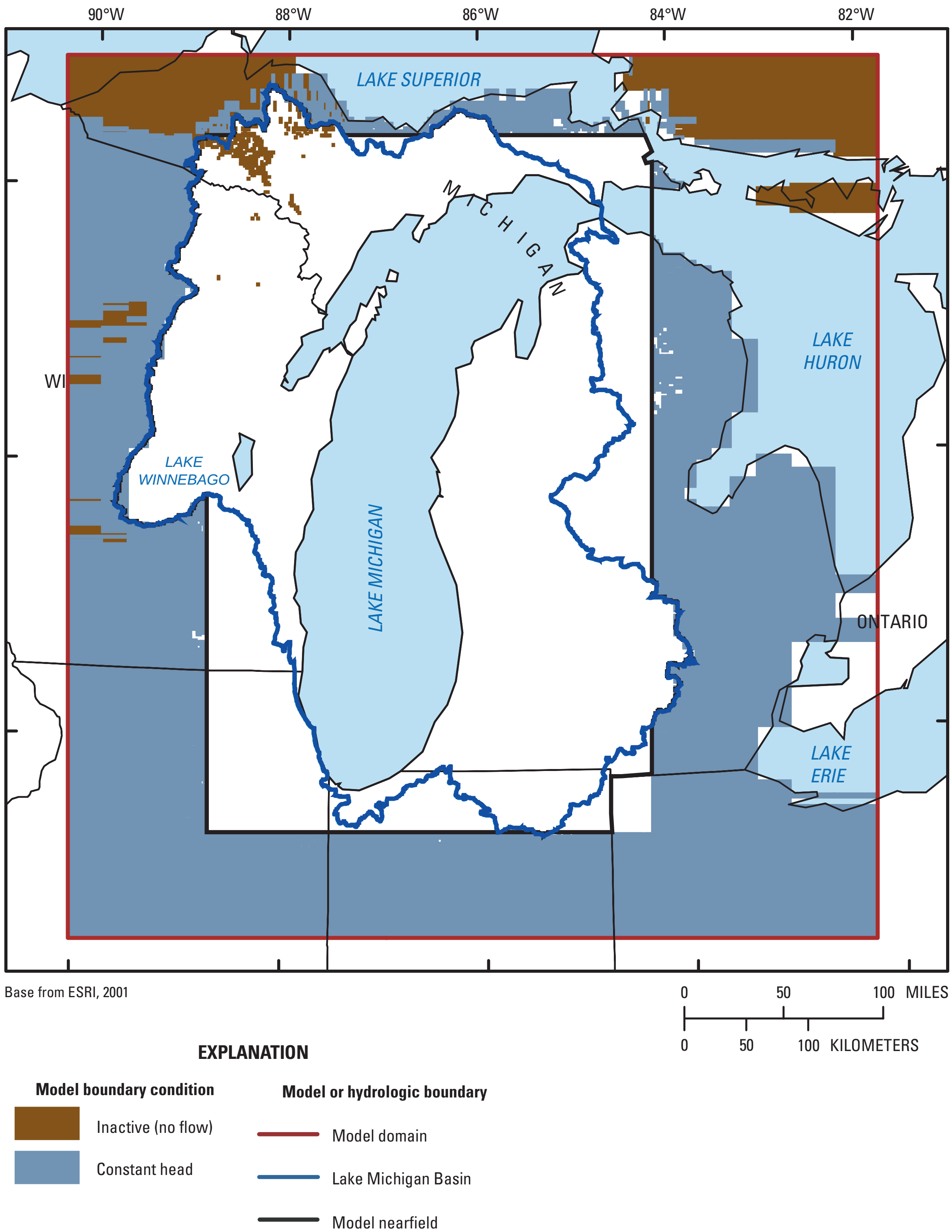

Figure 26. No-flow and constant-head boundary conditions. (The constant-head boundary conditions are applied only to the highest active cell at a row/column location. The inactive (no-flow) boundary conditions are applied to all layers at the row/column location.)

4.4.2 Constant Head

Constant-head (CHD) boundaries were used to specify water-table elevations throughout most of the model farfield (fig. 26). The condition is applied to the highest active cell at a row/column location, which is usually, but not always, model layer 1. The CHD boundaries ensure that regional gradients in the shallow flow system in the model farfield are reasonable and provide a means of computing recharge (through the exchange between constant head and underlying active cells) rather than furnish it as an input. One drawback of this approach is that it is impossible to adjust parameters in the shallow flow system in the model farfield to better match observations of head and flow. Given that the role of the farfield is strictly limited to providing reasonable flux into and out of the nearfield, this constraint is acceptable.

The constant head specified for the topmost active farfield cell corresponds to the average stage in the highest order stream crossing the cell area. If streams are absent, but other surface-water features are present, the constant head equals the elevation of the largest lake in the cell. Because the lateral dimensions of the farfield cells are large (greater than 1 mi on a side, sometimes much greater), the area enclosed by almost all inland farfield cells contain at least one stream or lake. Most (83 percent) of the 8,873 constant-head cells in the model are assigned to layer 1; the remainder correspond to average stage elevations below the bottom of layer 1 and areassigned to lower layers, with all overlying layers converted to inactive cells (that is, they do not participate in the model solution). Constant-head cells in the LMB model are used only in the model farfield and are held constant through all stress periods.

4.4.3 General-Head Conditions

A large part of the model farfield represents Lake Superior, Lake Huron, Lake St. Clair, or Lake Erie (fig. 27). These areas are represented in the LMB model by head-dependent boundaries with the General Head Boundary (GHB) package. Each lake is assigned a constant stage (feet above vertical datum):

- Lake Superior = 601.10
- Lake Huron = 577.50
- Lake St. Clair =572.33
- Lake Erie = 569.20

The stages for Lake Superior, Lake Huron, and Lake Erie correspond to the National Oceanographic and Atmospheric Administration Low-Water Datum, which is referenced to the International Great Lakes Datum (1985). No low-water datum is reported for Lake St. Clair, however; it is possible to estimate a stage from the historical record (1918–2007) by using the average stage difference between Lake Huron and Lake St. Clair and the average difference between Lake Huron and Lake Erie (U.S. Army Corps of Engineers, Detroit District, 2006).

The fixed farfield lake stages based on the low-water datum nearly equal the average Lake Superior, Lake Huron, and Lake Erie levels measured in 2005, a period of much lower than average stage across the Great Lakes. Section 7 of this report, a discussion of a model sensitivity simulation, describes the effect on model results of using time-dependent lake levels matched to the historical record in place of constant lake stages.

In addition to the stage, the GHB boundary condition for farfield lakes also requires a conductance term that controls the amount of flow entering or leaving the lake for a given hydraulic gradient within a lake cell, based on the specified lake stage and the simulated groundwater level in the same cell. For this application, the conductance term has been set to fairly high values for all the lakes.[10] (The conductance term is equal to the product of the assumed vertical hydraulic conductivity of the lakebed and the area of the cell assumed to transmit flow, divided by the assumed thickness of the lakebed; the resulting units are feet squared per day.) As a result, the GHB cells function in way similar way to constant-head boundary conditions. A comparison run substituting constant heads for GHB conditions produced negligible difference in any nearfield results. The use of a GHB boundary rather than a simpler CHD boundary is intended to keep the accounting of lake flows separate from other flows in the model water budget.

The GHB cells in the model farfield are assigned to layer 1 except in areas where they overlie bedrock, in which case the GHB cells are assigned to a lower layer and all overlying layers at the row/column location are rendered inactive.

4.4.4 Specified Flux

The northern half of the western edge of the model domain lies along the north-south course of the Wisconsin River (shown in fig. 7*B*) in the model farfield. Most of the northern farfield model edge intersects Lake Superior, and most of the eastern farfield model edge intersects Lake Huron, Lake St. Clair, or Lake Erie. For these sides of the model, the surface-water bodies serve as constant-head boundary conditions. In contrast, the southern side and the southern half of the western side of the farfield model domain do not coincide with surface-water features; instead, the groundwater levels are influenced by deep wells pumped in northeastern Illinois. Pumping has probably caused drawdown on the order of tens of feet in the confined C-O aquifer system in this area, as indicated by a regional model (Meyer and others, 2009) recently constructed by the Illinois State Water Survey (ISWS).

[10] For the farfield lakes, the K_v of the lakebed is assumed to be 1 ft/d, the entire cell surface area is assumed to transmit flow, and the lakebed thickness is assumed to be 1 ft. These values give rise to large conductance values not only because the surface areas of farfield cells are large but also because the assumed lakebed is everywhere set to a very small thickness.

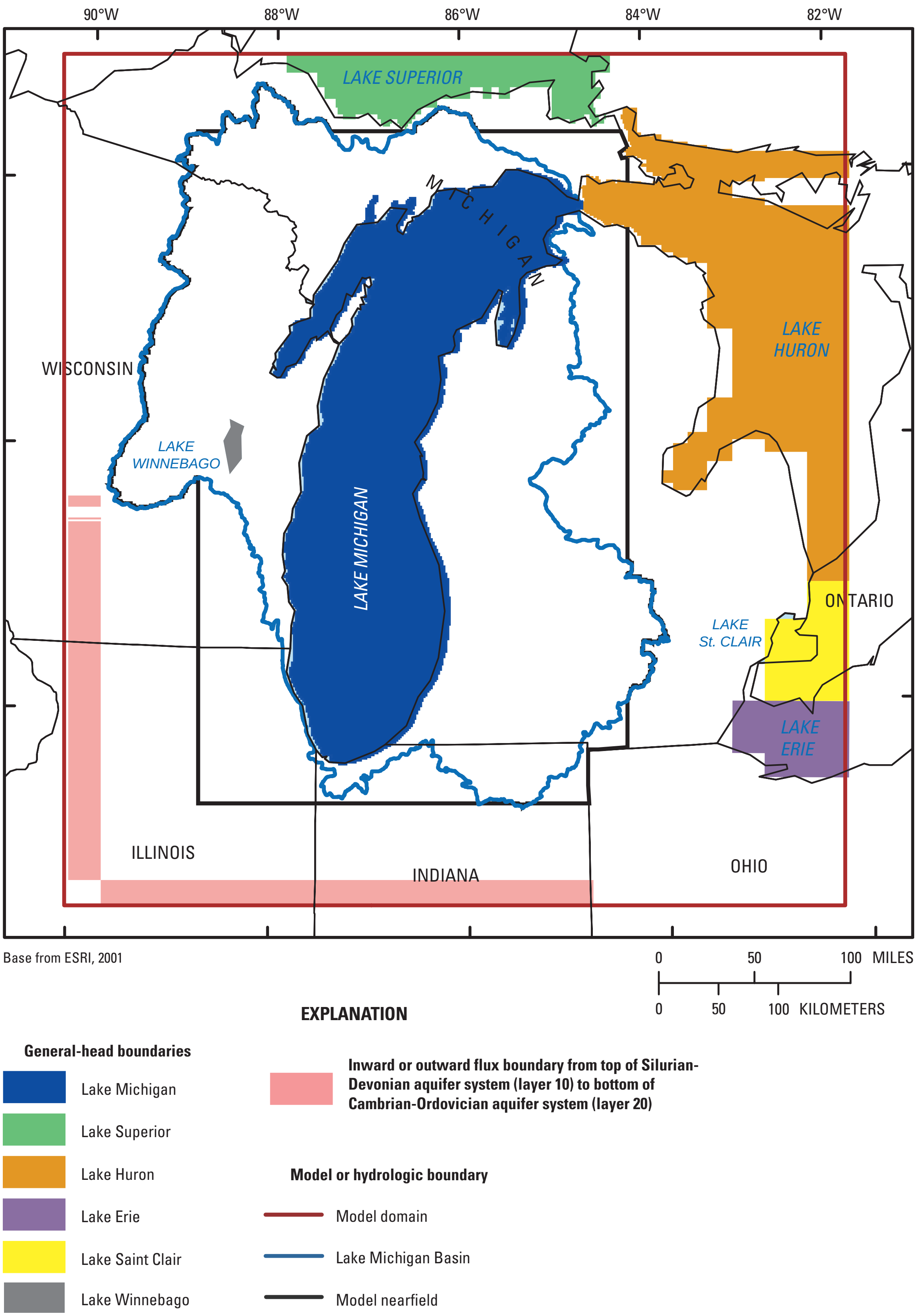

Figure 27. General-head and specified-flux boundary conditions. (The general-head boundary conditions apply to the highest active cell at a row/column location. The specified-flux boundary conditions apply to the bedrock cells in layers 10 to 20.)

Deep pumping is much more active west of Lake Michigan than east of the lake. (See discussion of groundwater withdrawals in this section.) Although shallow pumping centers tapping mostly unconfined aquifers produce restricted drawdown cones bounded by recharge (surface-water) boundaries, deep pumping centers tapping confined aquifers can produce drawdown cones affecting very large areas. Therefore, the possibility that a large drawdown cone associated with confined aquifers will violate the LMB model's edge boundary conditions is essentially limited to Wisconsin and Illinois. The drawdown cones from the major deep pumping centers around Green Bay and Milwaukee, Wis., do not extend beyond the LMB model nearfield (Conlon, 1998; Feinstein, Hart, and others, 2005; also the results from this modeling effort). Only the deep northeastern Illinois pumping center causes appreciable drawdown in the farfield and, therefore, only the farfield boundary conditions connected with this pumping center require special attention.

A constant-flux boundary was used to represent underflow to and from the southern side and the southern half of the western side of the model domain. Fortunately, the ISWS model uses the same pumping database for northeastern Illinois as the LMB model and similar model layers, so results of the ISWS model can be used to specify rates of underflow in the SLDV and C-O aquifer systems in the LMB model. Time periods used in the ISWS model are also similar to stress periods defined for the LMB model. Under predevelopment and early 20th century conditions, the flow simulated by the ISWS model across the LMB model boundary in Illinois, Indiana, and Wisconsin is at some locations inward with respect to the LMB model domain and at some locations outward. However, when increased withdrawals from northeastern Illinois are simulated, flow is almost entirely inward.

A constant-flux boundary was assigned in layers 10 through 20 by using the WEL package. One problem with using flux rates from the ISWS model is that uniform-density flow was assumed, rather than variable-density flow as in the LMB model. The effect of this constant-flux boundary on the LMB model was assessed through model sensitivity simulations (see section 7 of this report).

4.5 Nearfield Surface-Water Network

The nearfield surface-water network consists of

- streams of first order and higher,
- surface-water features designated as lakes or as wetlands, and
- Lake Michigan and Lake Winnebago (the large lake in northeastern Wisconsin; see fig. 1).

The streams, lakes, and wetlands constitute the inland surface-water network. They are represented as RIV cells, whereas GHB cells represent Lake Winnebago and Lake Michigan.

4.5.1 Inland Surface-Water Network

A surface-water database was compiled to represent streams and water bodies for the LMB model. The features of this database and how it is manipulated to generate inputs for both the farfield and nearfield of the model are described in appendix 2. In particular, the database serves to identify the location and quantify the stages and conductance terms used to represent streams and water bodies. The inland surface-water features are represented as RIV cells. The RIV boundaries representing streams are defined so that groundwater can discharge to a stream as base flow when the stream stage is below the simulated water table, and stream water can discharge to groundwater when the stage is above the simulated water table. The RIV boundaries representing lakes and wetlands are defined differently and can act only as discharge areas for groundwater whenever the ambient head is above the stage.[11] The treatment of water bodies as DRAIN boundaries was made to prevent one lake from simply routing water to an adjacent lake with a lower stage—an artifact of model construction that can distort the water budget for the model—whereas the ability of streams to lose water was maintained chiefly to allow surface water to act as a source of water to wells under stressed conditions.

The algorithm for assembling the stream input to the model associates a model cell with a stream only if at least part of the stream reach inside the cell (composed of one or more "stream arcs") is at least 8 ft wide; moreover, it associates a model cell with another water body only if the area of the lake or wetland inside the cell (defined as a "water-body polygon") is at least 20 acres (see appendix 2). In all, there are 63,398 cells that represent the water-table surface for the inland model nearfield (the remaining 25,289 nearfield cells correspond to Lake Michigan and Lake Winnebago). These width and area thresholds limit the percentage of inland nearfield cells with just streams to 27.5 percent, the percentage with just water bodies to 18.5 percent, and the percentage with both features to 11.1 percent. During model construction, this initial distribution left some areas of the nearfield with too great a distance between discharge points, leading to solutions with water-table elevations above the land surface. In these areas, the thresholds for including surface-water features were relaxed and minor surface-water features were added to the distribution, allowing the percentage of cells representing streams or stream and water bodies to increase to a total of 41.3 percent; the corresponding percentage representing just the water bodies increased to 19.0 percent.

[11] When the RIVBOT parameter for a cell in the RIV package input is identical to the STAGE, then the boundary condition in that cell acts the same as an entry in the DRN package and can only accept water. When RIVBOT is below the STAGE, then it can either accept or furnish water depending on the head elevation in the cell. In the LMB model, RIVBOT is set 1 ft below the stage for streams, but for water bodies it is equal to stage.

The distributions of the two types of surface-water features are shown in figures 28 *A* and *B*. As is pointed out elsewhere in this report, setting about 60 percent of the water-table cells to a RIV condition represents a compromise, one intended to insert a surface-water network into the model that is dense enough to prevent spurious water-table mounding with reasonable input parameters, but not so dense that the water-table solution is almost everywhere constrained by boundary conditions.

As in the case of the farfield GHB boundaries, the conductance assigned to any RIV cell is proportional to the assumed hydraulic conductivity of the bed material and the area across which exchange occurs and inversely proportional to the bed thickness. For all features, the bed thickness is assumed to be 1 ft, an arbitrary value. The area term depends on the type of feature. For cells intersecting at least one stream arc assigned at least 8 ft of width, the stream area is equal to the sum of the length of each arc multiplied by its width. The length is provided as a database attribute of the stream arcs, whereas the width is estimated as a function of the upstream distance from the stream arc to the streamhead (see appendix 2). For cells intersecting water bodies, the area assigned the conductance term is limited to a ring defined by the perimeter length of the water body inside the cell multiplied by a 20-ft width, assumed to represent the zone over which there is active exchange between the groundwater and the lake or wetland (see appendix 2).

The specified hydraulic conductivity of lakebeds (set everywhere to 2 ft/d) is assumed to be lower than for streambeds (set to 5 ft/d) but higher than for wetlands (set to 0.5 ft/d). The rationale for this ranking is that the bed materials of streams tend to be coarser than those of lakes, whereas wetlands tend to have the finest beds. The selected conductivity for streambeds is consistent with literature values (see, for example, Krohelski and others, 2000; Calver, 2001), but it is obvious that a single value for the three types of features cannot reproduce field behavior across the regional model nearfield. The extreme simplicity of the approach is mitigated in part by dividing the nearfield into zones based on categories of glacial material (see section 5.2) and adjusting the conductance in each zone during the calibration phase to better match field observations. However, it also must be recognized that the choice of the hydraulic conductivity of the bed exerts limited influence on the overall head and flux solutions (see last section in appendix 2).

The total conductance for any cell is the sum of the conductance terms calculated separately for each surface-water feature included in the model. For cells with both streams and water bodies, both feature types contribute to the total conductance. It is important to avoid assigning multiple RIV conditions to a single cell in a MODFLOW-2000/SEAWAT-2000 model so as to preclude spurious routing of water between them due to unequal stages.

If a water-table cell encloses only one surface-water feature, then the stage assigned the cell is the stage assigned the feature. Owing to the approximately 1-mi^2 size of the nearfield cells, however, it is very common for more than one surface-water feature to be enclosed. For this reason, it is necessary to derive a representative stage for the entire cell from some or all of the stages of the surface-water elements within it. For cells with only stream arcs or with both stream arcs and water-body polygons, the stage is calculated as the conductance-weighted average of individual stages assigned to the highest order streams in the cell (see appendix 2 for more detail). Because the streams of highest order are generally the biggest streams among the the cells, this method tends to associate the stage with the major stream rather than with its tributaries or adjacent water bodies. For water-table cells enclosing only water bodies, the stage is the conductance-weighted average of their stages.

The elevations of the stages assigned the RIV cells determine the layers to which they belong. If the stage of a particular inland surface-water feature falls below the bottom of layer 1 at a row/column location, then the boundary condition is assigned to the first layer whose bottom at that location is below the stage. In all, 89 percent of the RIV cells belong to layer 1; the rest are distributed mostly among bedrock layers in areas where streams cut through the unconsolidated material. Where the RIV cell is assigned below the top layer, then all overlying layers are inactive.

In the LMB model, the stages assigned the inland nearfield surface-water features are fixed through time. Stream stages, in fact, do change in time, but it is assumed that the water-table solution at the regional scale is not sensitive to this variation. The effect of many other assumptions and simplifications adopted in building the surface-water network are discussed at the end of appendix 2.

To depict more detail in the distribution of streams and water bodies included in the model, we mapped the entire surface-water network in one part of western Michigan (fig. 29*A*) and superimposed on top of it colored squares representing individual RIV cells, with a code that distinguishes the type of feature and the order of streams enclosed (fig. 29*B*). This sample area shows the density of the routed surface-water network and the relative frequency of streams, lakes/ponds, and wetlands (swamp/marshes). It demonstrates that all large features—for example, high-order streams—are included, and it indicates the extent to which small features—for example, first-order streams—are included or excluded. It also shows that cells typically contain more than one stream or water body.

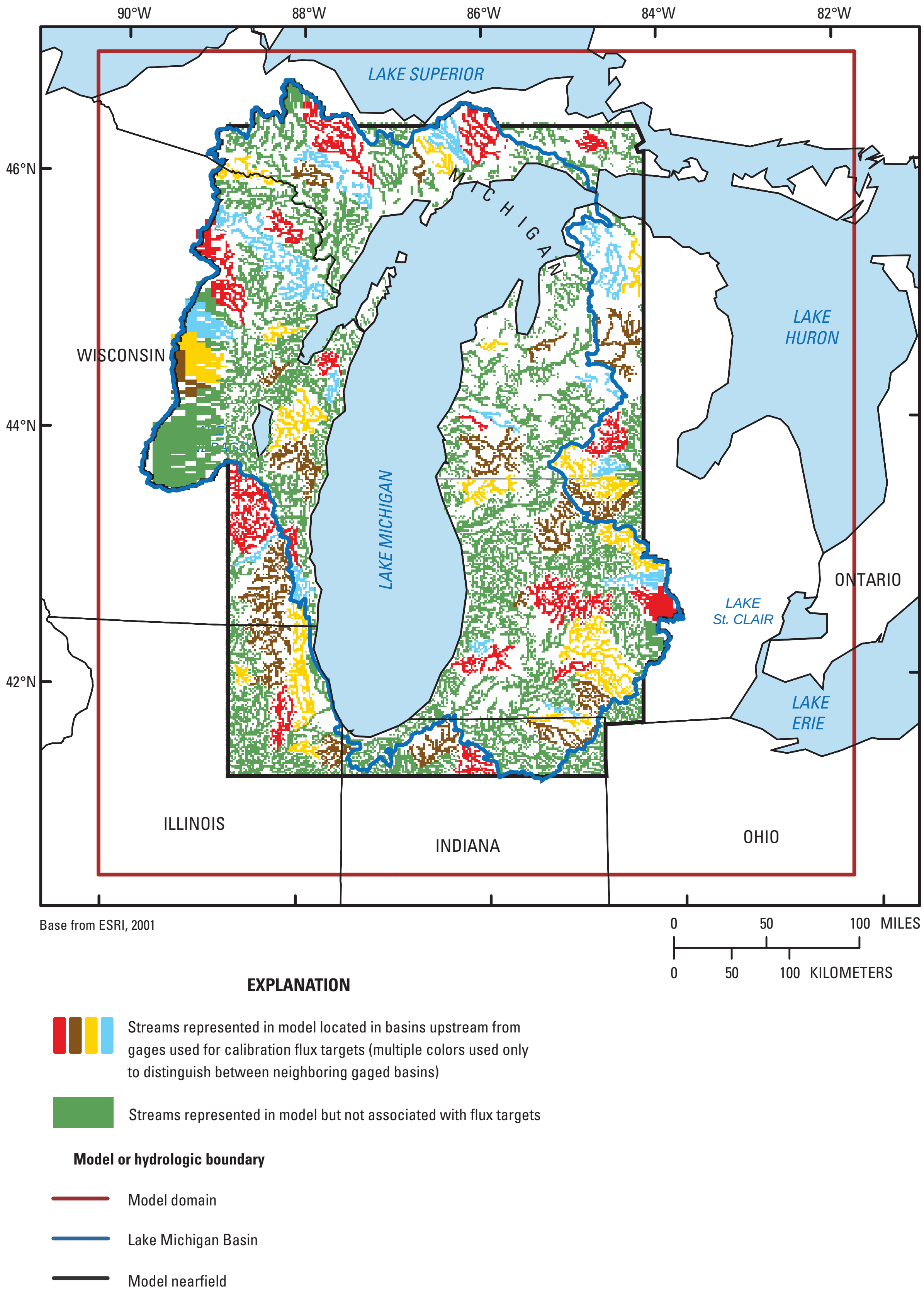

Figure 28*A*. Streams represented in model.

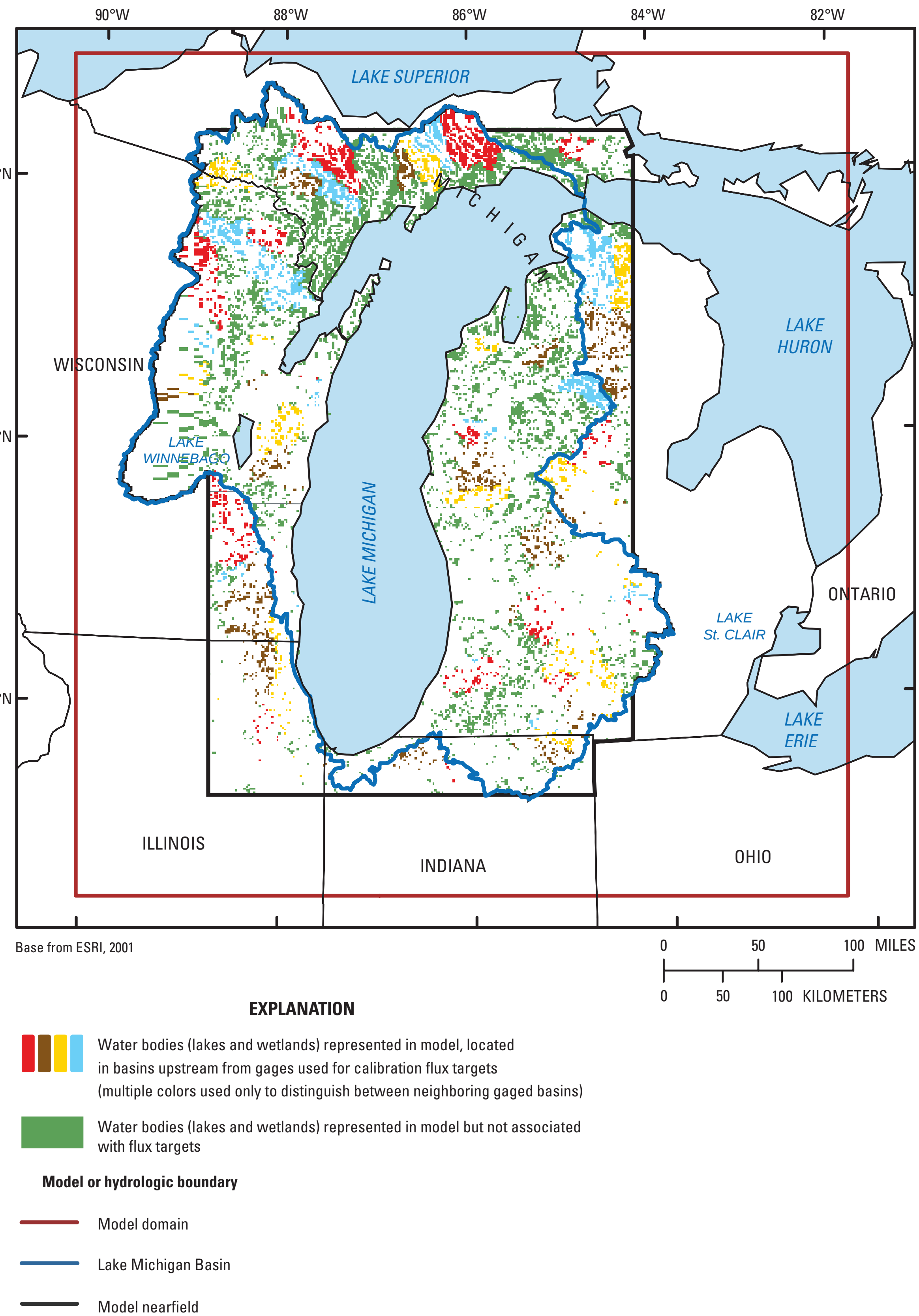

Figure 28*B*. Water bodies represented in model.

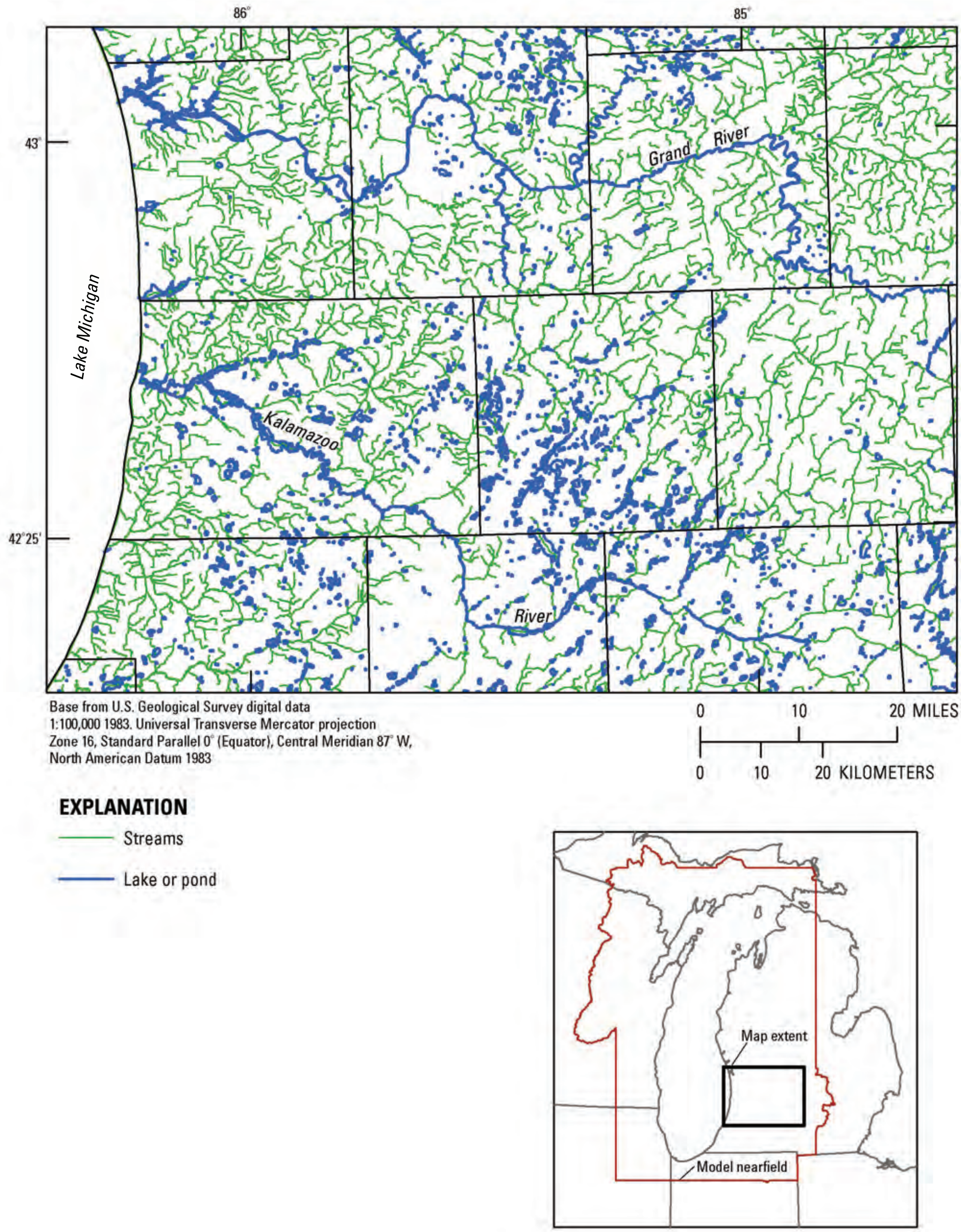

Figure 29*A*. Example surface-water network without model RIV cells.

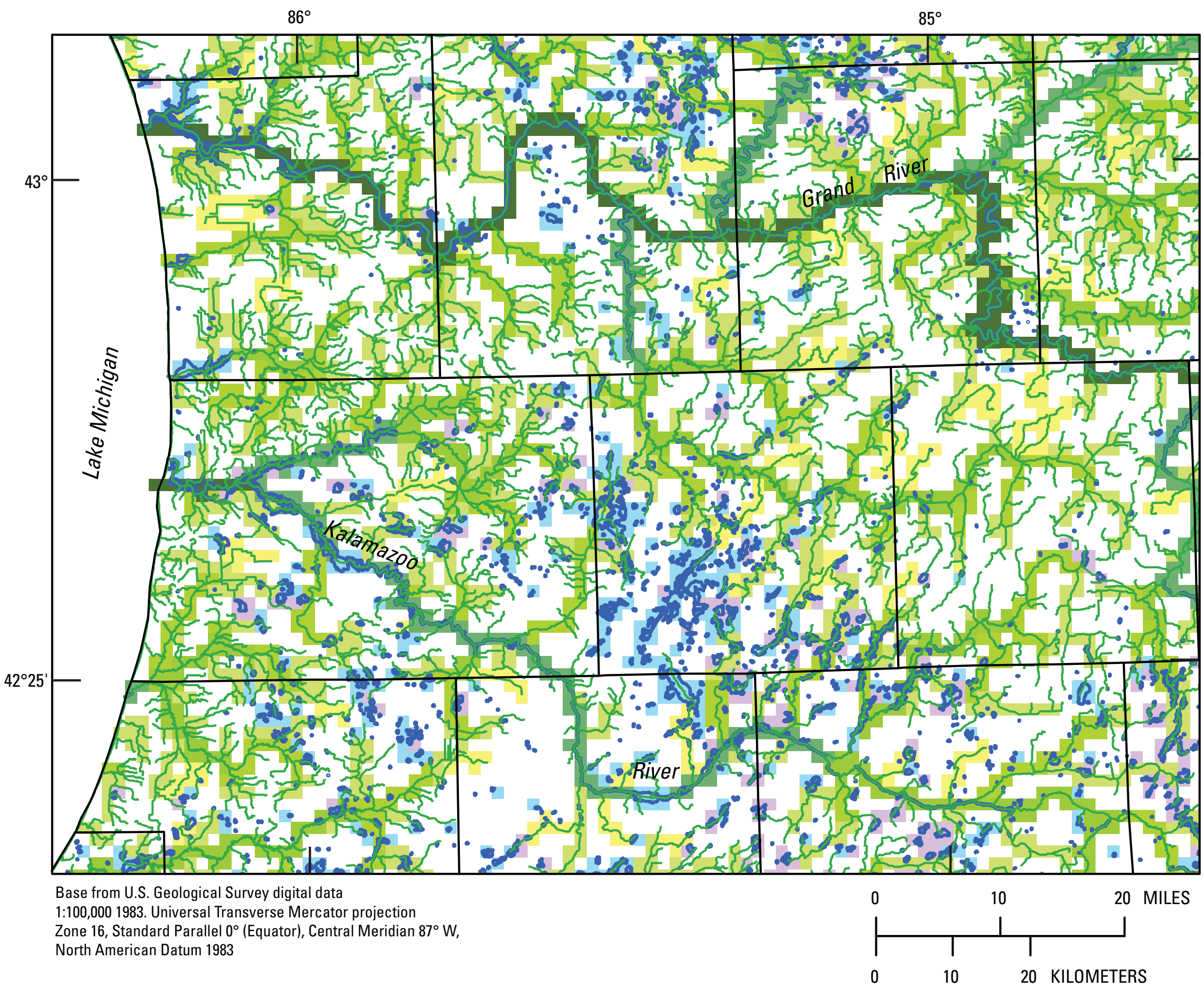

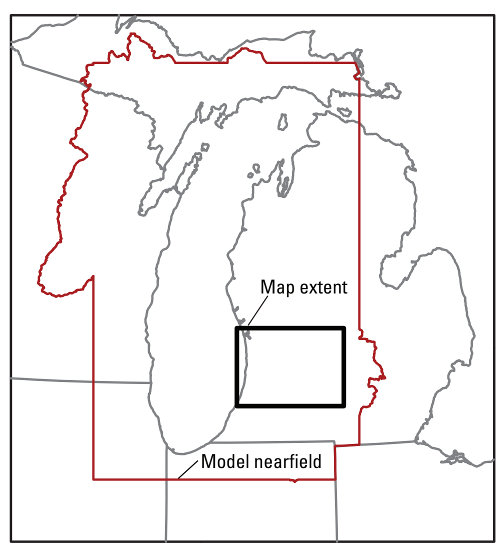

Figure 29*B*. Example surface-water network with model RIV cells.

4.5.2 Lake Michigan and Lake Winnebago

Lake Michigan and Lake Winnebago are represented as head-dependent boundaries by using GHB cells, similar to the way that Lake Superior, Lake Huron, Lake St. Clair, and Lake Erie are represented in the model farfield (fig. 27). The stage of Lake Winnebago, the largest inland lake in the model domain, is set to 747.0 ft on the basis of information in the surface-water datasets discussed in appendix 2; the conductance of the all its cells is equal to 5.0 E7, based on a surface area of 5,000 by 5,000 ft, a bed thickness of 1 ft, and a bed K_v assumed equal to 2 ft/d. The Lake Michigan stage is set to 577.5 ft, its low-water datum (identical to the stage for Lake Huron because the two lakes are hydraulically connected). As in the case of the farfield Great Lakes, the effect of substituting a time-dependent Lake Michigan stage for a fixed stage was assessed through model sensitivity (see section 7.2). The conductance of cells representing Lake Michigan is set to 2.5 E7, on the basis of a surface area of 5,000 by 5,000 ft, a bed thickness of 1 ft, and a bed K_v assumed equal to 1 ft/d. However, the connection of Lake Michigan to the groundwater system is represented much differently than is the connection in the case of the farfield Great Lakes. The latter function effectively as constant-head boundaries because the GHB conductance is so high. Although the conductance assigned Lake Michigan is also high and, consequently, presents very little resistance to flow across the GHB boundary, much more resistance is imposed by the full bed thickness attributed to the lake. That full thickness corresponds not to the 1-ft thickness of the GHB conductance term but instead to the mapped lakebed deposits of glacial and Holocene origin, discussed above in the "Model Layering" subsection. The greater the thickness and the lower the vertical hydraulic conductivity assigned to layers 1, 2, and 3 under Lake Michigan, the greater is the resistance to vertical flow discharging to the lake. The ease of lake discharge is also affected by the horizontal hydraulic conductivity of the unconsolidated and bedrock deposits underlying and adjacent to the lake. The hydraulic conductivities assigned to the QRNR and bedrock units in connection with the lake are discussed later in this section.

4.5.3 Summary of Farfield and Nearfield Surface-Water Inputs

Streams, water bodies, and the Great Lakes are essentially represented in the model farfield as constant heads that effectively define the water-table surface. In the model nearfield, the surface-water network is represented as head-dependent boundaries by using conductance terms that are related to stream order or to the thickness of underlying materials (as in the case of Lake Michigan). Lakes and wetlands in the model nearfield are effectively represented as drains that allow groundwater discharge but do not permit infiltration of surface water to the aquifer system. Table 6 lists the number of cells belonging to each boundary-condition type, their distribution in the nearfield/farfield, their distribution in QRNR/bedrock layers, and the number within the model domain.

4.6 Recharge

The LMB model represents the movement of water from the land surface into the groundwater-flow system in two ways. In the model *farfield*, the addition of water is controlled by the gradient between constant head cells at the top of the groundwater flow system and underlying cells deeper in the system. In the model *nearfield*, water is added to the water-table cells at the top of the saturated groundwater flow system at a specified rate in the form of recharge.

Recharge in the model nearfield varies spatially and through time. The rates reflect the evolution of land use, trends in temperature and precipitation, and factors involving hydrologic soil type, land surface slope, and soil-water capacity. Recharge was computed for each model cell and each stress period by using the Thornthwaite-Mather soil-water balance model (SWB) (Westenbroek and others, 2010). As stated by Westenbroek and others, the SWB model calculates spatial and temporal variations in recharge by use of commonly available GIS data layers in combination with tabular climatological data. The code is based on the modified Thornthwaite-Mather soil-water balance approach; components of the soil-water balance are calculated on a daily time step. Recharge calculations are made on a rectangular grid suitable for application to a regional groundwater-flow model.

The SWB model calculates *daily* recharge for each nearfield inland grid cell according to the following equation:

$$\begin{aligned} recharge &= (precip + snowmelt) \\ &\quad - (interception + outflow + ET) - \Delta\, soil\ moisture \end{aligned}$$

where

precip	is daily precipitation;
snowmelt	is water made available on days when temperatures are high enough to melt accumulated snowpack;
interception	is the amount of daily rainfall trapped by vegetation as a function of land-use type and season;
outflow	is daily surface runoff from a cell according to a curve number rainfall-runoff relation (U.S. Department of Agriculture, 1986) related to soil type, land use, surface condition, and antecedent runoff condition;
ET	is daily evapotranspiration from the root zone of the soil as a function of temperature and vegetation; and
Δ *soil moisture*	is the change in the amount of water stored in the root zone calculated according to the method of Thornthwaite (Thornthwaite and Mather, 1955).

Table 6. Surface-water boundary conditions.

River (RIV) cells		Number
Nearfield number		38,237
Farfield number		0
	Stream[1]	26,184
	Water body[2]	12,053
	Quaternary	34,218
	Bedrock	4,019
	Inside Lake Michigan Basin	27,613
	Outside Lake Michigan Basin	10,624
General Head Boundary (GHB) cells		**Number**
Nearfield number		25,290
Farfield number		2,771
	Quaternary	27,688
	Bedrock	373
	Inside Lake Michigan Basin *(Lake Michigan, Lake Winnebago)*	25,290
	Outside Lake Michigan Basin *(Lake Superior, Lake Huron, Lake St. Clair, Lake Erie)*	2,771
Constant Head (CHD) cells		**Number**
Nearfield number		0
Farfield number		8,873
	Quaternary	7,588
	Bedrock	1,285
	Inside Lake Michigan Basin	0
	Outside Lake Michigan Basin	8,873

[1] RIV cells with stage greater than bed elevation, thereby allowing for outflow from stream to groundwater.

[2] RIV cells with stage equal to bed elevation, thereby precluding outflow from water body to groundwater.

In using this method, one assumes all the water that percolates on a given day below the rooting depth of vegetation is immediately transferred to the water table as recharge. The method does not account for lags due to movement and storage within the unsaturated zone below the soil root zone and above the water table. This limitation has little importance when daily values are integrated to compute average recharge rates at a cell location over extended periods (for example, for a 10-year model stress period).

The model modules are designed to take advantage of widely available GIS datasets and file structures. Refinements to the SWB recharge model implemented in this study include an algorithm for limiting winter recharge when soils are frozen, based on cumulative days of temperatures below freezing. One option available in the SWB recharge model—the routing of overland flow to allow for focused recharge—is not activated in the LMB application because of the coarse scale of the model grid. The SWB model is calibrated by adjusting model inputs such as rooting depth of vegetation to produce an improved match between year 2000 recharge and base-flow estimates at the gaged outlets of the watersheds (Westenbroek and others, 2010). More information on the compilation of recharge calibration targets is given in section 5 (and appendix 7) of this report.

For the application of the SWB method to the LMB domain, spatially interpolated arrays of daily minimum temperature, maximum temperature, and precipitation were derived from time series recorded at more than 800 meteorological stations providing data for part or all of the 101-year period from 1900 to 2000. The daily results of the recharge generator were averaged to yield a yearly value for each nearfield model cell. The yearly values were, in turn, averaged over stress-period intervals to produce cell-by-cell arrays for the 10 stress periods extending between 1900 and 2000. The predevelopment and 1864–1900 stress periods were assigned the same rates as the 1901–1920 stress period, whereas the 2001–5 stress period was assigned the same rate as the 1991–2000 stress period. Because the SWB model calculates recharge partly as a function of land use, and given that only two land-use maps were available for the LMB domain—one for about 1910 and one for 1990, land use was assumed to evolve from the 1910 to the 1990 condition in a linear fashion with respect to time. In effect, recharge arrays were calculated by stress period for both conditions and weighted by time elapsed until or after 1950. In this way, recharge in earlier stress periods more strongly reflect the early-20th-century land use, whereas recharge for later stress periods reflect the late-20th-century land use, and recharge for 1950 is an average of the two.

The results of the SWB recharge model for the LMB nearfield show both temporal and spatial trends. If the recharge rates at all nearfield cells are averaged on a yearly basis and grouped by stress period, it is possible among the upward and downward trends to identify an increase in recharge around 1970 (fig. 30). This increase is consistent with findings of other investigators working at the scale of the Great Lakes Basin (Hodgkins and others, 2007).

The SWB model simulates a range of annual recharge rates within the model nearfield between 3 and 11 in. However, average recharge rates for the 12 stress periods specified in the LMB model range only from 6.80 to 8.84 in. The nearfield-wide average for the stress periods before 1970 is close to 7 in/yr; the average for the stress periods after 1970 is almost 8 in/yr.

In all the nearfield, recharge was computed by the SWB method on a cell-by-cell basis for 10 time intervals. Some intervals correspond to multiple stress periods, but most coincide with a single stress period (fig. 30). The average for any given period hides a fair degree of cell-by-cell spatial variability incorporated into the LMB model. Recharge maps for three sample time intervals—1901 to 1920 (fig. 31*A*), 1971 to 1975 (fig. 31*B*), and 1991 to 2005 (fig. 31*C*)—show an overall spatial range of 0 to 16 in/yr and illustrate areas of consistently higher or lower than average recharge. Higher recharge rates are computed for a north-to-south belt near the eastern shoreline of Lake Michigan that extends from the northern Lower Peninsula of Michigan into Indiana. Recharge in this area is enhanced by moisture from Lake Michigan carried by the prevailing winds from west to east, sometimes also by areas of coarse soil underlain predominantly by glacial outwash. Lower recharge rates are computed for a belt along the western side of Lake Michigan in Wisconsin and Illinois, which is associated with generally fine soils underlain by clayey tills. The maps also show a few zones of very low recharge (for example, a north-to-south span in the Upper Peninsula of Michigan north of Green Bay and an area in southern Michigan). The shallow unconsolidated part of the flow system is very thin in these areas and, on the assumption that the near-surface bedrock severely limits infiltration, the recharge rates are assumed to be small and were reduced to 0.5 in/yr. Recharge also was reduced to 0.5 in/yr in the urbanized vicinity of Chicago. These combined changes caused the global average nearfield recharge rate to decrease by 3 percent relative to the original average rate generated by the SWB recharge model.

The recharge rates computed by the SWB model adjusted through model calibration are described in section 5.

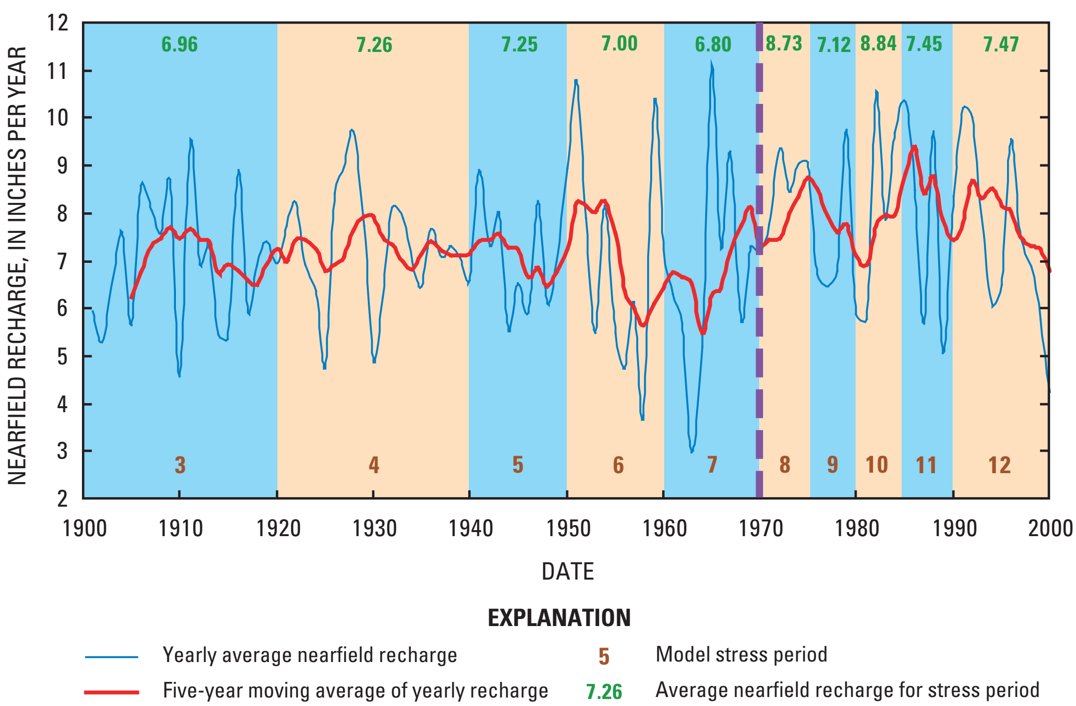

Figure 30. Recharge trends for the inland nearfield area of the model.

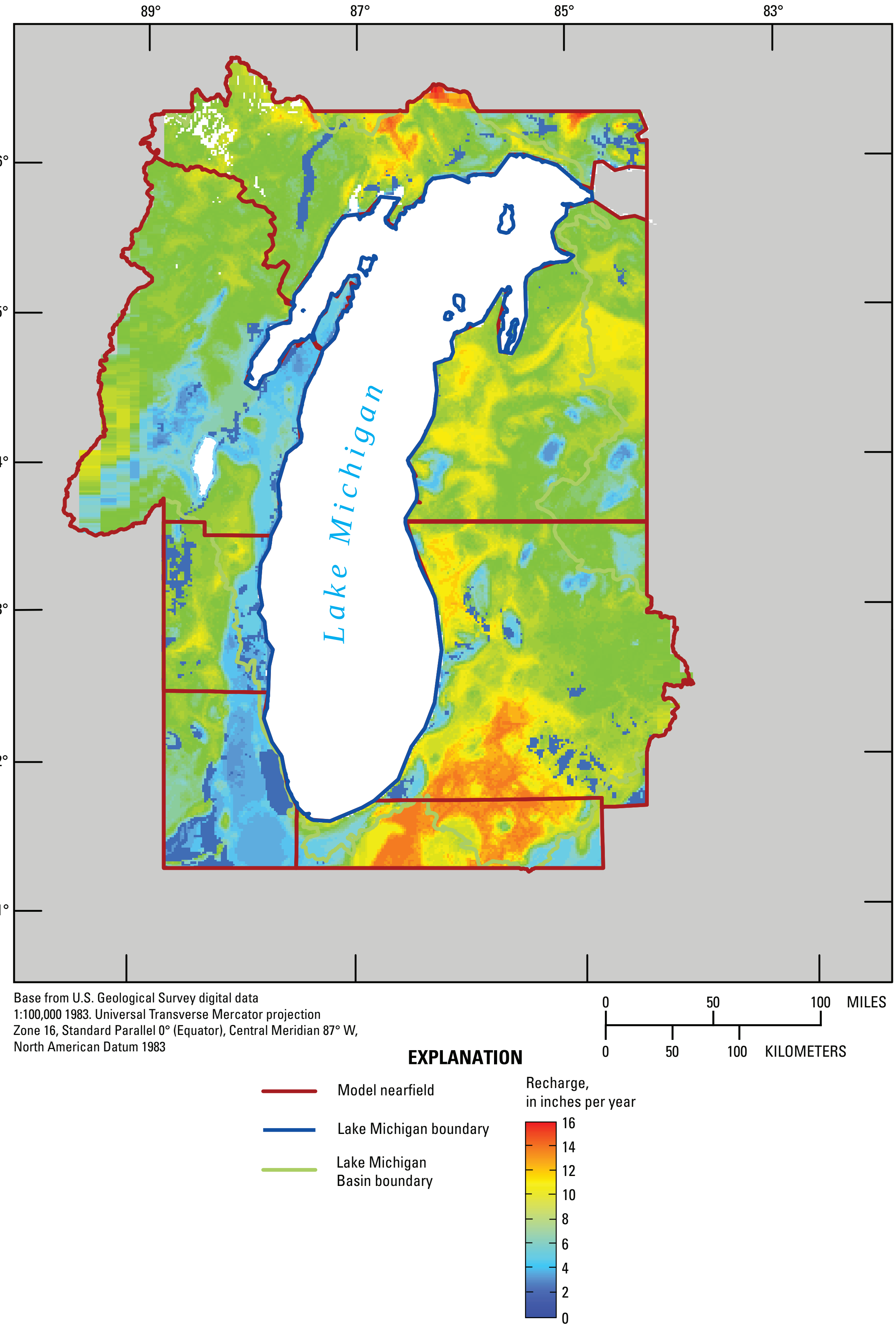

Figure 31*A*. Recharge distribution: 1901–20.

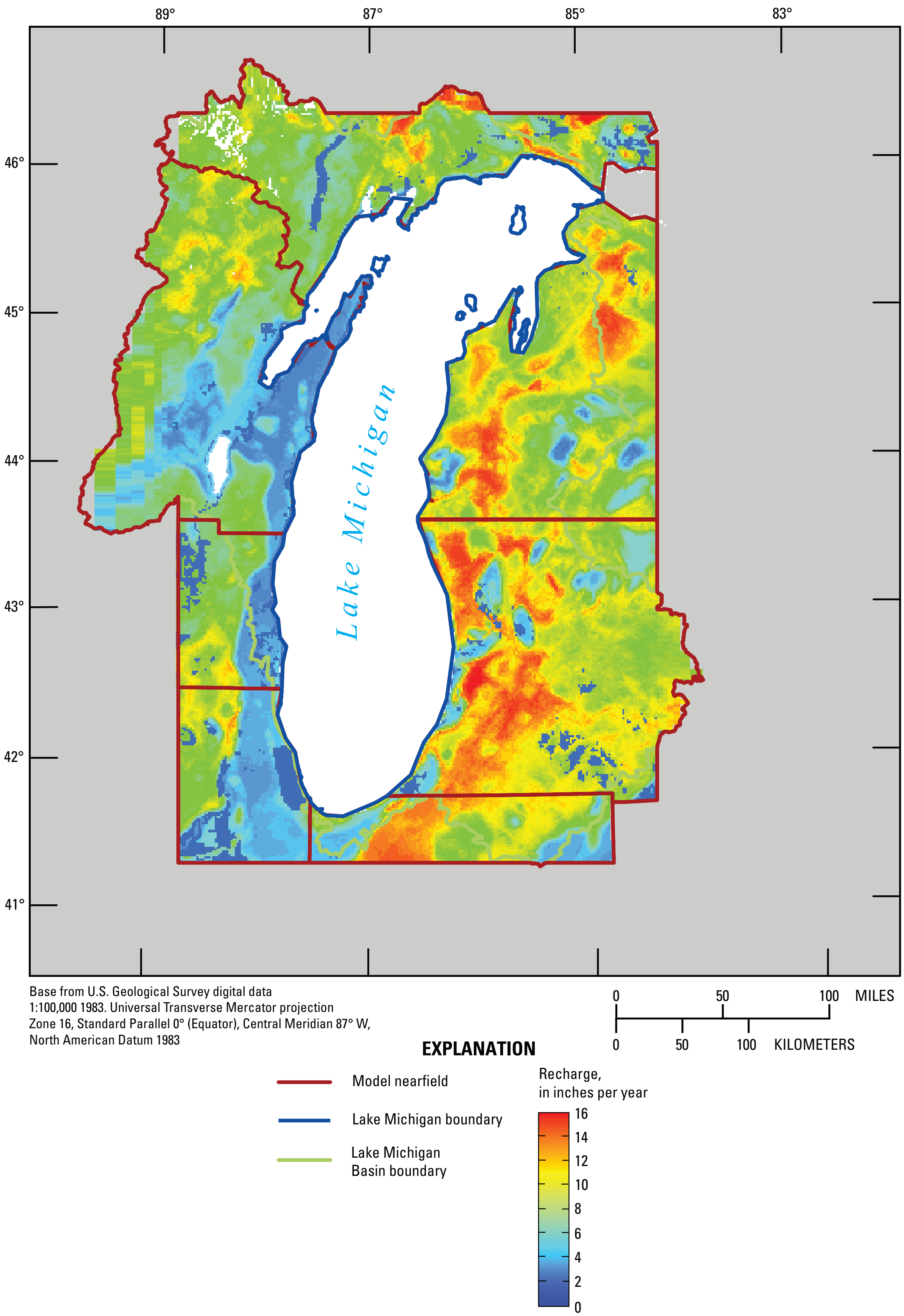

Figure 31*B*. Recharge distribution: 1971–75.

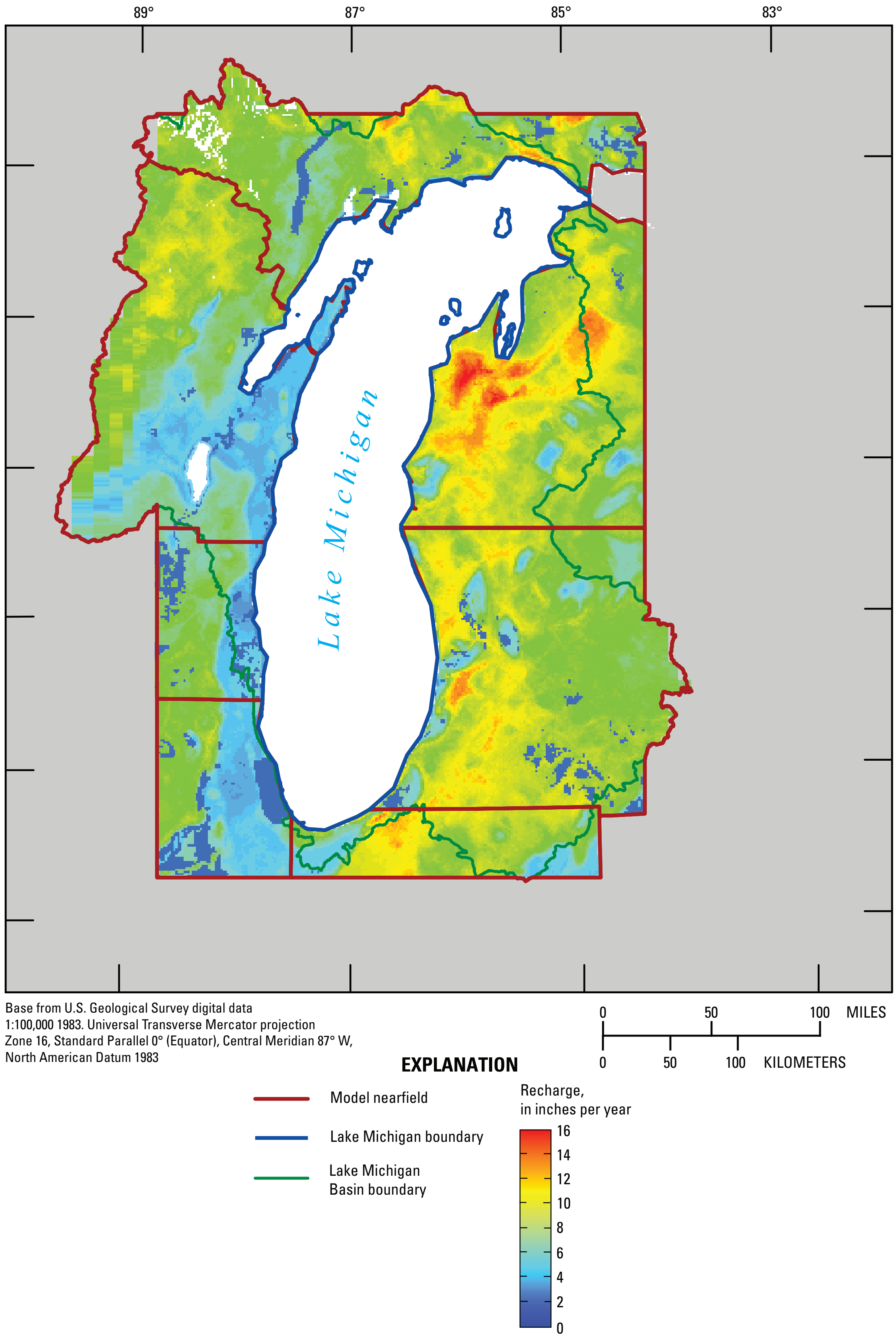

Figure 31*C*. Recharge distribution: 1991–2005.

4.7 Well Withdrawals

Three types of stresses in the LMB model change through time: boundary fluxes in the southwestern corner of the grid, recharge, and well withdrawals. Boundary fluxes function as sources or sinks of water depending on location and depth. Recharge is a source of water that is spatially distributed and applied to the water table. Well withdrawals are point sinks that can draw from any layer or combination of layers in the model and from any model cell as long as it is not assigned a constant head and as long as it is not pinched (that is, the unit it represents has some thickness).

A database of historical pumping constructed for the LMB model is described in Buchwald and others (2010). It documents the range of methods that support the tabulations of pumping by individual wells for all the nearfield and part of the farfield from 1864 through 2005. Four water-use categories are considered in the database: public supply, industrial/commercial, irrigation/golf course, and aquaculture. The well withdrawals are located by subregion and by depth according to what aquifer system or systems are pumped.

4.7.1 Database Limitations

The compilation of historical pumping rates for the LMB model has several limitations. Domestic pumping is not included because, although the number of domestic wells is large compared to those in other water-use categories, households generally use relatively small amounts of groundwater and pump it from shallow aquifers; the drawdown cone around each well is commonly buffered by nearby surface water unless recharge is very small (Bradbury and Rayne, 2009). In addition, most of the pumped water is returned to groundwater through onsite septic systems. In Wisconsin, it is estimated that domestic wells account for 23 percent of total groundwater withdrawals (Lawrence and Ellefson, 1982), but less than half the amount is thought to be consumed (Solley and others, 1998); estimates of return rate have been as high as 80 to 90 percent (Topper, 2007; Cherkauer, 2007). Together these estimates of extraction and return suggest that omission of domestic wells from the database underestimates total withdrawals by 5 percent.[12]

Pumping from the other water-use categories is typically almost all consumed rather than returned to the groundwater system. Even for irrigation, between 70 and 100 percent of the pumped water is estimated to be consumed by evapotranspiration (Shaffer and Runkle, 2007), so gross rates of withdrawals for irrigation can be fairly equated in most cases with net rates. In this study, the term “high-capacity wells” refers to those pumped at rates greater than 70 gal/min—equal to 0.1 Mgal/d—whereas low-capacity wells are those pumped at rates less than 70 gal/min. Although there are more low-capacity than high-capacity wells in the LMB model, high-capacity wells account for most of the total discharge. For 2001 to 2005, the model database contains 6,764 low-capacity wells and 2,381 high-capacity wells, but the combined discharge from the former is only 200.50 Mgal/d, whereas the discharge from the latter is 892.86 Mgal/d.

A second limitation of the LMB water-use database is that coverage of the model farfield is incomplete. Pumping information in these areas was only collected for high-capacity wells that pump from deep, confined aquifers that typically give rise to regional cones of depression. Pumping from the shallow flow system in the model farfield was assumed to have a negligible effect on flow between the nearfield and farfield. Given the hydrogeology of the model domain and the patterns of water use, it is reasonable to conclude that deep, confined pumping since 1864 is much more likely to have occurred west of Lake Michigan in Wisconsin and Illinois than east of the lake in Michigan and Indiana. To test this assumption, a survey of both shallow and deep pumping wells was done for the year 2004 in parts of Michigan and Indiana within the model farfield. In Michigan, 745 wells pumped a total of about 48 Mgal/d, and only 7.5 percent discharged from deep wells. In Indiana, 954 wells pumped about 42 Mgal/d, and 10 percent discharged from deep wells. On the basis of these findings, the error in omitting pumping from the deep flow system in the model farfield in Michigan and Indiana is acceptable. However, in order to minimize any error from omitting farfield pumping east of Lake Michigan, historical pumping was tabulated for the farfield area of all Michigan and Indiana counties that straddle the farfield/ nearfield boundary, as well as for the Monroe County industrial pumping center near Lake Erie in southwestern Michigan.[13] It should be noted that farfield pumping in the entire model domain west of Lake Michigan (that is, in Illinois and Wisconsin) was included by using the same database coverage applied to the nearfield.

[12] The most likely areas where omission of domestic pumping can lead to simulation errors are around high-density residential communities served by both domestic wells and by sewers or holding tanks. There are few examples in the LMB model domain. One is the city of Mequon north of Milwaukee, which before 2000 is estimated to have pumped 3 Mgal/d from domestic wells, but this water was not returned to the subsurface (Feinstein, Eaton, and others, 2005). Since 2000, some of that pumping has been replaced with Lake Michigan supply.

[13] No water-use data at all were compiled for Ohio. The state is outside the Lake Michigan Basin, and pumping is limited and mostly from shallow aquifers; accordingly, it is expected that the drawdown cones would be restricted in size and have little influence on the exchange of water between the model farfield and nearfield.

As expected, the entries to the water-use database become gradually more complete with time after 1864. For example, data sources for public-supply withdrawals in Michigan are sparse before the late 1970s, whereas the detailed Illinois surveys of public-supply, industrial-commercial, and irrigation discharge only begin in the early 1960s. The Illinois pumping before then was approximated by assigning all estimated discharge to only seven pumping centers. Some of the inevitable gaps in spatial and withdrawal information were handled by special estimation methods[14] so that, on balance, the inputs to the model are believed to accurately reflect overall historical trends with respect to amounts withdrawn from each aquifer system (Buchwald and others, 2010).

4.7.2 Transfer of Database to Model

Not all the entries in the water-use database have been transferred to the model. Some farfield wells in inactive and constant-head cells are excluded because they would have no effect on the model simulation. In addition a small number of farfield and nearfield wells that, according to the model stratigraphy, are in pinched units also are omitted. The elimination of all these wells reduces the pumping tabulated in the original database by about 13 percent for the last stress period, a decrease that is representative of the reductions for other stress periods and which mostly affects withdrawal rates in the farfield. The total number of individual pumping wells active in at least one model stress period is 13,312.

Pumping for each stress period is input to the LMB model by means of two SEAWAT-2000 packages. For wells that penetrate only one layer, the WEL package is employed. For wells that penetrate multiple model layers, the Multi-Node Well (MNW) package is used to divide the total withdrawal among layers on the basis of transmissivity and the hydraulic gradient between the well and the aquifer (Halford and Hanson, 2002). Two additional inputs are required by the MNW package for each well: the borehole radius and the "skin" resistance, the latter referring to the disturbed interval around the well. They are set, respectively, to 0.5 ft and to 5 ft^2/d for all multilayer wells to promote numerical stability. The MNW package allows for circulation through the pumped borehole (water can exit some layers penetrated by the well while entering others, but the the prescribed sink discharge is maintained). Whenever input of horizontal hydraulic conductivity to the model is modified, the MNW package also automatically resets the exchange between the well and the penetrated model layers as a function of the resulting aquifer transmissivity. This recalculation of pumping rates internal to the MNW package is a significant advantage because it eliminates the need for any manual updating of rates during the automated calibration process described in section 5.

[14] For example, in Wisconsin, pumping from industrial wells was estimated as a function of one or more of the following: pump capacity, approved normal daily pumpage, and an industry-specific withdrawal coefficient. Details on all estimation methods are given in Buchwald and others (2010).

In addition to the 1,306 pumping wells represented in the model, 4 injection wells are represented near Kalamazoo in the southern Lower Peninsula of Michigan. These wells are used in the model to account for the return of cooling water from pharmaceutical plants, water which is pumped from and then infiltrated back the QRNR aquifer system through constructed wetlands, ponds, or lakes (Luukkonen and others, 2004). The return infiltration began in the 1960s and continued through 2005, varying in quantity from 5.7 to 10.1 Mgal/d.

One other sink is also represented by the WEL input package: the Deep Sewer Tunnel System under Milwaukee, Wis. The 19.4-mi-long tunnel was installed in the early 1990s through the shallow Silurian dolomite in the SLDV aquifer system, some of which is highly fractured. The installation collects combined-sewer overflow during rainstorms and stores it for later treatment. Studies by the Milwaukee Metropolitan Sewage District estimate average groundwater discharge to the Deep Tunnel as 2.8 Mgal/d during dry periods (Dunning and others, 2004; Feinstein and others, 2003). The water is subsequently treated and pumped into Lake Michigan. In the LMB model, the groundwater discharge at the 2.8 Mgal/d rate is withdrawn for the 1991–2000 and 2001–5 stress periods from the Silurian bedrock (layer 11) over 20 cells that coincide with the tunnel geometry. Although Chicago is also underlain by a deep-tunnel system, that tunnel intersects mostly competent dolomite and is thoroughly grouted where rock is fractured (Knoerle, Bender, Stone & Associates, 1977), so little or no groundwater discharges to the tunnel.

4.7.3 Pumping Totals in Model

The 1,306 pumping wells in the model are distributed between the nearfield (77 percent) and the farfield (23 percent). The subregion with the largest number of wells is Northeastern Illinois; the smallest number is in the Upper Peninsula of Michigan (table 7). Over 40 percent of the nearfield wells are public supply; nearly all the remainder is split evenly between the industrial/commercial and irrigation/golf course categories. The QRNR system contains the most nearfield wells, followed by the C-O and SLDV systems.

The number of active wells and their pumping vary greatly by stress period and by aquifer system (table 8). For example, around 1900, the model database contains only 108 active nearfield wells pumping 16 Mgal/d, more than half of which is drawn from the C-O aquifer system. By 2000 there are 7,252 active nearfield wells pumping 841 Mgal/d, more than half of which is drawn from the QRNR aquifer system. The total nearfield pumping increased for each stress period through the early 1980s, when the Chicago diversion of Lake Michigan replaced groundwater extraction and caused a dip in use. The upward trend resumed in the 1990s but reached a plateau in the last stress period (2001–5), due in part to decreased withdrawals in southeastern Wisconsin (fig. 32). The trend of farfield withdrawals entered in the model is consistently upward for the entire simulation period.

Table 7. Number of pumping wells by subregion, water-use category, and aquifer system.

[Wells active for any model stress period are counted in totals]

Nearfield totals	
Total =10,255	
Number by subregion	
1,384	SLP_MI
333	NLP_MI
79	UP_MI
1,808	NE_WI
1,180	SE_WI
1,784	N_IND
3,687	NE_ILL
Number by water-use category	
4,431	Public supply
2,877	Irrigation/golf courses
2,896	Industrial/commercial
51	Aquiculture
Number by aquifer system (assigned to aquifer system of lowest layer penetrated)	
4,971	QRNR
144	PENN
153	MSHL
2,042	SLDV
2,945	C-O
Farfield totals	
Total = 3,051	
Number by subregion	
3,051	Farfield
Number by water-use category	
1,003	Public supply
1,444	Irrigation/golf courses
596	Industrial/commercial
8	Aquiculture
Number by aquifer system (assigned to aquifer system of lowest layer penetrated)	
1,119	QRNR
10	PENN
21	MSHL
231	SLDV
1,670	C-O

Table 8. Pumping by stress period and aquifer system.

[Table includes only pumping from wells; it excludes injection wells and inflow to the Milwaukee Deep Tunnel. Mgal/d, million gallons per day]

Aquifer system	Number of wells	Pumping (Mgal/d)
Predevelopment (stress period 1)		
QRNR nearfield	0	0
PENN nearfield	0	0
MSHL nearfield	0	0
SLDV nearfield	0	0
C-O nearfield	0	0
Total nearfield	0	0
Farfield	0	0
Oct. 1864–Oct. 1900 (stress period 2)		
QRNR nearfield	39	4.77
PENN nearfield	9	.97
MSHL nearfield	4	1.70
SLDV nearfield	0	.00
C-O nearfield	56	8.59
Total nearfield	108	16.04
Farfield	14	1.35
Oct. 1900–Oct. 1920 (stress period 3)		
QRNR nearfield	69	8.98
PENN nearfield	16	4.17
MSHL nearfield	7	2.69
SLDV nearfield	16	.50
C-O nearfield	144	39.88
Total nearfield	252	56.22
Farfield	38	6.17
Oct. 1920–Oct. 1940 (stress period 4)		
QRNR nearfield	135	19.40
PENN nearfield	30	10.05
MSHL nearfield	12	11.64
SLDV nearfield	46	1.99
C-O nearfield	298	71.60
Total nearfield	521	114.68
Farfield	86	12.02

Table 8. Pumping by stress period and aquifer system.—Continued

[Table includes only pumping from wells; it excludes injection wells and inflow to the Milwaukee Deep Tunnel. Mgal/d, million gallons per day]

Aquifer system	Number of wells	Pumping (Mgal/d)
Oct. 1940–Oct. 1950 (stress period 5)		
QRNR nearfield	335	51.66
PENN nearfield	32	17.31
MSHL nearfield	20	16.43
SLDV nearfield	126	7.83
C-O nearfield	408	101.14
Total nearfield	921	194.37
Farfield	141	29.81
Oct. 1950–Oct. 1960 (stress period 6)		
QRNR nearfield	482	91.07
PENN nearfield	45	23.68
MSHL nearfield	27	26.91
SLDV nearfield	191	12.23
C-O nearfield	487	127.14
Total nearfield	1,232	281.04
Farfield	265	46.25
Oct. 1960–Oct. 1970 (stress period 7)		
QRNR nearfield	999	183.20
PENN nearfield	54	31.74
MSHL nearfield	34	35.28
SLDV nearfield	1,322	60.34
C-O nearfield	1,081	172.27
Total nearfield	3,490	482.82
Farfield	984	122.72
Oct. 1970–Oct. 1975 (stress period 8)		
QRNR nearfield	1,276	228.09
PENN nearfield	83	41.21
MSHL nearfield	46	30.01
SLDV nearfield	1,494	104.83
C-O nearfield	1,159	234.48
Total nearfield	4,058	638.61
Farfield	1,186	176.48

Table 8. Pumping by stress period and aquifer system.—Continued

[Table includes only pumping from wells; it excludes injection wells and inflow to the Milwaukee Deep Tunnel. Mgal/d, million gallons per day]

Aquifer system	Number of wells	Pumping (Mgal/d)
Oct. 1975–Oct. 1980 (stress period 9)		
QRNR nearfield	1,778	276.55
PENN nearfield	83	41.21
MSHL nearfield	58	31.68
SLDV nearfield	1,695	118.18
C-O nearfield	1,346	266.58
Total nearfield	4,960	734.19
Farfield	1,670	197.09
Oct. 1980–Oct. 1985 (stress period 10)		
QRNR nearfield	2,578	332.38
PENN nearfield	109	39.99
MSHL nearfield	83	32.16
SLDV nearfield	1,499	119.36
C-O nearfield	1,311	272.05
Total nearfield	5,580	795.94
Farfield	1,851	220.00
Oct. 1985–Oct. 1990 (stress period 11)		
QRNR nearfield	2,945	340.95
PENN nearfield	110	40.07
MSHL nearfield	83	31.83
SLDV nearfield	1,635	119.70
C-O nearfield	1,338	223.59
Total nearfield	6,111	756.14
Farfield	2,049	234.37
Oct. 1990–Oct. 2000 (stress period 12)		
QRNR nearfield	3,787	465.87
PENN nearfield	123	38.17
MSHL nearfield	127	45.47
SLDV nearfield	1,705	104.25
C-O nearfield	1,510	187.10
Total nearfield	7,252	840.85
Farfield	2,419	264.48

Table 8. Pumping by stress period and aquifer system.—Continued

[Table includes only pumping from wells; it excludes injection wells and inflow to the Milwaukee Deep Tunnel. Mgal/d, million gallons per day]

Aquifer system	Number of wells	Pumping (Mgal/d)
Oct. 2000–Oct. 2005 (stress period 13)		
QRNR nearfield	3,704	465.69
PENN nearfield	130	40.58
MSHL nearfield	130	41.37
SLDV nearfield	1,360	91.38
C-O nearfield	1,416	191.78
Total nearfield	6,740	830.79
Farfield	2,407	262.57

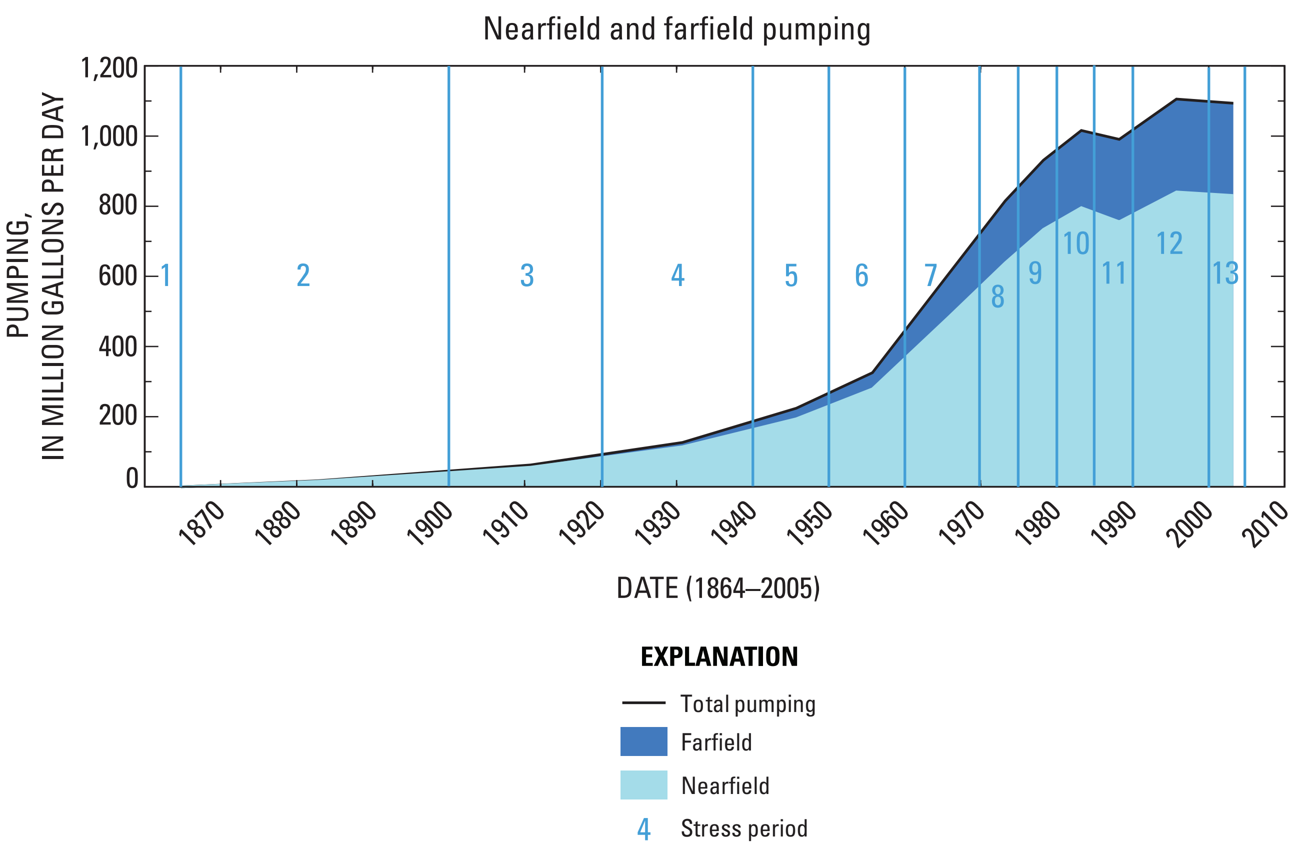

Figure 32. Total nearfield and farfield pumping through time.

The withdrawal trends by model subregion (fig. 33*A*) show that the share of nearfield pumping attributable to northeastern Illinois dropped sharply around 1980, whereas the share attributable to the southern Lower Peninsula of Michigan increased sharply, especially in the 1980s and 1990s. Other regions show subtle inflections over time. For example, the increased use in northeastern Wisconsin slowed in the 1950s because the city of Green Bay public water supply switched sources from well water to Lake Michigan water. The withdrawal trends by water-use category in the model nearfield (fig. 33*B*) show the predominance of the public-supply category; pumping for irrigation exceeds industrial withdrawal around 1990. The trends by aquifer system (fig. 33*C*) show that the effect of the Chicago lake diversion for water supply was to reduce C-O withdrawals relative to QRNR pumping. The contribution of the SLDV system rose abruptly around 1960, whereas the PENN and MSHL share remains small and stable through time.

The spatial distribution of groundwater withdrawals by water-use category is illustrated for the periods 1941 to 1950 (fig. 34*A*), 1976 to 1980 (fig. 34*B*), and 2001 to 2005 (fig. 34*C*). The large circles in the public-supply and industrial/commercial categories coincide with the major pumping centers in the SLP_MI (for example, around Lansing, Kalamazoo, and Grand Rapids), in NE_WI (around the city of Green Bay), in SE_WI (near and west of Milwaukee), and in NE_ILL (communities bordering Chicago).

The distribution of pumping wells indicates a widespread distribution of shallow wells throughout the model domain and concentrated areas of deep wells in areas west of Lake Michigan. In general, the number of wells drawing from both unconfined/semiconfined aquifers and from confined aquifers increases over time, although local trends in the spatial distribution of shallow and deep pumping are highly variable (figs. 35*A*–*C*). However, when the number and discharge of shallow versus deep pumping is tabulated not only by aquifer system (table 9*A*) but also by state (table 9*B*), it is evident how different is the water use in Michigan and Indiana is from that in Wisconsin and Illinois. The states east of Lake Michigan depend on pumping from the shallow part of the flow system, largely from the QRNR aquifer system. The states west of the lake utilize both shallow and deep wells. The deep pumping centered around Green Bay in NE_WI, around Milwaukee in SE_WI, and outside Chicago in NE_ILL acts to generate large interfering cones of depression that extend far under Lake Michigan. The pumping input to the LMB model allows the propagation of the stresses to be followed through time and across a very large area.

4.8 Hydraulic Conductivity

Every cell in the model is assigned a value for horizontal and for vertical hydraulic conductivity. For the QRNR aquifer system in the upper three upper model layers, values of K_h and K_v vary by cell. In contrast, for bedrock aquifer systems in layers 4–20, the K_h and K_v vary by zones, with blocks of cells sharing a common value. The methods for selecting K values also differ for the QRNR and bedrock aquifer systems. In addition, different methods are used to estimate the K of inland QRNR deposits and QRNR deposits under Lake Michigan and the farfield Great Lakes.

4.8.1 QRNR Deposits Below Inland Areas

The hydraulic conductivity assigned to QRNR deposits in inland areas is based on the type of glacial material and the granular texture of the material—its “coarse fraction.” The coarse fraction is defined as the proportion of a depth interval for which the driller descriptions in well logs gives precedence to sand and gravel (or related terms such as “cobbles”) over silt and clay (or related terms such as “hardpan”).

The QRNR deposits in the LMB model are divided into six categories: clayey till, loamy till, sandy till, fine stratified deposits (often derived from lake sediments), medium and coarse stratified deposits (associated with outwash sediments), and organic deposits. The distribution of glacial categories is based on surficial mapping by Fullerton and others (2003)[15] and supplemented by unpublished mapping in support the LMB model in 2006 by the Wisconsin Geological and Natural History Survey and David Mickelson, emeritus professor of glacial geology at the University of Wisconsin-Madison.[16] The distribution of glacial categories in the top layer (extending to a maximum depth of 100 ft from land surface) is complex (fig. 36*A*) and reflects the movements of different lobes of the Laurentian ice sheet (see appendix 1, section 1). The glacial categories of the second layer (from 100 to 300 ft below land surface) and third layer (more than 300 ft below land surface) reflect bedrock valleys in Wisconsin and are often filled with fine-grained deposits (figs. 36*B* and *C*). Outside of Wisconsin, the type of glacial material at depths below 100 ft has not been mapped at the LMB model regional scale.

---

[15] The surficial units present in the LMB model domain in the map prepared by Fullerton and others, 2003, were assigned to model glacial categories according to the following scheme approved by Professor Mickelson:
Clayey till = 3 units (ta, tc, td); Loamy till = 5 units (tb, tj, tk, tl, tm);
Sandy till = 0 units (none present);
Fine stratified = 3 units (EL, lc, la); Medium stratified = 7 units (al, ag, ed, es, gs, ca, Lu);
Coarse stratified = 7 units (gg, gl, lk, ls, kg, kt, ci); Organic = 7 units (ha, hb, hc, hd, he, hp, hs).

[16] The supplemental mapping satisfies two objectives: (1) to extend the mapping of glacial categories to layers 2 and 3 in Wisconsin and (2) to confirm across the model domain that the surficial glacial categories corresponding to the surficial units mapped by Fullerton are characteristic of the full 100-ft thickness of layer 1, and, if not, to assign the predominant categories that apply for the layer 1 thickness. For example, the remapping of layer 1 accounts for the substitution of sandy till for other surficial deposits in parts of northern Wisconsin and the substitution of clayey till for surficial fine-stratified deposits near Saginaw Bay area in eastern Michigan.

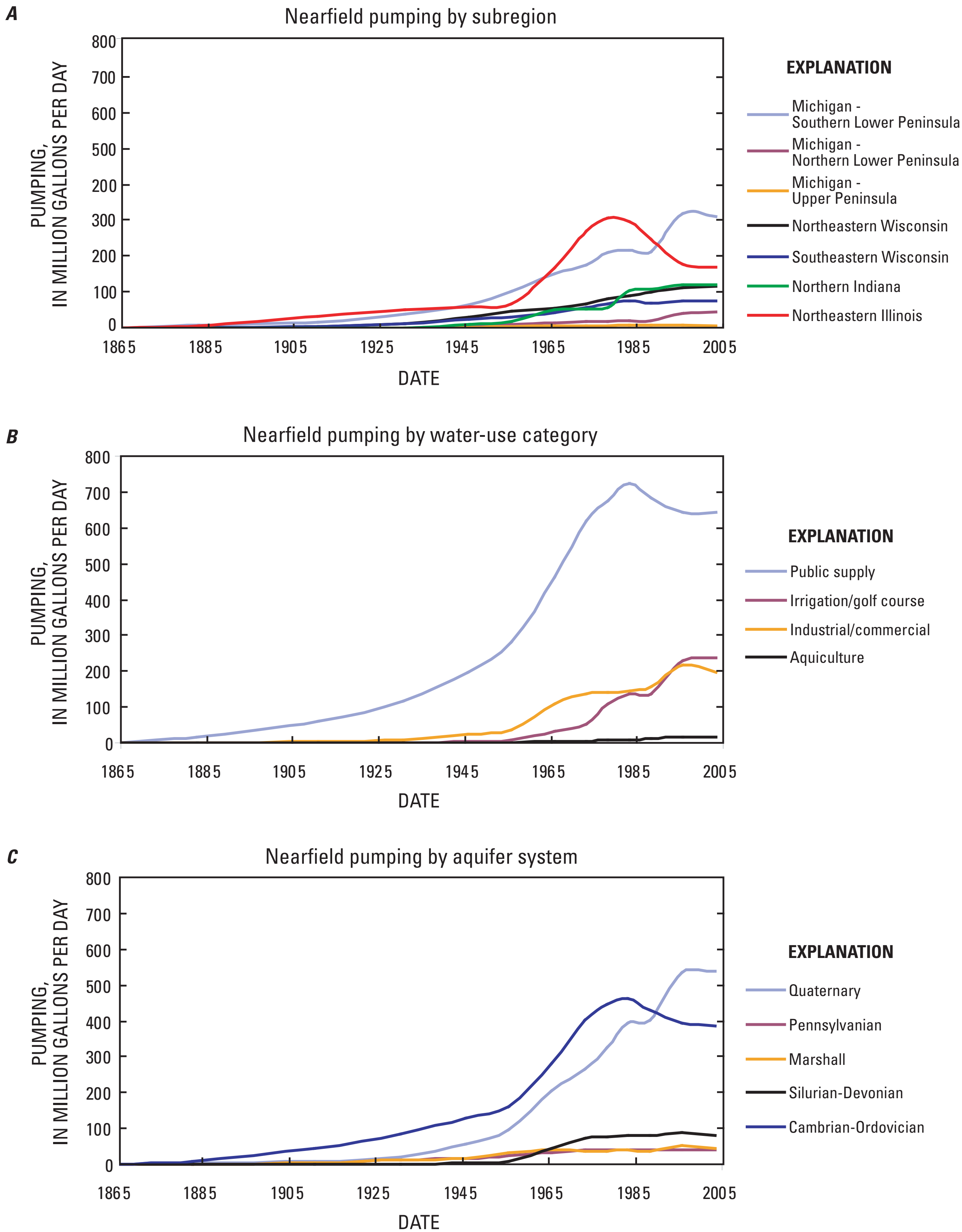

Figure 33. Nearfield pumping through time by *A*, subregion; *B*, water-use category; and *C*, aquifer system.

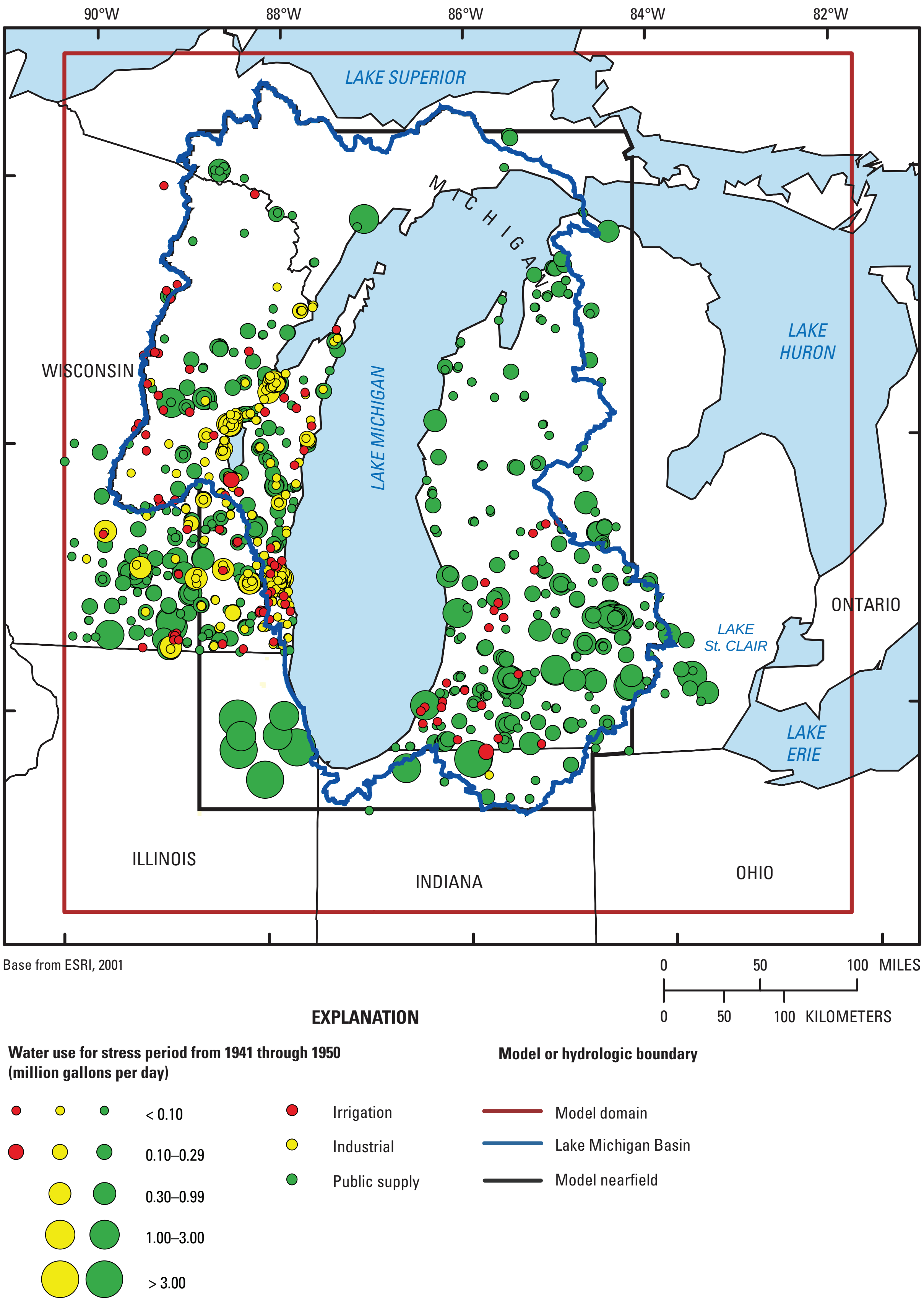

Figure 34*A*. Spatial distribution of pumping by water-use category: 1941–50.

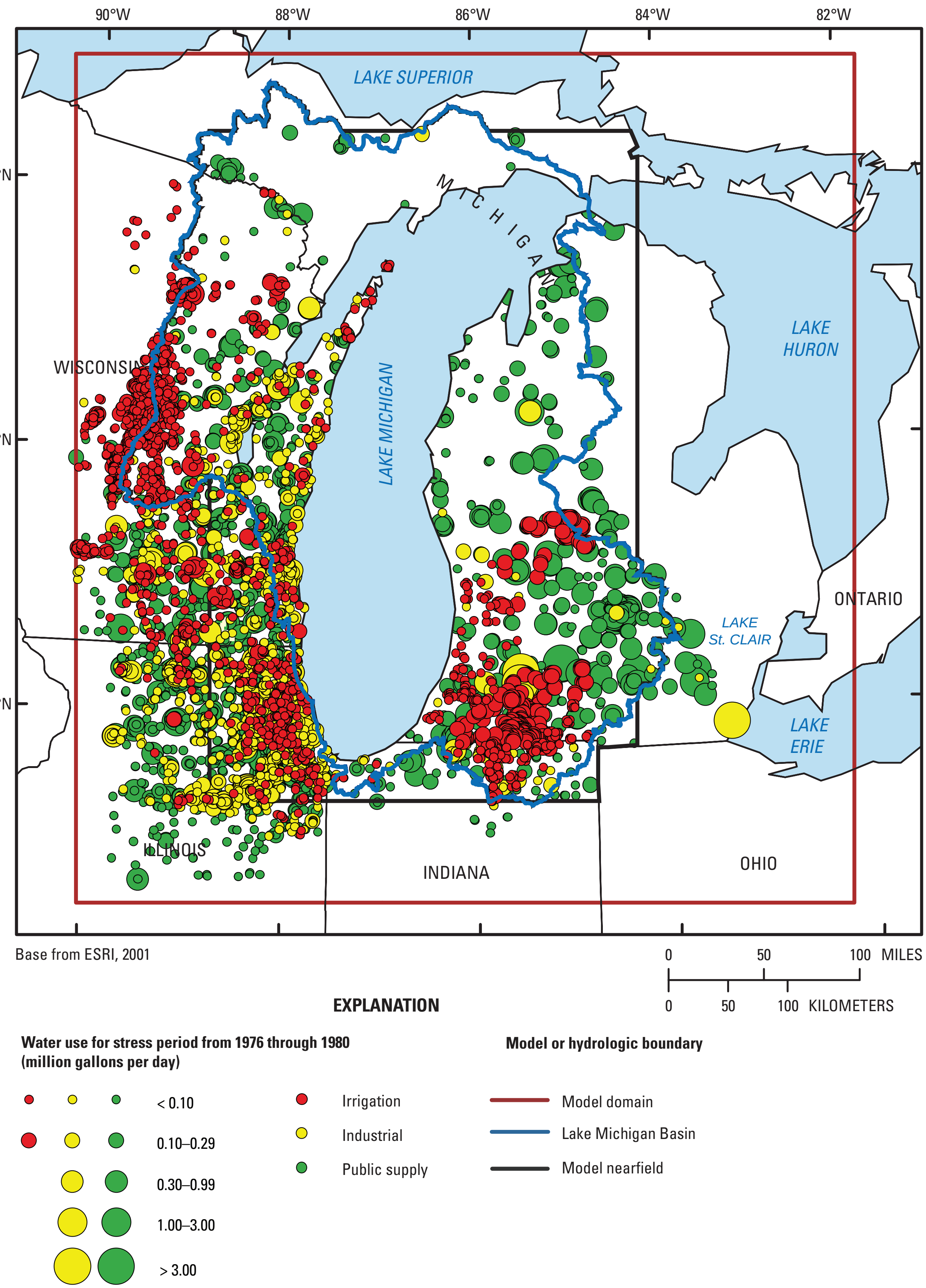

Figure 34*B*. Spatial distribution of pumping by water-use category: 1976–80.

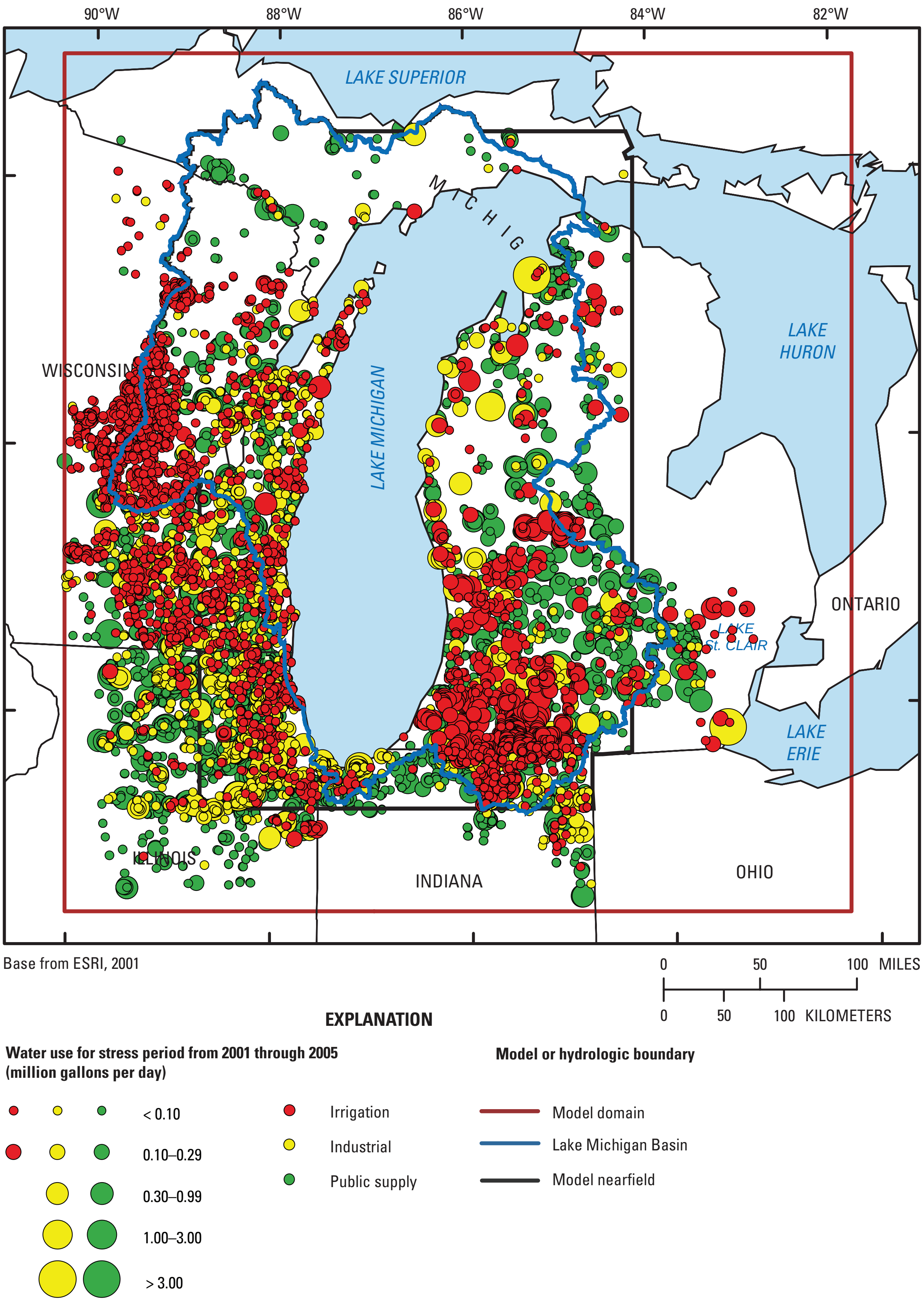

Figure 34*C*. Spatial distribution of pumping by water-use category: 2001–5.

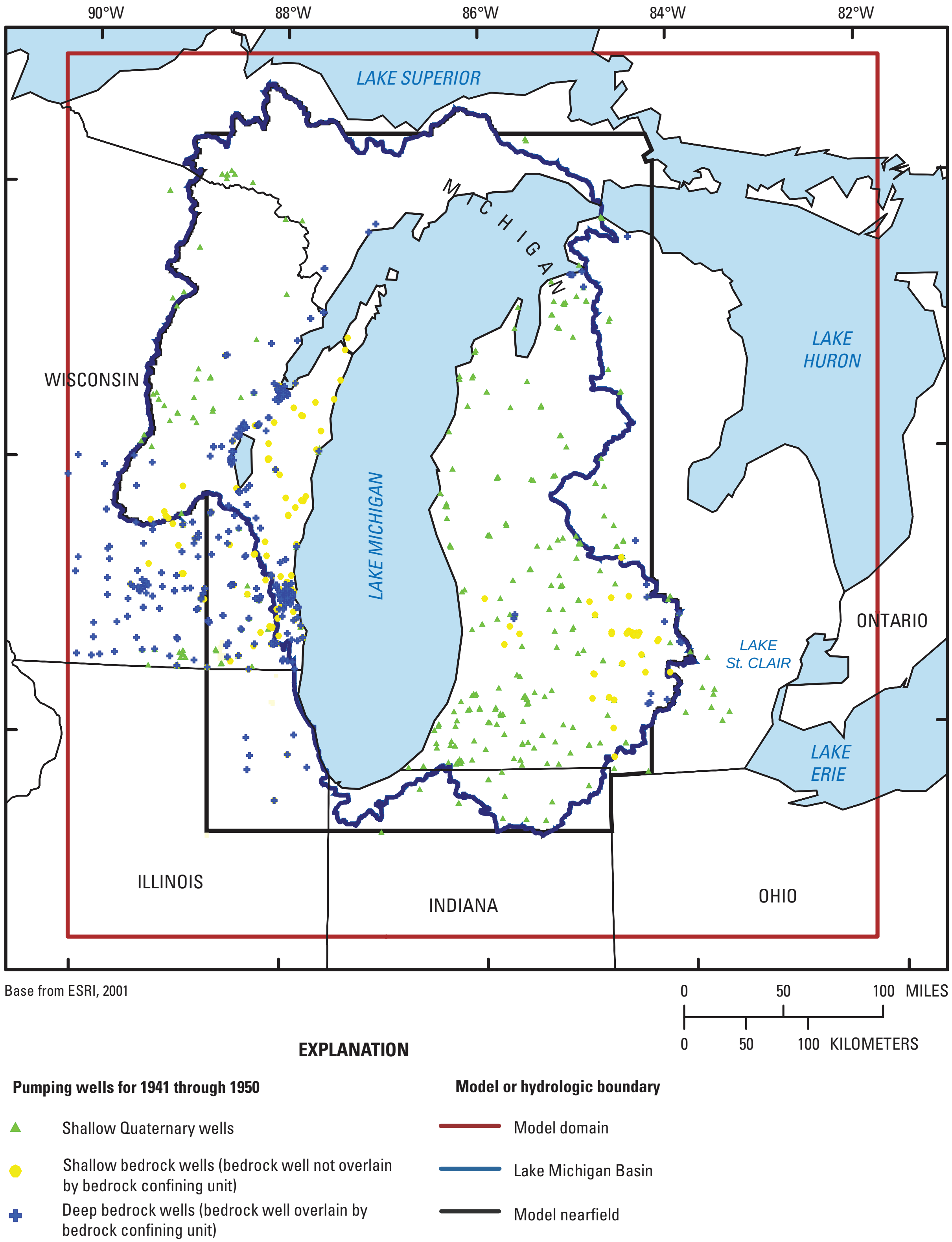

Figure 35*A*. Spatial distribution of shallow Quaternary, shallow bedrock, and deep bedrock wells: 1941–50.

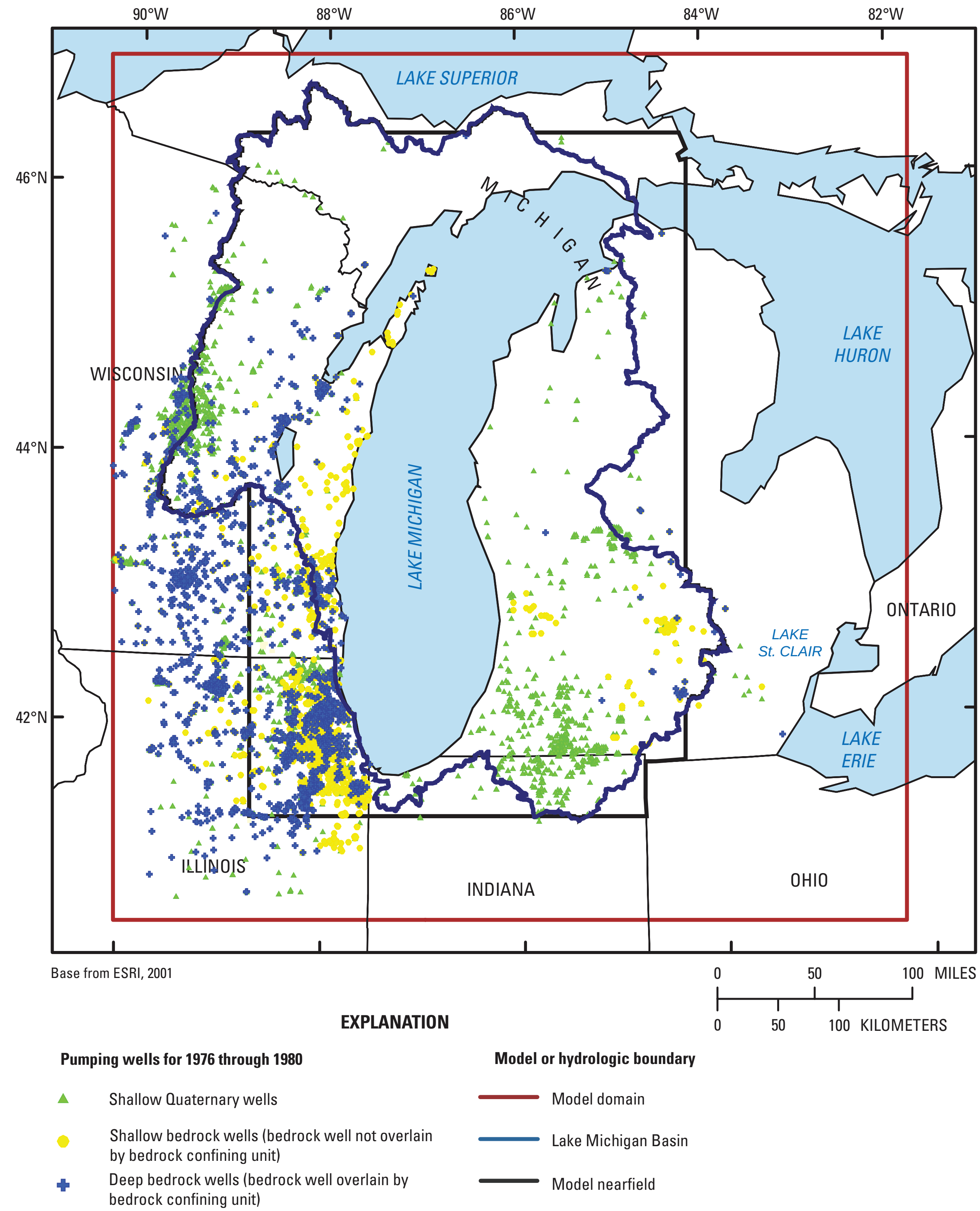

Figure 35*B*. Spatial distribution of shallow Quaternary, shallow bedrock, and deep bedrock wells: 1976–80.

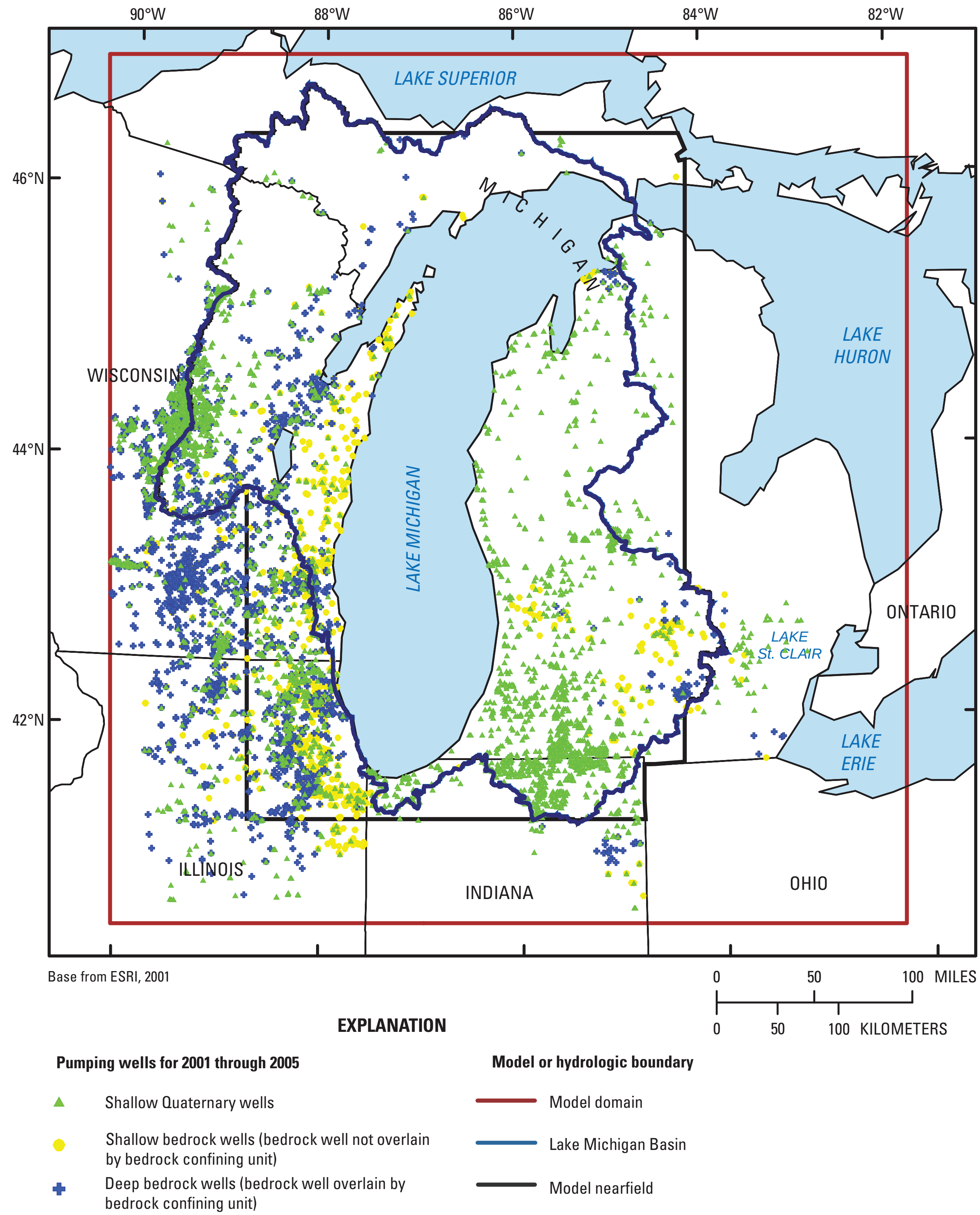

Figure 35*C*. Spatial distribution of shallow Quaternary, shallow bedrock, and deep bedrock wells: 2001–5.

Table 9. Shallow compared to deep withdrawals.

Shallow withdrawals include pumping from wells that penetrate unlithified Quaternary deposits plus pumping from shallow bedrock. Shallow bedrock withdrawals are from wells open to aquifers above the uppermost bedrock confining unit. Deep withdrawals are from wells that penetrate to bedrock aquifers that are below the uppermost bedrock confining unit. The uppermost bedrock confining unit at any row or column location in the model corresponds to the most shallow layer that is more than 5 feet thick and is assigned a vertical hydraulic conductivity less than or equal to 0.001 foot per day. If no bedrock confining unit is encountered, then the entire model thickness falls within the shallow part of the flow system at that location.

Shallow wells can be considered to pump under unconfined conditions when at the water table or when any overlying QRNR deposits are coarse grained, or under semiconfined conditions when any overlying QRNR deposits are fine grained. Deep wells all pump under confined conditions.

Mgal/d, million gallons per day.

9*A*. Shallow and deep withdrawals through time for entire model domain.

Withdrawal zone	Number of wells in model	Percentage of total number	Withdrawal in model (Mgal/d)	Percentage of total withdrawals
		1941–50		
Shallow QRNR	366	34	56.5	25
Shallow bedrock	192	18	34.1	15
Deep bedrock	504	48	133.5	60
		1976–80		
Shallow QRNR	2,449	37	322.8	35
Shallow bedrock	2,029	31	185.4	20
Deep bedrock	2,152	32	423.1	45
		2001–5		
Shallow QRNR	4,694	51	537.8	49
Shallow bedrock	1,841	20	173.3	16
Deep bedrock	2,612	29	382.3	35

9*B*. Percentages of withdrawals by state for 2001–5 in model nearfield.

State	With-drawal (Mgal/d)	Shallow QRNR (percent)	Shallow bedrock (percent)	Deep bedrock (percent)
Michigan	348	72.3	22.2	5.5
Indiana	117	98.9	1.1	.0
Wisconsin	193	27.3	20.5	52.2
Illinois	167	23.4	16.4.	60.2

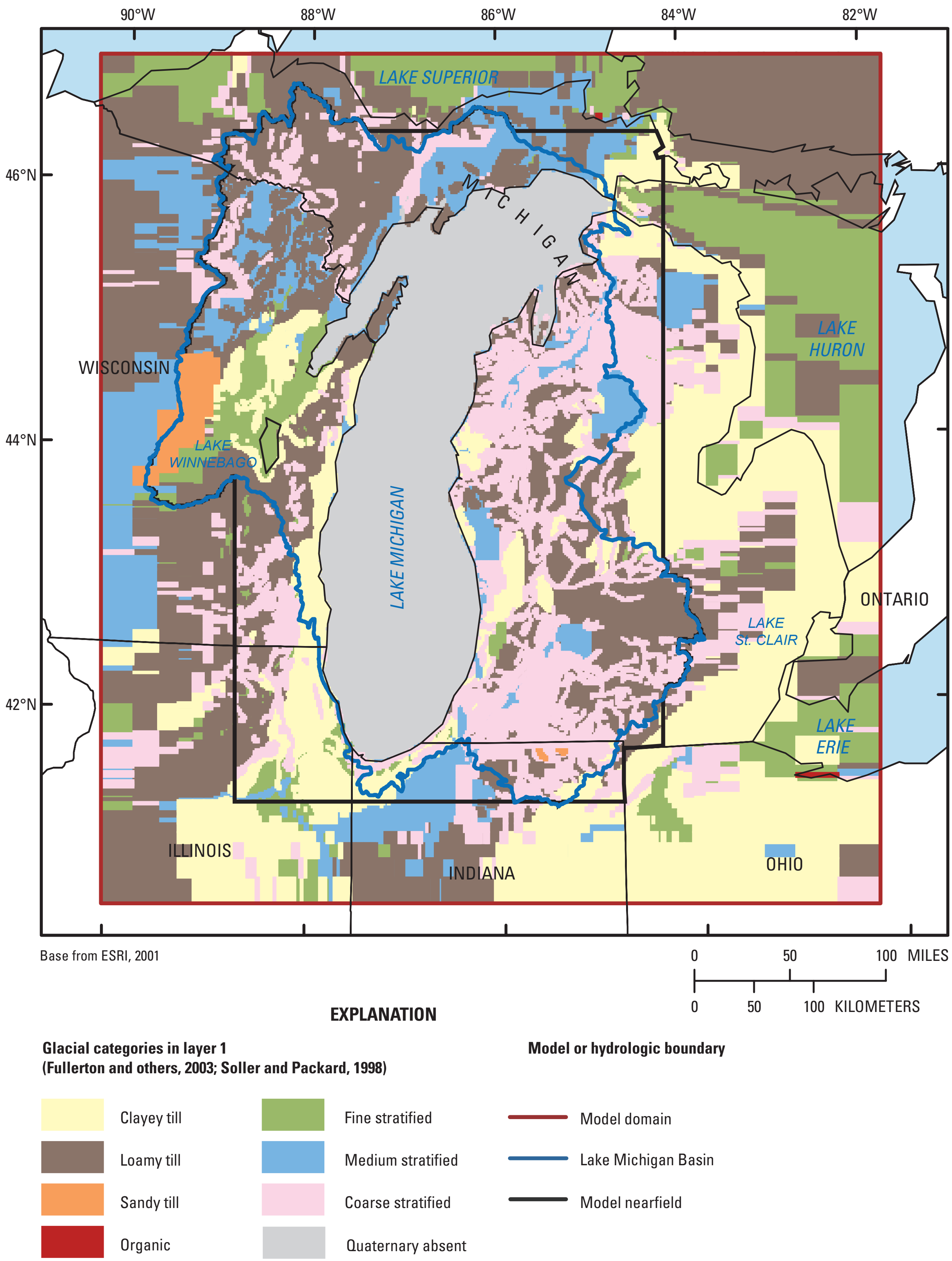

Figure 36*A*. Glacial categories in model layer 1.

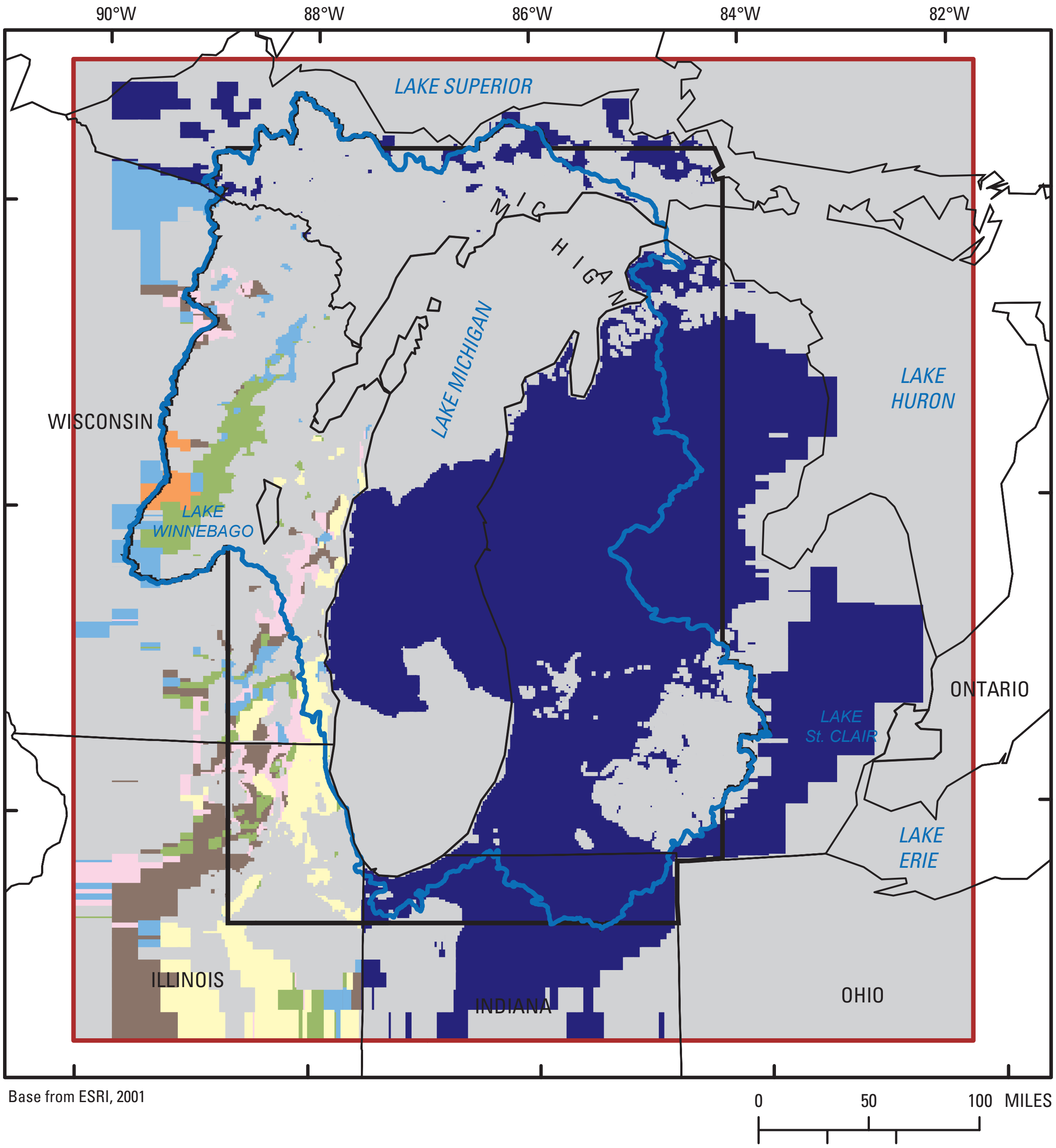

EXPLANATION

Glacial categories in layer 2
(Fullerton and others, 2003; Soller and Packard, 1998)

- Clayey till
- Loamy till
- Sandy till
- Unknown
- Fine stratified
- Medium stratified
- Coarse stratified
- Quaternary absent

Model or hydrologic boundary

- Model domain
- Lake Michigan Basin
- Model nearfield

Figure 36*B*. Glacial categories in model layer 2.

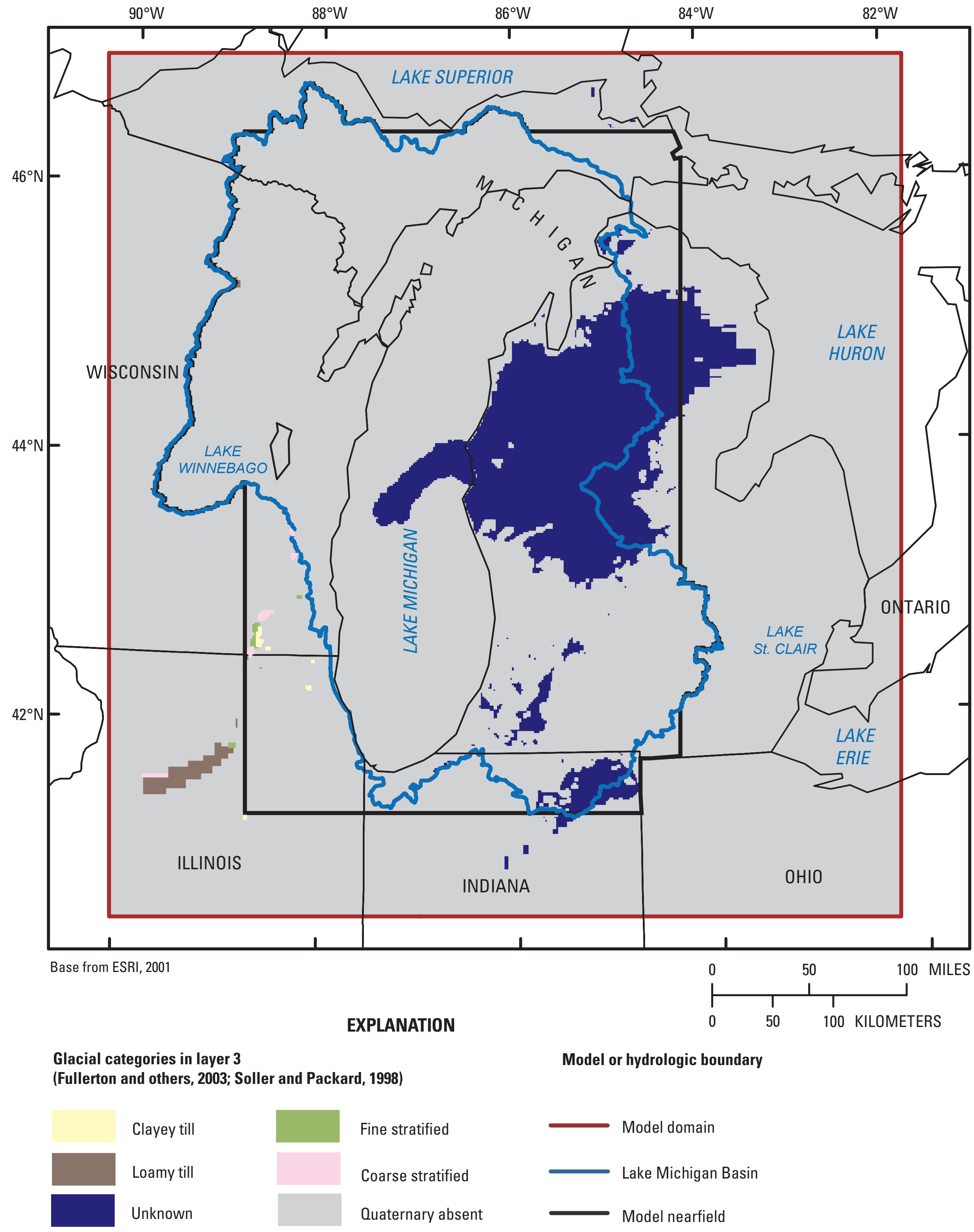

Figure 36*C*. Glacial categories in model layer 3.